Oncolytic Virotherapy using Reovirus for Canine Tumors

（犬の腫瘍に対する腫瘍溶解性レオウイルス療法の検討）

The United Graduate School of Veterinary Science
Yamaguchi University

Masaya IGASE

March 2019

TABLE OF CONTENTS

GENERAL INTRODUCTION

Canine cancer, such as, mammary grand tumor, melanoma, osteosarcoma, and histiocytic sarcoma is recently an increasing cause of death in adult dogs. Canine mammary gland tumor is the most common neoplasm in female dogs. Complete surgical resection is the best treatment available for canine mammary gland tumor as no other effective systemic therapy has been established so far. Canine melanoma is among the most aggressive cancers, exhibiting the ability to readily metastasize to other organs such as the lung, lymph nodes, and liver. Naturally occurring canine melanoma is considered a preclinical model of human melanoma (Gillard, M. *et al*., 2013, Hernandez, B. *et al*., 2018). Osteosarcoma is the common primary bone neoplasm in dogs and occured frequently in the appendicular skeleton (Dernell, WS. *et al*., 2007). Even though amputation is the standard local treatment for canine osteosarcoma, the suitable treatment against metastatic osteosarcoma has not been developed. Canine histiocytic sarcoma is known as a rapidly growing, aggressive fatal neoplastic disease which originates from dendritic cells (Fulmer, AK. and Mauldin, GE., 2007). Histiocytic sarcoma represents approximately 1% of canine cancers of the lymphoreticular system (Clifford, CA. *et al*., 2013). Also, human histiocytic sarcoma

represents such a rare disease and similar characteristics of disease (Dalia, S. *et al*., 2014, Hedan, B. *et al*., 2011). Chemotherapy with lomustine and doxorubicin is a common treatment in canine histiocytic sarcoma. However, it is often associated with the acquisition of multi-drug resistances, leading to poor prognosis (Skorupski, KA. *et al*., 2007, Rassnick, KM. *et al*., 2010). Due to the aggressive characteristic of these tumors and its refractory to conventional therapy, a new effective therapy against cancer is needed. In the recent study, various new therapeutic approaches have been developed in human oncology and some of them are used for veterinary medicine.

Now, a lot of candidates as a novel cancer treatment have been investigated in the world. In particular, it is thought that cancer immunotherapy may be positioned as the major breakthrough in cancer treatment, following the success of small molecular inhibitors (Farkona, S. *et al.*, 2016). Cancer immunotherapy is defined as a treatment for modulation of immune system to fight cancers, and includes monoclonal antibodies, immune checkpoint inhibitors, cancer vaccine, and oncolytic viruses. Among them, I have been working with the oncolytic virotherapy to apply it to veterinary medicine.

Oncolytic virotherapy is one of the latest strategies for cancer therapy.

Generally, oncolytic viruses specifically replicate and kill the tumor cells without affecting normal cells. Viruses released from infected-tumor cells attack the other tumor cells again. In addition to direct cytotoxicity, oncolytic viruses also have immune-stimulatory effects against tumors (Marelli, G. *et al*., 2018, Filley, AC. and Dey, M., 2017, Rajani, K. *et al*., 2016, Mostafa, AA. *et al*., 2018). Many viruses, adenovirus, coxsackie virus, herpes simplex virus, measles virus, Newcastle disease virus, parvovirus, poliovirus, reovirus, retrovirus, vaccinia virus and vesicular stomatitis virus have been developed for oncolytic virotherapy, and some of them are currently in human clinical trials (Fukuhara, H. *et al.*, 2016, Marelli, G. *et al.*, 2018). Most of the oncolytic viruses are genetically modified to reduce the pathogenicity, to enhance the specificity to tumor cells, and to transduce the therapeutic gene. Using genetically modified oncolytic virus in a clinical setting in small animal medicine has a big hurdle because of the difficulty in management of the animals treated with the recombinant virus and the subsequent viral excretion. On the other hand, some viruses including reovirus and myxoma virus have been discovered to be naturally occurring oncolytic viruses without a requirement of any gene-modifications (Fukuhara, H. *et al.*, 2016,

Marelli, G. *et al.*, 2018). In canine cancers, a total of 13 viral species were reported as the candidates of oncolytic virotherapy (Sanchez, D. *et al.*, 2018). However, there has been only limited number of reports regarding the available of oncolytic virus against canine cancers. Our laboratory has focused on oncolytic virotherapy using reovirus, which is naturally occurring non-recombinant virius, and the previous PhD. student, Dr. Hwang Chung Chew, first reported the anti-tumor effects of reovirus in canine mast cell tumor and lymphoma (Hwang, CC. *et al*., 2013, Hwang, CC. *et al*., 2016).

Reovirus is a double-strand RNA virus with low pathogenicity in humans. Even though all three serotypes of reovirus (type I Lang, type II Jones, and type III Dearing) has the oncolytic ability, the serotype III Dearing strain has always been used in human studies (Alloussi, SH. *et al.*, 2011). Reovirus has shown selective infection in transformed or malignant tumor cells with a preference to replicate in these cells (Duncan, MR. *et al*., 1978, Hashiro, G. *et al*., 1977, Coffey, MC. *et al*., 1998). Oncogenic Ras-transformed cells are highly susceptible to reovirus infection, and non-transformed cells did not allow the translation of viral genes and viral replication. The major difference between reovirus susceptible and non-susceptible cells lines in the

ability of the cells to phosphorylate PKR (dsRNA-activated protein kinase). In cases of reovirus infection in susceptible cells, Ras activation will inhibit the phosphorylation of PKR and allow the expression of viral proteins before the release of viral progeny. However, it has also been reported that reovirus can exert oncolysis independent of this pathway in some tumor cells (Twigger, K. *et al*., 2012). In addition, reovirus shows the oncolytic activity against a wide range of human cancers such as brain, gynecologic, colorectal, breast, prostate, pancreatic, lung, head and neck, bone and soft tissue, skin, and hematological cancer or sarcoma (Kim, M., 2015). The most significant study involving REOLYSIN®, which is GMP grade reovirus, was the Phase III study of intravenous (IV) administration of reovirus in combination with carboplatin and paclitaxel in patients with metastatic or recurrent head and neck cancers. Even though this study was conducted on expanded groups consisting of patients with certain disease conditions, the progression free survival of patients treated with the reovirus combination therapy had a statistically significant response (http://www.oncolyticsbiotech.com/news/oncolytics-biotech-inc-announces-positive-top-line-data-from-reo-018-randomized-study-of-reolysin-in-head-and-neck-cancers/).

Another remarkable finding was presented in the most recent conclusion of the Phase II metastatic breast cancer study, where results have shown that REOLYSIN® in combination with paclitaxel had a statistically significant increase in median overall survival as compared to paclitaxel alone (17.4 vs 10.4 months). More interestingly, the overall survival in patients with mutated p53 metastatic breast cancer more than doubled (20.9 months) when given the combination treatment. This remarkable finding was acknowledged by the U.S. FDA with the Fast Track designation (http://www.oncolyticsbiotech.com/news/oncolytics-biotech-inc-announces-fda-fast-track-designation-for-reolysin-in-metastatic-breast-cancer/). In contrast, there is only limited information about anti-tumor effects of reovirus on canine tumors, as shown in our laboratory's previous report about mast cell tumor and lymphoma. Therefore, main purpose of this thesis is to provide the basic and clinical evidences on the feasibility of reovirus as an attractive cancer therapy in a wide range of canine cancers.

In Chapter 1, *in vitro* cytotoxicity of reovirus was examined in canine solid tumor cell lines (melanoma, mammary gland tumor, and osteosarcoma). I also assessed reovirus infectivity, production of progeny viruses and the relationship between Ras

activation status and reovirus susceptibility in those cell lines.

In Chapter 2, I examined *in vitro* and *in vivo* cytotoxicity of reovirus against canine histiocytic sarcoma cell lines and peripheral blood monocyte-derived immature dendritic cells. Moreover, I confirmed the relationship between the oncolytic activity and innate immune response to reovirus in histiocytic sarcoma and immature dendritic cells. To my best knowledge, there are very few reports about the effects of oncolytic virus (morbillivirus and ECHO-7 virus) in canine and human histiocytic sarcoma (Pfankuche, VM. *et al*., 2016, Pfankuche, VM. *et al*., 2017, Alberts, P. *et al*., 2016). Therefore, the data on the oncolysis of reovirus in histiocytic sarcoma cells is important to provide the evidence for rational use of oncolytic viruses in clinical trials.

Reovirus has been used in multiple clinical trials in human cancer patients, primarily in combination with conventional chemotherapeutic drugs such as paclitaxel, gemcitabine and carboplatin (Clements, D. *et al*., 2014), radiation, and small molecule inhibitors (Pol, J. *et al*., 2014, Pol, J. *et al*., 2015, Vacchelli, E. *et al*., 2013), with the intent of enhancing the efficacy of oncolytic therapy. However, there still needs to identify new candidate drugs for use in combination therapy with oncolytic viruses for

treating human cancers. In Chapter 3, I examined the synergistic anti-cancer effects of a combination of reovirus and various chemotherapeutic drugs (paclitaxel, gemcitabine, carboplatin and toceranib) in canine mammary gland tumor cell lines. In addition to that, to develop a new combination approach for oncolytic virotherapy using reovirus, I screened a large number of small molecule inhibitors in combination with reovirus in canine melanoma. I successfully identified an inhibitor of the ataxia telangiectasia mutated protein (ATM). Here, I reported the first evidence to my knowledge that the cytotoxicity of reovirus is potentiated by inhibition of ATM in canine melanoma cell lines. I also showed that ATM inhibition increases reovirus replication by up-regulating proteolysis of endosome-localized reovirus particles. Notably, reovirus was able to induce the phosphorylation of ATM without inducing DNA damage. As in canine cancers, the combination of reovirus and an ATM inhibitor yielded enhanced cytotoxicity in several human cancer cell lines. The analysis and result are discussed in Chapter 4.

In Chapter 5, aligned with the exciting progress in human clinical trials, I conducted the first reovirus clinical study in dogs with various spontaneously occurring

tumors. Based on information of studies in mouse models and healthy dogs (data not shown), I reached a prior conclusion that reovirus administration is safe and non-pathogenic in dogs. Following that, with consent from dog owners, reovirus administration was carried out in 19 tumor-bearing dogs while referring to information of human clinical trials. The primary objectives of this study were to determine the safety profile of reovirus in dogs with tumors, while identifying a recommended dosing regimen. At the same time, data on the pharmacokinetics of viral shedding, immune response and efficacy of reovirus against cancers in immunocompetent canine patients, which are essential for the establishment of a future pivotal study, was also collected.

From all my experiments, we found that reovirus was a promising effective treatment against canine cancers. My supervisor, *Prof. Takuya Mizuno* says to me "The Clinic to Bench, Bench to Clinic are important for us". This phrase inspired me and motivated to work my PhD study hard. Hopefully with the completion of my PhD, I strongly believe that oncolytic virotherapy using reovirus has the potential to be one of the next generation cancer therapeutics in dogs.

MATERIALS & METHODS

Reovirus

The Dearing strain of reovirus serotype 3 (Reolysin®; GMP grade reovirus) was obtained from Oncolytics Biotech Inc. (Calgary, Canada). Infectious subviral particles (ISVPs) were produced just before use, and were generated according to the protocol of Alain, T. *et al*. 2006. Briefly, reovirus (2.835 x10^8 Plaque-forming unit (PFU)) was digested with chymotrypsin-HCl (2 μg; Roche Diagnostics K.K., Tokyo, Japan) for 30 min at 37°C. The digestion was terminated by adding phenymethylsulphonyl fluoride (5 mM in ethanol) and shifting the reaction to 4 °C.

Cell lines

Canine mammary gland tumor (MGT) cell lines (CIP-p, CIP-m, CTB-p, CTB-m, CHM-p, CHM-m CNM-m (Nakagawa, T. *et al*., 2006), CHMp-13a and CHMp-5b (Murai, K. et al., 2012)), canine osteosarcoma cell lines (Abrams, D17, Gracie, MacKinley and Moresco (Maeda, J. *et al*., 2012)), canine malignant melanoma cell lines (CMeC1, CMeC2, KMeC, LMeC (Inoue, K. *et al*., 2004), CMM10, CMM12 (Yoshitake, R. *et al*., 2017) CMGD2 and CMGD5 (Bianco, SR. *et al*., 2003)) and canine

histiocytic sarcoma cell lines (CHSA(CHS-5), CHSS(CHS-7), CMHM(CHS-2) (Azakami, D. *et al*., 2006) and MHT-2 (Ito, K. *et al*., 2013)) were used in this thesis. Also, human cancer cell lines (A549, T-24, A2058, Colo679, and DLD-1) were used. All canine MGT and six canine malignant melanoma cell lines (CMeC1, CMeC2, KMeC, LMeC, CMM10 and CMM12) were kindly provided by Dr. Nakagawa (University of Tokyo, Tokyo, Japan). Two canine malignant melanoma (CMGD2 and CMGD5) and all canine ostersarcoma cell lines were kindly provided by Dr. Modiano (University of Minnesota, St Paul, MN) and Dr. Thamm (Colorado State University, Fort Collins, CO), respectively. Canine histiocytic sarcoma cell lines were kindly provided by Dr. Bonkobara (Nippon Veterinary and Life Science University, Tokyo, Japan). All of the human cancer cell lines (A549, T-24, A2058, Colo679, and DLD-1), a mouse L929 fibroblastic cell line (used for the titration of viral progeny) and a human Burkitt's lymphoma cell line Raji (used as a positive control in the Ras GST pull-down assay) were obtained from the Cell Resource Center for Biomedical Research (Institute of Development, Aging and Cancer, Tohoku University, Sendai, Japan). All cell lines except CHSA, CHSS, CMHM, MHT-2 and A2058 were grown in the R10 complete

medium (RPMI1640 supplemented with 10% fetal bovine serum (FBS), 100 U/ml penicillin, 100 μg/ml streptomycin and 55 μM 2-mercaptoethanol). Remaining cell lines (CHSA, CHSS, CMHM, MHT-2 and A2058) were grown in D10 complete medium (DMEM supplemented with high glucose, 10% FBS, 100 U/ml penicillin, 100 μg/ml streptomycin, and 55 μM 2-mercaptoethanol). All cell lines were maintained at 37°C in a humidified 5% CO_2 incubator.

Reagents

The pan-caspase inhibitor Z-VAD-FMK (Calbiochem, Billerica, MA) was used in inhibition of apoptosis assay. Poly IC as the positive control of TLR3 agonist was purchased from TOCRIS Bioscience (Minneapolis, MN). Paclitaxel, carboplatin and gemcitabine were obtained from SIGMA-ALDRICH® Corporation (St. Louis, MO). Toceranib (SU11654) was obtained from Adooq Bioscience (Irvine, CA). The ATM inhibitors KU55933 and KU60019 were obtained from AdooQ Bioscience.

Drug screening

To identify the new combination drug, we screened the SCADS inhibitor kit (The Ministry of Education, Culture, Sports, Science and Technology, Tokyo, Japan), which includes 285 signaling pathway inhibitors. The canine melanoma cell line CMeC1 was plated in 96-well plates containing each inhibitor, with or without reovirus at an MOI of 100 PFU per cell, and the plates were incubated for 48 hr. After treatment, cell growth inhibition was evaluated by use of the Cell Counting Kit-8 (CCK-8; Dojindo, Kumamoto, Japan) according to the manufacturer's instructions.

Cell proliferation assay

In Chapters 1, 2 and 3, cell growth inhibition by reovirus was assessed by methylthiazole tetrazolium (MTT) assay, according to the previously published method (Yang, WQ. *et al*., 2003). Briefly, each cell line was seeded at an optimized number (1250 cells for CIP-p, CIP-m, CHM-p and CHM-m; 2000 cells for CMeC1, KMeC and LMeC, 2500 cells for CTB-p; 3000 cells for Abrams, Gracie, Moresco, CMeC2, CHMp-13a and CHMp-5b; 5000 cells for CTB-p, CNM-m, D17, MacKinley, CMGD2 and CMGD5; 10,000 cells for CHSA, CHSS, CMHM and MHT-2) in 96-well plates

and was simultaneously mock-infected or infected with reovirus at MOI of 0.1, 1.0, 10, 100 and 1000 PFUs per cell in triplicates. Cells were cultured for 72 hr before 3-(4,5-dimethylthiazol-2yl)-2,5-diphenyltetrazolium bromide (MTT) reagent was added into the culture for 4 hr, and the MTT assay was performed to assess cell proliferation by measuring the absorbance in the plates.

In Chapter 4, each cell line was seeded at an optimized number in 96-well plates and mock-infected or infected with reovirus at an MOI of 10 or 100 PFU per cell in the presence of the ATM inhibitor KU60019 at 1.25, 2.5, 5.0 or 10 μM; assays were performed in triplicate wells. Cells were cultured for 48 hr before adding the CCK-8 reagent. The cell proliferation rate was calculated by measuring absorbance.

All experiments were repeated at least three times.

Cytotoxicity assay

In Chapter 1 and Chapter 3, each cell line was seeded at an optimized number (3000 cells for CIP-p, CTB-p, CHM-p, CHMp-13a, CHMp-5b, CHM-m, Abrams, Gracie, Moresco, CMeC1, CMeC2, KMeC and LMeC; 5000 cells for CIP-m, CTB-m,

CNM-m, D17, MacKinley, CMGD2 and CMGD5) in 96-well plates in triplicates. Then, cells were and infected with mock or reovirus at MOI of 70 PFUs per cell in triplicates. At 72 hours post-infection (hpi), live and dead cells were counted with 0.25% trypan blue.

In Chapter 4, each cell line was treated with reovirus at an MOI of 10 or 100 and KU60019 at 2.5 or 10 μM; assays were performed in triplicate wells. Cells were cultured for 48 hr before performing the trypan blue exclusion test.

All experiments were repeated at least three times.

Evaluation of apoptosis with flow cytometric analysis

To determine that the reovirus-induced cell death was apoptosis, PE Annexin V Apoptosis Detection Kit I (BD Biosciences, San Jose, CA) was used in Chapter 2. Canine histiocytic sarcoma cell lines were treated with reovirus at MOI of 10 for 48 hr. Harvested cells were washed in cold PBS, and re-suspended at 1 $x10^5$ in Binding buffer. Then, cells were incubated for 15 min at room temperature with PE-Annexin V and 7-AAD.

In Chapter 3, CHMp-13a and CHMp-5b were treated with reovirus at MOI of 70 for 24 and 48 hr. Adherent cells were collected, washed with cold PBS, and 3 x 10^5 cells were resuspended in 30 µl of PBS. Next, cells were incubated for 15 min at room temperature in the dark in cold 1 x binding buffer containing Annexin V-FITC antibody, according to the manufacturer's instructions (Miltenyi Biotech, Auburn, CA). The cells were pelleted and resuspended in cold 1 x binding buffer. Cells were stained with 1.5 µl of propidium iodide (PI) at 1 µg/ml.

Stained cells were analyzed using BD Accuri C6 Flow Cytometer (BD Biosciences). Analyses were performed with FlowJo software ver. 10.1 (FlowJo LLC, Ashland, OR).

Measurement of inhibition of apoptosis

To evaluate that the apoptosis induced by reovirus was dependent on caspase signaling pathway, the inhibition assay of cell death by irreversible pan-caspase inhibitor Z-VAD-FMK (Calbiochem) was performed. In Chapter 2 and Chapter 3, canine histiocytic sarcoma cell lines and canine MGT cell lines were seeded at 10,000

cells or 3,000 cells per well, respectively, in a 96-well plate in triplicates. To each well, Z-VAD-FMK was added at 50 μM for 1 hour before reovirus infection at MOI of 10 or 70. After 72 hours incubation, viable and non-viable cells were counted using 0.25% trypan blue.

In Chapter 4, canine melanoma cell lines (CMeC1 and KMeC) were seeded at 5,000 cells per well in 96-well plates. Z-VAD-FMK (Calbiochem) was added to triplicate wells at a concentration of 50 μM for 1 hr before the cells were treated with reovirus (MOI 100) and KU60019 (indicated concentration). After 48 hr, cell proliferation and cell viability were evaluated by CCK-8 and trypan blue exclusion test, respectively.

All experiments were repeated at least three times.

In vitro synergy assay

Experiments in Chapter 3 were performed as described in the *in vitro* cell proliferation assay using 0.25, 0.5, 1, 2 and 4 times of the IC50 (half maximal inhibitory concentration) dose as calculated by CompuSyn (ComboSyn, Inc., Paramus, NJ, USA)

using a combination of reovirus and paclitaxel, carboplatin, gemcitabine or toceranib.

The synergistic effects of reovirus and the chemotherapeutic agents on cell proliferation were assessed by calculating the combination-index (CI) values using the CompuSyn software. Using the Chou and Talalay method, CI provides a quantitative measure of the degree of interaction between two or more agents (Chou, TC., 2010, Chou, TC. and Talalay, P., 1984). The CI value offers quantitative definitions that depict synergism (CI<1), additive effect (CI=1) and antagonism (CI>1).

Reovirus replication

Reovirus replication was examined by western blotting analysis using anti-reovirus antibody (produced by our laboratory (Hwang, CC. *et al*., 2013)). In Chapter 2, canine histiocytic sarcoma cell lines were seeded at 2.5 $x10^5$ cells/ well in 6-well plates and treated with reovirus (MOI 10). After 24 and 48 hours, cells were harvested and stored at -80°C pending use for western blotting. In Chapter 4, each cell line was seeded in 6-well plates and treated with reovirus (MOI 10 or 100) and KU60019 (2.5 μM) for 24 and 48 hr. In some experiments examining the reovirus proteins at early stages, wells

were rinsed to remove unbound reovirus following adsorption. Briefly, CMeC1 was plated in 6-well plates and cultured before use. On the following day, cells were exposed to reovirus (MOI 100) for 1 hr at 4°C. Then, cells were washed and cultured in the presence of KU60019 (2.5 μM) for 6, 12, or 24 hr at 37°C. Cells were harvested at the indicated time points and stored at -80°C pending use for western blotting. Western blotting analysis was carried out as described the below section.

Production of viral progeny

Cell culture supernatant of samples from cytotoxicity assay was collected and kept at -80°C until analysis. Viral progeny was measured by 50% tissue culture dose ($TCID_{50}$) assay on L929 cells as previously described (Hwang, CC. *et al*., 2013). L929 cells were seeded at 10,000 cells per well in 96-well plates. Serial ten-fold dilutions of the stock virus or the culture supernatant from cytotoxicity assay were prepared before being added into the wells. After 144 hr of incubation, cytopathogenic effects (CPE) in the wells were recorded and $TCID_{50}$ was calculated. Titration of the viral progeny was performed on all the supernatants obtained from three independent cytotoxicity assays.

Reovirus infectivity

Reovirus infectivity of the cell lines was quantified by flow cytometry. Cell lines used in Chapter 1 were infected with reovirus at MOI of 70 for 24 hr (CMGD2), 48 hr (CIP-p and CNM-m) or 72 hr (all remaining cell lines). In Chapter 3, CHMp-13a and CHMp-5b were infected with reovirus at MOI of 70 for 48 hr. Cells were harvested and resuspended in PBS before being fixed and permeabilized with BD Cytofix/ Cytoperm Kit (BD Bioscience). Intracellular viral proteins were stained with rabbit anti-reovirus polyclonal antibody (produced by our laboratory). The staining of primary antibody was followed by incubation with anti-rabbit IgG PE antibody (Santa Cruz Biotechnology, Santa Cruz, CA). Serum from healthy rabbit (Life technologies, Tokyo, Japan) was used as the isotype control. The stained cells were analyzed using Cyflow Space (Partec GmbH, Munster, Germany) or BD Accuri C6 Flow Cytometer (BD Biosciences,), and the results were analyzed using FlowJo software (FlowJo LLC).

Plasmid construction

The human *ATP6V1G1* gene was amplified by PCR using 141-LCL (human EBV-lymphoblastoid cell line) cDNA as a template and the primers YTM1658 (5'-GCTTGCCTTGCTCTCAGAAT -3') and YTM1659 (5'-TAAAATGCCACTCCACAGCA -3') as the primers; the resulting product was cloned into the pBluescript SK (-) vector, yielding a construct designated pBs-hATP6V1G1). The nucleotide sequence of the insert was confirmed using a Big Dye Terminator v3.1 Cycle Sequencing kit (PerkinElmer, Inc., Waltham, MA). The human *ATP6V1G1* gene then was subcloned into the pMxs-IP retroviral vector (kindly provided by Dr. T. Kitamura (The University of Tokyo)), yielding a plasmid (designated pMx-IP-PA-hATP6V1G1) encoding a PA epitope-tagged version of the V-ATPase G1 protein.

Genome editing

A small guide RNA (sgRNA) targeting canine *ATM*, 5'-TAGTTTCAGGATCCCGAATC -3', was designed through the online CRISPR design tool (http://crispr.mit.edu/); the resulting sgNRA was synthesized and subcloned into the lentiCRISPRv2 plasmid which was gift from Dr. Feng Zhang (Sanjana, NE. *et al*.,

2014) (obtained from Addgene (Cambridge, MA) as accession #52961). The plasmid and packaging vectors were transfected to HEK293T to produce the lentivirus expressing an sgRNA targeting *ATM*. After transduction with the lentivirus, canine melanoma cell lines were cultured in the presence of puromycin (Sigma Aldrich Japan K.K., Tokyo, Japan; 0.6 - 5.0 μg/ml) to select for stably transduced cells. Individual clones were isolated by the limiting dilution method and further analyzed by western blotting to confirm that the cells no longer produced ATM protein. The resulting clones were used for further experiments.

Generation of normal canine immature dendritic cell and reovirus infection

Peripheral blood mononuclear cells (PBMCs) were isolated from three healthy beagles. PBMCs were cultured for 7 days with 33 ng/ml of canine interleukin-4 (caIL-4) and 40 ng/ml of canine granulocyte-macrophage colony-stimulation factor (GM-CSF) (R&D Systems, Minneapolis, MN) to differentiate into immature dendritic cells (normal DCs) (Mito, K. *et al*., 2010). Normal DCs were then used for following experiments in Chapter 3.

RNA isolation, cDNA, and real-time PCR

Total RNA was harvested from cells using ISOGEN II (NIPPON GENE, Tokyo, Japan), and cDNA was synthesized using ReveTra Ace qPCR RT kit (TOYOBO, Osaka, Japan) according to the manufacture's instructions. Real-time PCR was performed using QuantiTect SYBR Green PCR kit (Qiagen, Valencia, CA) and CFX touch real time PCR analysis system (Bio-rad Laboratories, Hercules, CA) as per the manufacture's protocol. The following primer were used: canine *IFN-α* (Jassies-van der Lee, A. *et al*., 2014) forward 5'-TGGGACAGATGAGGAGACTCTC-3' and reverse 5'-GAAGACCTTCTGGGTCATCACG-3'; canine *IFN-β* (Shoji, M. *et al*., 2015) forward 5'-CCAGTTCCAGAAGGAGGACA-3' and reverse 5'-TGTCCCAGGTGAAGTTTTCC-3'; canine *RPL13A* forward 5'-GCCGGAAGGTTGTAGTCGT-3' and reverse 5'-GGAGGAAGGCCAGGTAATTC-3'; and canine *HPRT* forward 5'-CACTGGGAAAACAATGCAGA-3' and reverse 5'-ACACTTCGAGGGGTCCTTTT-3'. In our study, ribosomal protein *RPL13A* and hypoxanthine phosphoribosyl transferase *HPRT* were used as reference genes

(Boerkamp, KM. *et al*., 2014). After the PCR, all products were analyzed by the melting curves to confirm the amplification of other genes. The relative mRNA expression levels of *IFN-α* and *IFN-β* were calculated as ΔCt from the difference between expression of the reference gene. All ΔCt values were converted to $2^{-\Delta Ct}$ (Kambayashi, S. *et al*., 2015). Experiment was repeated at least three times.

Cell cycle analysis

Canine melanoma cells were treated with reovirus (MOI 100) and KU60019 (2.5 μM) for 24 and 48 hr. Cells were trypsinized and washed in Phosphate-buffered saline (PBS) and fixed in 70 % ice cold ethanol at -30 °C for at least 24 hr. The fixed cells were re-suspended in PBS supplemented with 0.1 mg/ml of RNase (Nacalai Tesque, Kyoto, Japan) and incubated for 30 min at room temperature. The digested cells then were incubated with 0.1 mg/ml of propidium iodide (PI; Nacalai Tesque) for 5 min and analyzed using a BD Accuri C6 Flow Cytometer (BD Biosciences). Data were analyzed using FlowJo software ver. 10.1 (FlowJo LLC).

Western blotting

In Chapter 1, to detect the PARP cleavage, cells were seeded at 5.0 x 10^5 cells and mock infected or infected with reovirus at MOI of 70 for 48 hr before being harvested and lysed at 4°C with NP40 lysis buffer [(1% NP40, 10 mM Tris-HCl (pH 7.5), 150 mM NaCl, 1 mM EDTA) supplemented with protease inhibitor cocktails (Nacalai Tesque), 1 mM Na_3VO_4, and 50 mM NaF]. In Chapter 2, to evaluate the mechanism of cell death, canine histiocytic sarcoma cell lines were seeded at 2.5 x10^5 cells in 6-well plate before being infected with mock or reovirus at MOI of 10. After 24 and 48 hours, cells were harvested and lysed with NP40 lysis buffer. In Chapter 3, CHMp-13a and CHMp-5b were seeded at 2.5 x 10^5 cells, and mock-infected or infected with reovirus at MOI 70. In order to evaluate the synergistic effects of the combination treatments, CHMp-5b cells were seeded at 2.5 x 10^5 cells, and treated 0.5 times the calculated IC50 dose of the single or a combination of the cytotoxic agents. In order to confirm the inhibition of caspase 3 activation, both of the cell lines were seeded at 2.0 x 10^5 cells in 6-well plates. Z-VAD-FMK was added at 50 μM for 1hr before the cells were infected at MOI 70. After 48 or 72 hr incubation, cells were harvested and lysed at

4°C with NP40 lysis buffer. In Chapter 4, cells were plated at 3 x10^5 cells per well in 6-well plates and treated with reovirus (MOI 10 or 100) and KU60019 (2.5 μM) for 24 and 48 hr. For short-term incubation, CMeC1 were plated, and on the following day, cells were treated as shown above (see *Reovirus replication*). Harvested cells were lysed at 4°C with NP40 lysis buffer.

These lysates were subjected to SDS-PAGE, and proteins then were transferred to Hybond PVDF membrane (GE Healthcare Bio-Sciences, Pittsburgh, PA). The membrane was blocked with Tris buffered saline (TBS) containing with 0.05% Tween20 (Polyoxyethylene sorbitane monolaureate) and 5% skim milk, followed by addition of the primary antibodies. Rabbit anti-PARP antibody (NeoMarkers, Fremont, CA) was used as primary antibody in Chapter 1. Mouse monoclonal anti-TLR3 antibody (40C1285.6) was obtained from Novus Biologicals (Littleton, CO). Mouse monoclonal anti-RIG-I antibody (D-12), mouse monoclonal anti-TRIF antibody (E-7), and mouse monoclonal anti-IRF3 antibody (D-3) were obtained from Santa Cruz Biotechnology. Rabbit polyclonal anti-MAVS antibody was obtained from Proteintech (Rosemont, IL). Rabbit monoclonal anti-phospho-IRF3 (Ser396) antibody (4D4G),

rabbit monoclonal anti-cleaved caspase-3 (Asp175) antibody, rabbit monoclonal anti-MDA-5 antibody (D74E4), and rabbit monoclonal anti-phospho-TBK1 (Ser172) antibody (D52C2) were obtained from Cell Signaling Technology (Danvers, MA). Theses primary antibodies were used in Chapter 2. Rabbit anti-PARP antibody and rabbit monoclonal anti-cleaved caspase-3 (Asp175) antibody were used in Chapter 3. The primary antibodies in Chapter 4 are listed in Table IV-1. Horseradish peroxidase (HRP) -conjugated goat anti-rabbit IgG (Jackson ImmunoResearch, West Grove, PA), HRP-conjugated goat anti-mouse IgG (Merck Millipore, Darmstadt, Germany) and rabbit anti-goat IgG HRP (Bethyl Laboratories, Montgomery, TX) were used as the secondary antibodies. Beta-actin and vinculin, housekeeping proteins, were used as a loading control, and were detected using mouse anti-beta-actin monoclonal antibody (Sigma-Aldrich Japan K.K), goat anti-beta-actin antibody (Santa Cruz Biotechnology) or mouse monoclonal anti-vinculin antibody (eBioscience). The labeled proteins were detected using the ECL reagent (PerkinElmer). The intensity of the bands was determined by ImageJ software ver. 1.48.

LysoTracker-Red staining

CMeC1 cells were cultured on microcover glasses (Matunami Garasu Kogyo, Osaka, Japan) in the wells of a 12-well plate. On the following day, cells were exposed to reovirus (MOI 100) for 1 hr at 4°C. Then, cells were washed and cultured in the presence of KU60019 (2.5 μM) for 24 hr at 37°C. After treatment, cells were incubated with LysoTracker-Red DND-99 (Invitrogen, Carlsbad, CA) for 30 min at 37°C, followed by fixation with 4% paraformaldehyde. The coverslips were mounted onto glass slides with Molecular Probes Prolong Gold with DAPI (Invitrogen) for staining of nuclei. Samples were visualized at a 100x magnification using LSM710 confocal microscope (Carl Zeiss, Oberkochen, Germany). Images were analyzed by using ZEN software 2012 (Carl Zeiss). The percentage of LysoTracker-Red-positive CMeC1 cells was quantified by flow cytometric analysis as described above.

Measurement of cathepsin B activity

Cathepsin activity was determined with a Cathepsin B Activity Assay Kit (PromoCell, Heidelberg, Germany), according to the manufacturer's instructions.

CMeC1 cells were cultured in 6-well plates. Then, cells were treated with reovirus (MOI 100) and KU60019 (2.5 μM) for 24 hr. After treatments, cells were lysed with CB Cell Lysis Buffer, followed by mixing with the CB Reaction Buffer. The cell lysate was incubated at 37°C for 1 hr with 200 μM CB Substrate Ac-RR-AFC. Cathepsin activity was measured in an ARVO X4 fluorometer (PerkinElmer). The fluorescence values were normalized to values obtained for a mock-treated sample after subtraction of background autofluorescence.

Co-immunoprecipitation of V-ATPase units

A plasmid encoding PA epitope-tagged-human V-ATPasse protein G1 (pMx-IP-PA-hATP6V1G1) was stably transfected into A549 cells using the retroviral method. Briefly, PLAT-GP packaging cells, kindly provided by Dr. T. Kitamura (The University of Tokyo), were transfected with either pMx-IP (empty vector) or pMx-IP-PA-hATP6V1G1 using the PEI transfection reagent (Polysciences, Inc., Warrington, PA) according to the manufacturer's instructions. After a 48-hr incubation, the supernatant containing the retrovirus was collected and added to A549 cells along with 5 μg/ml

polybrene (Sigma-Aldrich). Puromycin was used for selection and maintenance of A549 cells expressing the transfected V-ATPase-encoding gene. A549/ATP6V1G1 cells were seeded at 3 x10^6 cells per 10-cm dish. Then, cells were treated with reovirus (MOI 100) and KU60019 (2.5 μM) for 24 hr. Cells were harvested and lysed as described above. The PA-tag immunoprecipitation assay was performed as previously described (Fujii, Y. *et al*., 2014, Fujii, Y. *et al*., 2016), with modifications. Each lysate was transferred to a 1.5-ml microcentrifuge tube and incubated with the Sepharose-conjugated anti-PA-tag antibody (clone NZ-1), which was kindly provided by Dr. Kato (Tohoku University), on a rotating wheel for 1 hr at 4°C to immunoprecipitate the epitope-tagged ATP6V1G1 protein. The samples were washed five times with lysis buffer. SDS loading buffer with 2-mercaptoethanol was added to the sample, and the mixture then was heated to 100°C for 5 min. The proteins were separated on a 10-20% SDS-PAGE gel and analyzed by western blotting as above.

GST pull-down assay for Ras status

Ras activation status of the cell lines was evaluated with the GST pull-down

assay as previously reported (Hwang, CC. *et al*., 2013). Briefly, vector that expresses GST fused with Ras-binding domain (RBD) of Raf-1 was constructed. Then, *E. coli* competent cell JM109 was transformed with this vector and GST-RBD was extracted with lysis buffer. Extracted proteins from the cells were mixed with glutathione-sepharose 4B beads (GE Healthcare, Tokyo, Japan) for 1 hr before washing with lysis buffer. Ras activation status of each cell lines was evaluated after GST pull-down. Western blotting was carried out as previously described using mouse anti-pan-Ras (Calbiochem) and goat anti-mouse IgG HRP (Zymed Laboratories).

Tumor xenograft mouse experiment

In Chapter 2, Eight to 10-week-old NOD/ShiJic-scid (NOD/SCID) mice were obtained from Kyudo Co. Ltd. (Saga, Japan) and studies were conducted in a specific pathogen-free area in accordance with the Yamaguchi University Animal Care and Use guidelines. CHSSv1 cell line was a subline derived from the tumors established on the NOD/SCID mouse subcutaneously xenografted with CHSS. CHSSv1 (4.0×10^6 cells in PBS) were implanted subcutaneously into the right flank of the mice under general

anesthesia. After inoculation, the size of the mass was measured with caliper every other day. Tumor weight was estimated from calipers measurements of two perpendicular dimensions of the tumors in millimeters using the formula: *Tumor Volume (mm^3) = 1/2 x Length (mm) x $Width^2$ (mm^2)*. Once the size of the mass reached 200 mm^3, one group of mice (n = 8) was treated intratumorally with reovirus at 1.0 $x10^8$ PFUs, and another group of mice (n = 7) was treated intratumorally with PBS. Tumor growth was assessed until the experimental endpoint (20 days post-injection) was reached or when tumor volume was excess 1200 mm^3. For immunohistochemical staining, collected tumors were fixed in 10% neutral buffered formalin and embedded in paraffin. Then, deparafinized samples were treated with Target Retrieval Solution (Dako, Glostrup, Denmark). Sections were incubated with rabbit anti-reovirus polyclonal antibody (produced in our laboratory), followed by Histofine Simple Stain MAX-PO (Nichirei Biosciences, Tokyo, Japan). Slides were subjected to 3-3-diaminobenzidine tetrachloride (Roche Diagnostics K.K.) staining before counterstaining with Meyer's hematoxylin.

In Chapter 3, Eight to nine-week-old NOD/ShiJic-scid (NOD/SCID) mice

were obtained from Kyudo Co. Ltd. and studies were conducted in a specific pathogen-free area in accordance with the Yamaguchi University Animal Care and Use guidelines. CHMp-5b cells (1.0×10^7 in 50 µl PBS) were implanted subcutaneously into the right flank of the mice under general anesthesia (day 1). 1.0×10^8 PFUs of live reovirus (experimental group; three male and five female mice) or UV-inactivated reovirus (control group; two male and five female mice) in 20 µl PBS were injected intratumorally 14 days after tumor transplantation. Tumour growth was determined by measuring the tumor volume (described above) with a caliper every other day until euthanasia at day 21. The method for immunohistochemical staining was same as Chapter 2.

Statistical analysis

The significance of differences between samples were determined by the Student's t-test or one-way factorial ANOVA test followed by multiple comparison using Turkey-Kramer test. Differences were considered statistically significant if the *p* values were less than 0.05. Multiple comparison tests were performed using JMP

software ver. 9.0 (SAS Institute Japan, Tokyo, Japan).

Clinical study design

The study was conducted at the Yamaguchi University Animal Medical Center (YUAMEC) with approval from the Ethics Review Board of the Joint Faculty of Veterinary Medicine of Yamaguchi University. All dogs were enrolled and treated with reovirus from May 2013 to February 2017. This study was opened to all dogs fulfilling the eligibility criteria, which included a signed owner informed-consent, a confirmed tumor diagnosis, a tumor that allows measurement, and a life expectancy of at least a month with standard therapy. The study events are shown in Table V-1.

Clinical treatment

Reovirus serotype 3 Dearing produced for the usage as investigational products in human clinical trials (REOLYSIN®, registered USAN name: pelareorep) was kindly provided by Oncolytics Biotech Inc. of Calgary, Canada. Each vial contained 1 mL of 4.5×10^{10} $TCID_{50}$/ mL reovirus and the vials were stored at -80°C.

The frozen virus was thawed and diluted to pre-calculated concentrations immediately before use. Reovirus was administered as IT in all accessible and defined tumors while IV was used in dogs with non-surface and inaccessible tumors. Reovirus was diluted in normal saline in 1 mL volume for IT administration while in cases where reovirus was given IV, reovirus was diluted in 50 mL normal saline given over 2 hours in small breed dogs or in 200 mL normal saline given over 1 hour in large breed dogs. No prophylactic medication was administered. As reovirus is a live virus, strict precautions such as wearing disposable gowns, gloves and masks were taken by the investigators and authorized personnel during virus administration in a sterile and isolated environment.

Virologic studies

Serum, saliva, urine and feces were collected at various time points for the examination of reovirus particles using specific reverse transcriptase polymerase chain reaction (RT-PCR). In brief, RNA was extracted using ISOGEN-LS (Nippon Gene, Toyama, Japan) from 250 µl samples and RT-PCR was performed with One Step SYBR® PrimeScript™ PLUS RT-PCR Kit (Takara Bio, Shiga, Japan) using forward

primer 5'-TGGGACAACTTGAGACAGGA-3' and reverse primer 5'-CTGAAGTCCACCATTTTGAA-3' specific for the *S1* gene of reovirus serotype 3 (Decaro, N. *et al*., 2005). Qualitative detection of viral complementary DNA was performed by electrophoresis analysis in 2% agarose gel. Infectivity assay was carried out in RT-PCR positive samples by co-culture in reovirus-sensitive L929 cells to determine the presence of live virus (Yang, WQ. *et al*., 2004).

Neutralizing anti-reovirus antibody (NARA) assay

NARA assay (White, CL. *et al*., 2008) was performed to detect antibody titers at baseline (pre-treatment) and at selected time points post-treatment. In brief, 4-fold dilutions of serum were treated with a constant titer of reovirus known to cause 80% cell death on L929 cells. The serum-virus mix was incubated for 1 hour to allow antibodies in the serum to bind and neutralize the virus, before incubation with L929 cells for 2 hours. The inoculum was replaced with fresh medium and cell survival was measured by MTT assay. Naïve dog serum was used as control for each NARA assay. NARA titer was expressed as the last dilution, where any neutralization occurred before

cell killing was resumed to that seen in the virus-only treated controls.

Evaluation of study dogs

Assessment of AE was performed according to the Veterinary Cooperative Oncology Group- Common Terminology Criteria for Adverse Events (VCOG-CTCAE) v1.1 guidelines (2016). AE was monitored throughout the study by using methods such as reporting by owners, physical examination, hematology and blood biochemistry. Relevant palliative and/ or supportive treatments were given in response to the AE at the discretion of the investigators. The target and non-target tumors were measured by caliper or photography before and after treatment. Non-surface tumors and tumor metastasis were measured using ultrasound and computed tomography (CT).

Whenever the physical condition of the dogs allowed general or local anesthesia, tumor biopsy was taken upon owners' consent. Biopsy samples were fixed in 10% neutral buffered formalin and embedded in paraffin before hematoxylin and eosin (H&E) for histopathological analysis. Deparafinized samples were treated with Target Retrieval Solution (Dako) before treatment with 3% hydrogen peroxidase and Protein

Block (Dako). Sections were incubated with rabbit anti-reovirus polyclonal antibody (1:500 dilution; produced in our laboratory) or rabbit immunoglobulin fraction of serum from non-immunized rabbit (isotype control; FLEX by Dako), followed by Histofine Simple Stain MAX-PO (Nichirei Biosciences). Slides were subjected to 3,3-diaminobenzidine tetrachloride (Roche Diagnostics K.K.) staining before counterstaining with Meyer’s hematoxylin. Reovirus-treated tumor samples from MCT xenograft mouse model were used as positive control (Hwang, CC. *et al*., 2013).

Chapter 1

The oncolytics effects of reovirus in canine solid tumor cell lines

SUMMARY

Oncolytic virotherapy is a new strategy for cancer treatment for humans and dogs. Reovirus has been proven to be a potent oncolytic virus in human medicine. Our laboratory has previously reported that canine mast cell tumor and canine lymphoma were susceptible to reovirus. In this chapter, canine solid tumor cell lines (mammary gland tumor, osteosarcoma and malignant melanoma) were tested to determine their susceptibility towards reovirus. I demonstrated that reovirus induces more than 50% cell death in three canine mammary gland tumor and one canine malignant melanoma cell line. The reovirus-induced cell death occurred via the activation of caspase 3. Ras activation has been shown to be one of the important mechanisms of reovirus-susceptibility in human cancers. However, Ras activation was not related to the reovirus-susceptibility in canine solid tumor cell lines, which was similar to reports in canine mast cell tumor and canine lymphoma. The results of this study highly suggest that canine mammary gland tumor and canine malignant melanoma are also potential candidates for reovirus therapy in veterinary oncology.

RESULTS

Inhibition of cell proliferation by reovirus in a dose-dependent manner

Firstly, examination of the susceptibility of canine solid tumors towards reovirus was conducted by infecting canine MGT, osteosarcoma and malignant melanoma cell lines with reovirus at various levels of MOI, and the inhibition of cell proliferation was assessed at 72 hpi using MTT assay (Fig. I-1). The results revealed that reovirus susceptibility varied among the cell lines.

Reovirus infection at a very high MOI of 1000 induced tremendous cell death in all the MGT cell lines except CTB-m (Fig. I-1A). At a lower MOI of 10, three of the MGT cell lines showed more than 50% of inhibition of cell growth, but the other four cell lines were less susceptible. Generally, canine osteosarcoma cell lines showed a lower susceptibility towards reovirus as compared to MGT and malignant melanoma (Fig. I-1B). The most reovirus-susceptible canine osteosarcoma cell lines, Abrams, MacKinley and Moresco, only showed approximately 50% inhibition of cell growth at MOI 1000, and all the other cell lines seemed to be minimally susceptible to reovirus at MOI 10.

As for canine malignant melanoma, all of the cell lines were highly susceptible to reovirus at MOI 1000 (Fig. I-1C). CMGD2 showed predominant growth inhibition at MOI as low as 1. In contrast, LMeC was not susceptible to reovirus at MOI of lower than 100. CMeC1 and KMeC were more susceptible to reovirus than CMeC2 and CMGD5. These results suggest that canine osteosarcoma cell lines are relatively non-susceptible to reovirus infection, but some of the MGT and malignant melanoma cell lines are highly susceptible to reovirus in a dose-dependent manner.

Reovirus-induced cytotoxicity

MTT assay quantifies the inhibition of cell proliferation through the reduction of total mitochondrial activity (van Meerloo, J. *et al*., 2011). In order to examine the reovirus-induced cell death directly, all the canine solid tumor cell lines were infected with reovirus at MOI 70, which is the titer of virus used for the cytotoxicity assay in mast cell tumor cell lines and lymphoma cell lines in our previous report (Hwang, CC. *et al*., 2013, Hwang, CC. *et al*., 2014), before trypan blue exclusion test was carried out to quantify the proportion of live and dead cells (Fig. I-2). The percentages of reovirus-

induced cell death assessed by the trypan blue exclusion test were consistent with the percentage of inhibition of cell proliferation by reovirus. These results indicate that the inhibition of cell proliferation by reovirus is mainly due to cell death.

Reovirus infectivity and production of reoviral progeny

Reovirus infectivity in the involved cancer cell lines was quantified by flow cytometric analysis of intracellular viral protein (Fig. I-3). In CTB-m and Gracie, reovirus proteins were not detected by flow cytometry, which was consistent with the low cytotoxicity in the reovirus-infected cell lines. However, reoviral proteins were detected in the cytoplasm of some of the cell lines, such as Abrams, D17, CMeC2 and LMeC, even though they showed low cytotoxicity after reovirus infection. Reoviral proteins were detected in all the other cell lines at various levels. Although there were some exceptions, the combination of these results shows that the detection of reoviral proteins correlates with the reovirus-induced cell death.

In order to determine if reovirus-susceptible cell lines can support viral production, I measured the amount of viral progeny by $TCID_{50}$ assay. Fig. I-4 represents

the fold increase of viral titer as compared with input viral titer in the culture supernatant. Increment of titer in culture supernatant from reovirus-infected CTB-p, CTB-m, and Gracie cells showed less than 1, which suggested that these cell lines did not produce any virus. The remaining cell lines produced a certain amount of viral progeny, which were consistent with the detection of viral proteins and reovirus-induced cell death. Among the less susceptible canine MGT cell lines, reoviral proteins were detected in CTB-p (Fig. I-3), even though it did not support any production of viral progeny (Fig. I-4). Canine MGT cell line CTB-m and canine osteosarcoma cell line Gracie had a no increment of reovirus titer, which were consistent with no detection of reoviral proteins (Fig. I-3). The canine osteosarcoma and malignant melanoma cell lines (Abrams, D17, CMeC2, and LMeC) were less susceptible to reovirus, but produced viral progeny after reovirus infection, which was consistent with detection of viral proteins by flow cytometry in all these cell lines. These results indicate that viral proteins and the production of viral progeny can be detected not only in cell lines highly susceptible, but also in some of the cell lines less susceptible to reovirus.

PARP cleavage as indicator of apoptosis induced by reovirus

Previous reports have shown that reovirus-induced cell death was due to apoptosis (Clarke, P. *et al*., 2004, Connolly, JL. *et al*., 2000, Hwang, CC. *et al*., 2013). Therefore, I investigated the cleavage of PARP, which is a hallmark of caspase-dependent apoptosis, in reovirus-infected canine MGT, osteosarcoma and malignant melanoma cell lines. The most reovirus-susceptible (CNM-m, MacKinley and CMGD2) and the least reovirus-susceptible cell line (CTB-m, Gracie and LMeC) were chosen from each of the tumor type (Fig. I-5). Prominent cleaved product was detected at 48 hpi in all of the cell lines highly susceptible to reovirus. No cleaved bands were observed in reovirus-infected CTB-m and Gracie at 48 hpi but surprisingly, cleaved PARP was detected in LMeC, which is less susceptible to reovirus.

Lack of correlation between Ras activation status and reovirus susceptibility

The baseline GTP-loading status of Ras among the cell lines involved in this study was determined in order to investigate the involvement of Ras activation as the molecular determinant for reovirus susceptibility. In canine MGT, CHM-p and CHM-m

have elevated Ras activities while Ras activation was not detected in the other cell lines (Fig. I-6A). Among the canine osteosarcoma cell lines, GTP-bound Ras was highly expressed only in D17 and Gracie (Fig. I-6B). In canine malignant melanoma, CMeC1, CMeC2 and LMeC have elevated Ras activities, as compared to CMGD2, CMGD5 and KMeC (Fig. I-6C). The collection of these results indicates that reovirus susceptibility is not correlated to the baseline status of Ras activation status among the canine solid tumor cell lines.

DISCUSSION

Our laboratory has previously reported that canine mast cell tumors are highly susceptible to reovirus infection (Hwang, CC. *et al*., 2013) but reovirus-susceptibility is less among the canine lymphoma cell lines (Hwang, CC. *et al*., 2014). In current human clinical studies using reovirus, solid tumors are the main targets (Vacchelli, E. *et al*., 2013). Thus, I focused on a panel of canine tumor cell lines established from solid tumors and tested their susceptibility towards the effects of reovirus. Due to the limited availability of cell lines in the veterinary field, solid tumor cell lines established from MGT, osteosarcoma and malignant melanoma were chosen in this study (Table I-1).

A total of six canine MGT cell lines, two canine osteosarcoma cell lines and four canine malignant melanoma cell lines were susceptible to reovirus, where more than 20% of the cells were killed after reovirus infection (Fig. I-2). Among the three types of canine tumors, the osteosarcoma cell lines were relatively less susceptible to reovirus infection. On the other hand, the canine MGT and malignant melanoma cell lines were mostly susceptible to reovirus. Similarly, human breast cancer cell lines and malignant melanoma cell lines have been shown to be susceptible to reovirus

(Errington, F. *et al*., 2008, Norman, KL. *et al*., 2002) and phase II clinical trials involving patients with breast cancer and malignant melanoma have been conducted (Vacchelli, E. *et al*., 2013). From the results of this study, it is suggested that canine MGT and malignant melanoma are potential candidates for reovirus treatment, but not so in osteosarcoma (Table I-1).

Flow cytometric analysis (Fig. I-3) showed that reovirus proteins were detected in most of the cell lines except in CTB-m and Gracie, which are less susceptible to reovirus infection. Generally, the results of the production viral progeny correlated with the detection of viral proteins among the cell lines, but not in CTB-p, where viral proteins were detected even though there was no production of viral progeny. In normal cases, reovirus infection should occur first before virus replication and cell death. However, in this study, reovirus infection and cell death took place without virus replication in CTB-p, which is inconsistent with the other results. Our hypothesis is that CTB-p might have a low efficiency in virus replication and/ or virus release from cells, leading to the low virus titer detected in the cell culture supernatant. However, this hypothesis remains to be proven and requires further investigation.

In order to elucidate the mechanism of cell death induced by reovirus in the canine solid tumor cell lines, PARP cleavage was examined in the most reovirus-susceptible and the least reovirus-susceptible cell line from each of the tumor type. My data showed that cell death in the cell lines most susceptible to reovirus, CNM-m, MacKinley, and CMGD2, was accompanied with PARP cleavage, indicating that reovirus induces cell death through a caspase-dependent manner (Fig. I-5), consistent with previous reports (Hwang, CC. *et al*., 2013, Marcato, P. *et al*., 2007). Among the three cell lines that were the least susceptible to reovirus, an unexpected result was discovered, where the cleavage of PARP was detected in LMeC. In order to confirm that PARP cleavage occurs with caspase 3 activation in LMeC, I examined the cleavage of caspase 3 with Western blotting. My results confirmed that caspase 3 was cleaved and therefore, activated after reovirus infection took place in LMeC (data not shown). Hence, I came to a conclusion that there possibly exists a mechanism where apoptotic cell death can be prevented in LMeC even with the activation of caspase 3. However, this phenomenon remains a mystery until further investigation.

Initial studies involving reovirus as an oncolytic virus have proven that

reovirus-induced cytotoxicity was observed in Ras-transformed cells but not in untransformed cells (Shmulevitz, M. *et al*., 2005, Strong, JE. *et al*., 1998). On top of that, various reports have cited that the activation of Ras signaling pathway plays a key role in enhancing reovirus disassembly, infectivity, viral replication and production viral progeny (Alain, T. *et al*., 2007, Marcato, P. *et al*., 2007, Shmulevitz, M. *et al*., 2010). In this study, the results showed that profound activation of Ras was observed in CHM-p, CHM-m, D17, Gracie, CMeC1, CMeC2, and LMeC as compared to Raji, which was used as a control for Ras activation. Among the cell lines with elevated Ras activities, D17 and Gracie are the least susceptible to reovirus infection. On the other hand, CIP-p, CIP-m, CTB-p, CNM-m, MacKinley, Moresco, KMeC and CMGD2, that have low or no expression of Ras activity, are highly susceptible to reovirus. These discrepancies were also observed in some of the human cancers (Sei, S. *et al*., 2009, Thirukkumaran, CM. *et al*., 2003, Twigger, K. *et al*., 2012, van Houdt, WJ. *et al*., 2008), canine mast cell tumor (Hwang, CC. *et al*., 2013) and canine lymphoma (Hwang, CC. *et al*., 2014). Indeed, I cannot completely deny that there exist other mechanisms of reovirus susceptibility besides the Ras signaling pathway. From my data, elevated Ras

activity has failed to serve as a predictive marker to define the susceptibility of a tumor cell line towards reovirus. Further studies need to be performed to elucidate the alternative mechanism(s) that is involved en route to discovering the molecular determinant of reovirus susceptibility.

Reovirus serves as an attractive option in cancer therapy. Besides the influenza-like symptoms, the side effects of using reovirus as a treatment for cancers are minimal (Rosen, L. *et al*., 1963). From the results of this study, it seems like reovirus as a monotherapy for cancers has limited efficacy. Different approaches using combination of reovirus with radiation or chemotherapy has been tested human clinical trials (Vacchelli, E. *et al*., 2013). Therefore, in order to increase the oncolytic effects of reovirus in canine MGT, osteosarcoma and malignant melanoma, further investigations on the synergistic effects of reovirus and chemotherapeutic agents in these canine cancers are currently being carried out.

In summary, this study suggested that reovirus is a potent oncolytic virotherapy in canine solid tumors such as MGT and malignant melanoma. However, I was unable to completely elucidate the mechanism of reovirus-induced cell death in

these cell lines. I wasalso unable to identify the molecular determinant of reovirus susceptibility in canine solid tumors in this study.

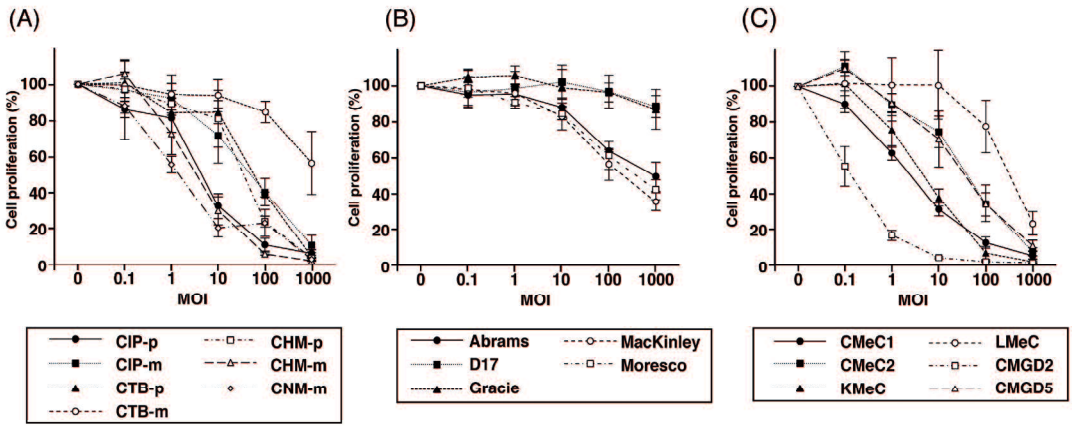

Fig. I-1. Cell proliferation of canine solid tumor cell lines infected with reovirus.

Canine mammary gland tumor (MGT) (A), osteosarcoma (B) and malignant melanoma (C) cell lines in triplicate wells were mock-infected or infected with reovirus at the indicated MOI. After 72 hours post-infection (hpi), cell proliferation was quantified by MTT assay. Mean ± SD, n=3.

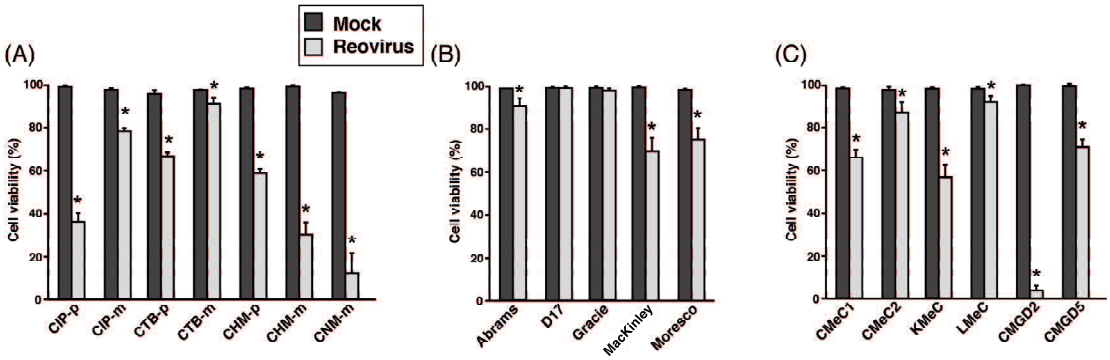

Fig. I-2. Cell viability of canine solid tumor cell lines infected with reovirus.

Canine MGT (A), osteosarcoma (B) and malignant melanoma (C) cell lines in triplicate wells were mock-infected or infected with reovirus at MOI 70. After 72 hpi, cell viability was quantified by trypan blue exclusion test. Mean ± SD, n=3, $*p < 0.05$.

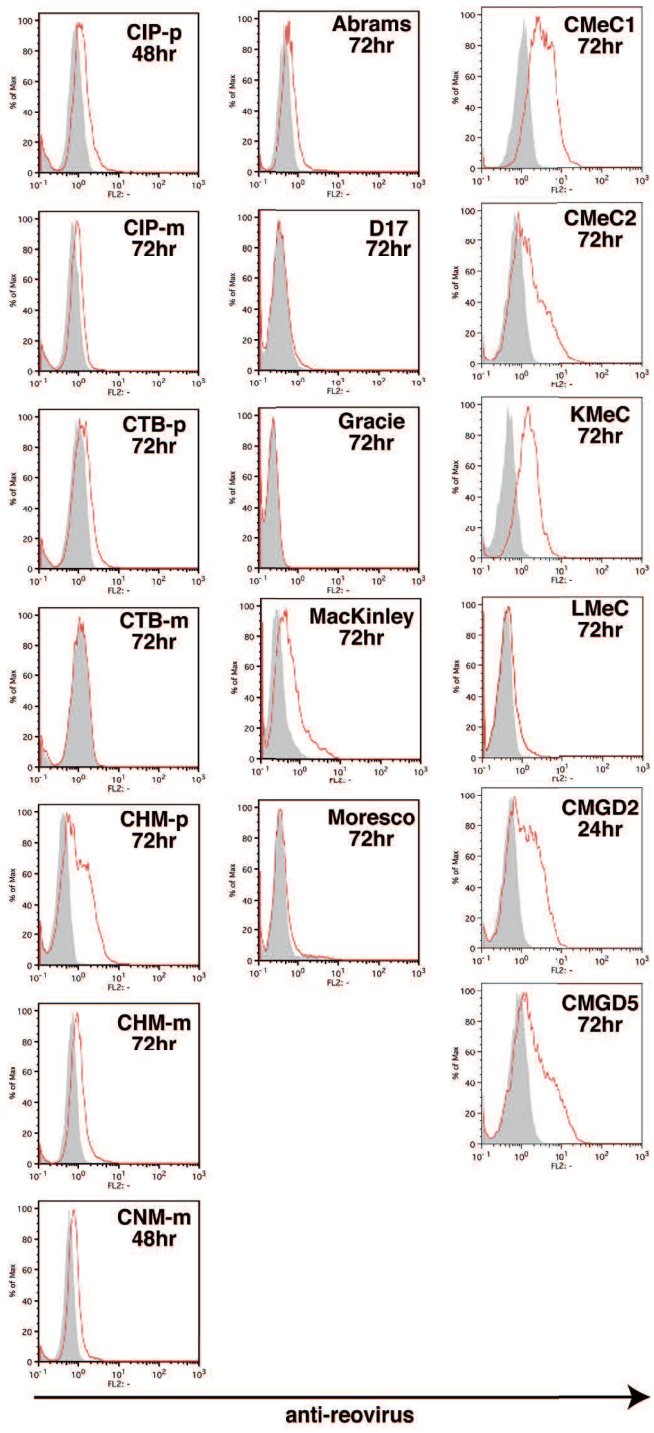

Fig. I-3. Reovirus infectivity in canine solid tumor cell lines.

Canine MGT (A), osteosarcoma (B) and malignant melanoma (C) cell lines were infected with reovirus at MOI 70. Reovirus-infected CMGD2 was harvested at 24 hpi.

CIP-p and CNM-m were harvested at 48 hpi. All remaining cell lines were harvested at 72 hpi. Cells were stained with rabbit polyclonal anti-reovirus antibody and analyzed by flow cytometry. The shaded regions and regions below the red line in the histograms indicate staining with isotype control and anti-reovirus antibody, respectively. Results shown are representatives from a minimal of two repeats.

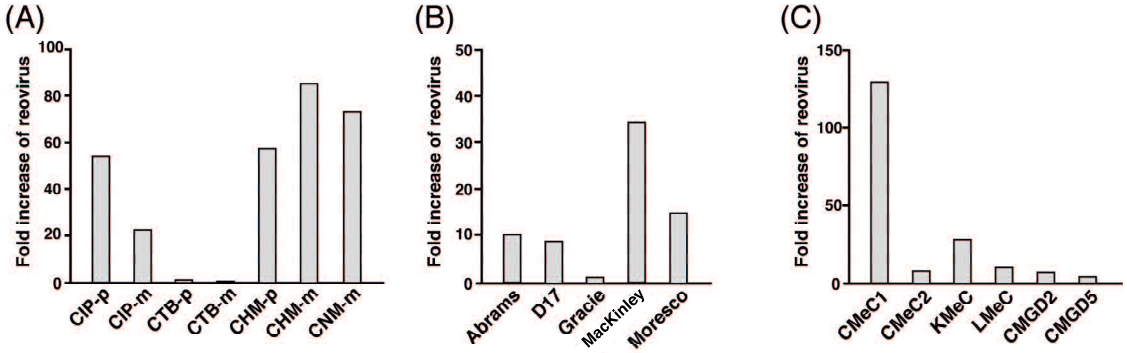

Fig. I-4. Production of viral progeny in reovirus-infected canine solid tumor cell lines. Supernatant of reovirus-infected (MOI 70) canine MGT (A), osteosarcoma (B) and malignant melanoma (C) cell lines was harvested at 72 hpi, and virus titer were determined by $TCID_{50}$ assay. The fold increase of reovirus represents the mean values calculated from the titer of progeny virus divided by the titer of input virus from three independent experiments.

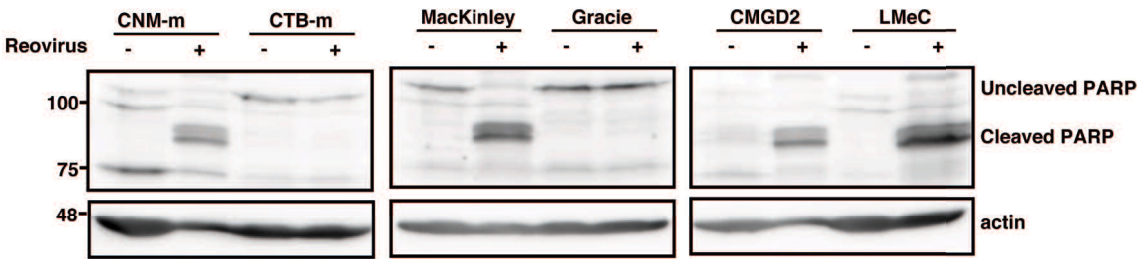

Fig. I-5. Poly (ADP-Ribose) Polymerase (PARP) cleavage in selected canine solid tumor cell lines after reovirus infection.

Whole cell lysates were prepared from mock-infected or reovirus-infected (MOI 70) CNM-m, CTB-m, MacKinley, Gracie, CMGD2 and LMeC at 48 hpi. Proteins were separated with SDS-PAGE before the cleavage of PARP was determined using Western blotting with anti-PARP antibody. Beta-actin was used as protein loading controls. Results shown are representatives from a minimal of two repeats.

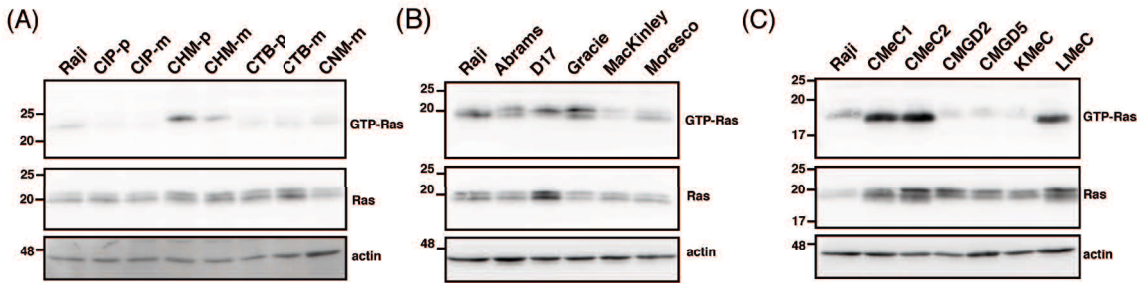

Fig. I-6. Ras activation status in canine solid tumor cell lines.

Ras-GTP from cell lysates of canine solid tumor cell lines was affinity-precipitated with GST-RBD protein. The affinity-precipitated Ras-GTP was subjected to SDS-PAGE, followed by Western blotting with anti-Ras antibody. Results shown are representatives from two repeats.

Table I-1. Summary of the effects of reovirus in canine tumor cell lines

tumor type	Cell line	Reovirus susceptibility[a]	Viral protein detection[b]	Viral progeny production[c]	Ras activation
MGT	CIPp	++	++	+++	−
	CIPm	+	++	+++	−
	CTBp	+	++	−	−
	CTBm	−	−	−	−
	CHMp	+	++	+++	+
	CHMm	++	++	+++	+
	CNMm	++	++	+++	−
OS	Abrams	−	++	+++	+
	D17	−	+	++	+
	Gracie	−	−	−	+
	Mackinley	+	++	+++	−
	Moresco	+	+	+++	−
MM	CMeC1	+	++	+++	++
	CMeC2	−	++	++	++
	KMeC	+	++	+++	−
	LMeC	−	+	++	++
	CMGD2	++	++	++	−
	CMGD5	+	++	+	−

[a] Reovirus susceptibility: − No significant difference between cell viability of mock and reovirus-infected cells; − <20% cell death; + 20–50% cell death; ++ >50% cell death.

[b] Viral protein detection: − No virus detection, + partly positive staining to viral protein; ++ positive staining to viral protein.

[c] Viral progeny production: − No increment as compared to input virus titer, + <5x increment of virus titer; ++ 5–10x increment of virus titer; +++ >10x increment of virus titer.

Chapter 2

The oncolytic effects of reovirus in canine histiocytic sarcoma cell lines

SUMMARY

Histiocytic sarcoma is rare and an aggressive fatal neoplastic disease with a poor prognosis in human. Dogs occur the spontaneously histiocytic sarcoma, which shows similar characteristic of disease in human. Therefore, the research of canine histiocytic sarcoma may be available as a translational model of human. In the current study, oncolytic reovirus has demonstrated preclinical and early clinical activity in human and canine cancers. However, anti-tumor effects of reovirus against histiocytic sarcoma are unknown. Here, I show that reovirus has oncolytic activity in canine histiocytic sarcoma cell lines *in vitro* and *in vivo* in Chapter 2. I found *in vitro* assay that reovirus can replicate and induce caspase-dependent apoptosis in canine histiocytic sarcoma. A single intra-tumor injection of reovirus suppresses the growth of subcutaneous tumor completely in NOD/SCID mice. Additionally, I demonstrate that cells highly expressed innate immune responses by reovirus infection were resistant to reovirus-induced cell death. In conclusion, oncolytic reovirus appears to be effective treatment options of histiocytic sarcoma, and warrants further investigation in early clinical trials.

RESULTS

Reovirus suppresses the cell proliferation in canine histiocytic sarcoma cell lines without correlation to Ras activation status

Firstly, susceptibility of canine histiocytic sarcoma cell lines to reovirus was examined by MTT assay. After 72 hours post-infection of reovirus (MOI 0.1, 1, and 10), the cell growth of all cell lines was suppressed in a dose-dependent manner (Fig. II-1A). CHSA, CHSS and CMHM showed more than 70% of inhibition of cell growth at MOI 10. In contrast, MHT-2 showed approximately 30% of inhibition at same titer, suggesting MHT-2 had a low sensitivity compared to other cell lines. And, the degree of cell viability was consistent with that of cell growth inhibition (Fig. II-2C).

The baseline GTP-loading status of Ras was determined to investigate the involvement of Ras activation as the molecular determinant for reovirus susceptibility in canine histiocytic sarcoma cell lines. Using Raji as the comparison for Ras activation (Igase, M. *et al*., 2015 (Chapter 1), Hwang, CC. *et al*., 2013, Hwang, CC. *et al*., 2016, Igase, M. *et al*., 2016 (Chapter 3)), all cell lines had Ras activation to some extent (Fig. II-1B), and of the four cell lines, MHT-2 expressed the highest GTP-bound Ras levels.

Comparing the susceptibility of each cell line to reovirus with their activated Ras status, this experiment clarified that there was not correlated.

Reovirus induced caspase-dependent apoptosis in canine histiocytic sarcoma cell lines

Our previous reports showed that caspase-dependent apoptosis was one of the mechanisms of reovirus-induced cell death in canine cancer cell lines (Igase, M. *et al*., 2015 (Chapter 1), Hwang, CC. *et al*., 2013, Hwang, CC. *et al*., 2016, Igase, M. *et al*., 2016 (Chapter 3)). Therefore, PE-Annexin V/ 7-AAD assay was carried out to confirm that the reovirus-induced cell death was apoptosis in canine histiocytic sarcoma cell lines (Fig. II-2A). After 48 hours post-infection of reovirus, all cell lines except MHT-2 showed that the percentages of early apoptotic cells (A+/7-AAD-) significantly increased as compared to mock infection. Moreover, in reovirus-infected CHSS, late apoptotic cells (A+/7-AAD+) were predominantly observed, and this indicated that cell death of CHSS started earlier than that of other cell lines.

Next, to evaluate the caspase activation, western blot analysis was performed

using anti-cleaved caspase-3 antibody, which was indicator of apoptosis. As shown in Fig. II-2B, cleaved caspase-3 was shown in all cell lines at 48 hours. In addition, to confirm that the cell death was occurred via caspase signaling pathway, each cell line was pre-treated with pan-caspase inhibitor, Z-VAD-FMK, before infection with reovirus (MOI 10). Trypan blue test showed that the reovirus-induced cytotoxicity was reversed by Z-VAD-FMK in all cell lines. In CMHM and MHT-2, cell death was almost completely inhibited, however, in CHSA and CHSS, approximately 50% of the cell death was inhibited (Fig. II-2C). These data revealed that reovirus infection induced apoptosis via caspase signaling pathway in canine histiocytic sarcoma cell lines, which were consistent with other canine tumor cell lines shown in our previous reports (Igase, M. *et al*., 2015 (Chapter 1), Hwang, CC. *et al*., 2013, Hwang, CC. *et al*., 2016, Igase, M. *et al*., 2016 (Chapter 3)).

Expression of viral structural proteins and production of progeny were caused by reovirus infection

To confirm the infectivity and replication of reovirus, reoviral structural

proteins were examined in canine histiocytic sarcoma cell lines after infection by western blotting. After 24 and 48 hours post-infection of reovirus (MOI 10), the synthesis of reoviral proteins was detected in all cell lines (Fig. II-3A).

The viral progeny was measured by $TCID_{50}$ assay to prove production of reovirus (as shown in Chapter 1). The viral progeny titer was dramatically increased in CHSA, CHSS and CMHM, but not in MHT-2 (Fig. II-3B). From these results, reovirus could replicate in all cell lines, but release of progeny was not observed in MHT-2. These data suggested that the released viruses might be attributed to the cytotoxicity induced by reovirus infection.

Low susceptibility of reovirus in canine immature dendritic cells

To assess the cytotoxicity of reovirus to normal cells, immature dendritic cells differentiated from PBMC were infected by reovirus (MOI 10), and cytotoxicity assay was performed after 72 hours post-infection. As a result, cell death by reovirus was not observed in immature dendritic cells derived from normal healthy dogs (Fig. II-4).

The gene expression of type I interferon was enhanced by reovirus infection

Previous works showed that mammalian reovirus was sensed by both Toll like receptor 3 (TLR3) and the RIG-I like receptor (RLR) pathway and activated host innate immune response such as type I interferon (Stanifer, ML. *et al*., 2016, Holm, GH. *et al*., 2007). It is widely accepted that innate immune response protects normal cells from virus replication (Akira, S. *et al*., 2006). In contrast to normal cells, dysfunction of innate immunity occurs during the evolution of cancers (Linge, C. *et al*., 1995, Matin, SF. *et al*., 2001, Sun, WH. *et al*., 1998). However, the precise mechanism between the production of interferon and the susceptibility of reovirus remains unknown. At first, to monitor the immune response in canine histiocytic sarcoma cell lines and normal DCs after reovirus infection, real-time PCR analysis was performed. Two kinds of reference genes, *RPL13A* and *HPRT*, were used, however only *RPL13A*, whose expression was more stable among the samples, was used for normalization of each gene. After 24 hours post-infection, the expression of *IFN-α* and *IFN-β* mRNAs in all cell lines except CMHM was significantly up-regulated by reovirus (Fig. II-5A, 5B). In particular, the immune response to reovirus in MHT-2 and normal DCs seemed to be stronger than

other cell lines. In contrast, the expression level of those genes after reovirus infection was very low in CMHM, which possibly have the dysfunction of innate immune response. This result showed that the expression levels of type I interferon were higher in reovirus-resistant cells than in reovirus-susceptible cells.

The molecular mechanism of the innate immune response in canine histiocytic sarcoma cell lines

Many genes are known to be involved in innate immune response in double-strand RNA virus-infected cells (Akira, S. *et al*., 2006). When RNA virus incorporates into cells, viral RNA is initially recognized by TLR3 or RIG-I. Mitochondrial antiviral-signaling protein (MAVS) and TRIF work in the virus-infected cells as an innate immune adapter protein. And, phosphorylation of MAVS and TRIF induces the IRF3 activation, which has a role in transcription of interferons (Liu, S. *et al*., 2015). To assess the molecular differences between reovirus-susceptible and reovirus-resistant cells, we first examined the expression of these genes. The expression of these proteins was observed in all histiocytic sarcoma cell lines, but RIG-I was expressed only in

CHSA (Fig. II-7A). In normal DCs, all these proteins except MAVS were expressed (Fig. II-7B). As same as CHSA, RIG-I was expressed in normal DCs (Fig. II-7B). Although RIG-I was not expressed on three canine histiocytic sarcoma cell lines (CHSS, CMHM, and MHT-2) in the uninfected culture condition, poly IC, analogs of dsRNA, treatment induced the expression of RIG-I in both of CHSS and MHT-2, but not CMHM (Fig. II-7C). In addition, IRF3 activation was induced by poly IC treatment in all cell lines except CMHM (Fig. II-7C). This result indicated that CMHM had defect in innate immune system, probably due to the lack of RIG-I expression.

Melanoma differentiation associated gene 5 (MDA5) is the sensor of viral RNA in cytoplasm as similar to RIG-I (Kang, DC. *et al*., 2002). TBK1 and IKKα/β are downstream signaling mediators of innate immune response (Akira, S. *et al*., 2006). In order to determine whether reovirus induced the interferon response in canine histiocytic sarcoma cells, I monitored IRF3 phosphorylation, RIG-I up-regulation and other innate immune signaling molecules (MDA5, TBK1, IKKα/β) expression over the time course by western blotting. Western blotting analysis showed that reovirus induced the phosphorylation of IRF3 in CHSS and MHT-2 until 24 hours post-infection, but

RIG-I was up-regulated in all cell lines except CMHM (Fig. II-6). In addition, the expression of MDA5 was induced by reovirus infection in all cell lines. I also found that reovirus infection phosphorylated TBK1 in all cell lines, but not IKKα/β. However, among histiocytic sarcoma cell lines, MHT-2 demonstrated that reovirus infection strongly triggered the response of innate immunity as compared to other cell lines, supporting the results of Fig. II-5A and B.

From these results, canine histiocytic sarcoma cells may impair the activity of innate immune responses during the tumorigenic transformation.

Reovirus injection regressed the tumor growth in CHSSv1 xenograft mouse models

In order to show the effect of reovirus using *in vivo* anti-tumor potential of reovirus, CHSSv1 (derived from CHSS) subcutaneous xenograft model was established in severe immunodeficiency (NOD/SCID) mice and treated intratumorally with a single injection of reovirus. All mice were treated with reovirus or PBS after the size of mass reached 200 mm^3. Tumor growth was suppressed completely after single injection of reovirus in all treated mice, as compared to PBS-treated mice (Fig. II-5A). However,

black tail syndrome, which reported as a possible side effect (Hwang, CC. *et al*., 2013, Loken, SD. *et al*., 2004), was observed in four out of eight reovirus-injected NOD/SCID mice. The result of IHC staining for reoviral proteins showed the infection of reovirus in the reovirus-injected tumor (Fig. II-5B). These results indicated that reovirus infected the canine histiocytic sarcoma cells and suppressed the growth of mass *in vivo*.

DISCUSSION

The development of oncolytic reovirus as a cancer therapy has been currently expanded in human and dogs (Hwang, CC. *et al*., 2018 (Chapter 5), Clements, D. *et al*., 2014). However, reovirus therapy against rare tumors such as histiocytic sarcoma and angiosarcoma has not been investigated in human medicine, as well as veterinary medicine. In the present study, I examined the effects of oncolytic reovirus in four canine histiocytic sarcoma cell lines *in vitro* and *in vivo*. In addition, I evaluated the innate immune response induced by reovirus infection in canine histiocytic sarcoma cell lines as compared to normal DCs.

As a result of *in vitro* study, I found that three out of four cell lines were strongly susceptible to reovirus without correlation to Ras activation status. In the PE-Annexin V/7-AAD assay, all cell lines except MHT-2 showed the increase of apoptotic fraction after 48 hours post-infection of reovirus, as shown in Fig. II-2A. However, in all cell lines including MHT-2, caspase-3 was activated. In addition to caspase-3 activation, I found that the reovirus-induced cytotoxicity was reversed by Z-VAD-FMK in all cell lines. Although the reason why PE-Annexin V/ 7-AAD assay did not detect

the apoptosis in MHT-2 remains unknown, this may reflect the low sensitivity of Annexin V because the degree of reovirus-induced cell death was low at the time point of analysis in MHT-2. In consideration of these results, I observed that reovirus induced the caspase-dependent apoptosis in canine histiocytic sarcoma cell lines, consistent with our previous reports (Igase, M. *et al*., 2015 (Chapter 1), Hwang, CC. *et al*., 2013, Hwang, CC. *et al*., 2016, Igase, M. *et al*., 2016 (Chapter 3)).

MHT-2 showed the lowest amount of progeny virus, which is consistent with lowest susceptibility of reovirus. Other three cell lines showed the high increment of progeny virus, but its degree differed by each cell line. Although few progeny of reovirus was observed in MHT-2, the synthesis of reovirus structure proteins was observed at 24 and 48 hours after infection. I obtained the similar result in Chapter 1 using one of canine mammary gland tumor cell lines, CTB-p. I have proposed a hypothesis that CTB-p might have a low efficiency in virus release from cells, which leads to the lower production of progeny virus detected in the culture supernatant. The present case of MHT-2 was similar to our previous result. From these results, it is implied that production of reovirus is correlated to reovirus susceptibility in canine

histiocytic sarcoma cell lines. Still, further studies will be necessary to prove those correlations.

Histiocytic sarcoma is originated from a histiocytic lineage including dendritic cells in dogs as well as human (Moore, PF., 2014, Emile, JF. *et al*., 2016). The cell death was not observed in the immature DCs differentiated from PBMC of normal healthy beagles in this study. This result was consistent with the previous studies, in which reovirus families including mammalian reovirus and rotavirus can infect and stimulate human immature dendritic cells, but not induce cell death (Errington, F. *et al*., 2008, Narvaez, C. *et al*., 2005, Ilett, EJ. *et al*., 2011). In addition, canine immature dendritic cells strongly induced type I interferon by reovirus infection without showing any cytotoxicity, which is also consistent with previous reports that reovirus-infected immature dendritic cells are activated the production of proinflammatory cytokines type I interferon, TNF-alpha, and IL-6, because reovirus does not inhibit the DC maturation and function. However, in contrast to dendritic cells, the innate immune response was weaker in all canine histiocytic sarcoma cell lines except for MHT-2. From western blotting results of Fig. II-7 and Fig. II-6, we revealed that canine histiocytic sarcoma

cell lines were not capable of activating innate immunity by reovirus even though TLR3 agonist poly IC could induce the phosphorylation of IRF3 in all lines excepting CMHM. Therefore, canine histiocytic sarcoma may lack the mechanism of innate immunity against reovirus, or reovirus proteins themselves may suppress the activation of innate immune response. However, these possibilities remain to be proven and requires further investigation.

Consistent with *in vitro* study, the *in vivo* study demonstrated that reovirus injection suppressed the tumor growth completely in the canine xenograft mouse model using CHSSv1. This data proposes that oncolytic reovirus has potential to become one of the therapeutic options for canine histiocytic sarcoma.

In conclusion, my results suggested that canine histiocytic sarcoma cell lines were very susceptible to oncolytic reovirus *in vitro* and *in vivo*. Although the robust correlation between the innate immune response and reovirus cytotoxicity remains unknown, cells highly expressed type I interferon by reovirus infection were resistant to reovirus-induced cell death. Histiocytic sarcoma is rare, aggressive and high mortality in human (Dalia, S. *et al*., 2014, Pileri, SA. *et al*., 2002). Therefore, my study using

canine histiocytic sarcoma might be translated to human clinical trials for oncolytic virotherapy. In addition, in the future, I hope that expression profiling for innate immune molecules can be used to determine the suitability of oncolytic reovirus for cancer therapy in dogs with histiocytic sarcoma.

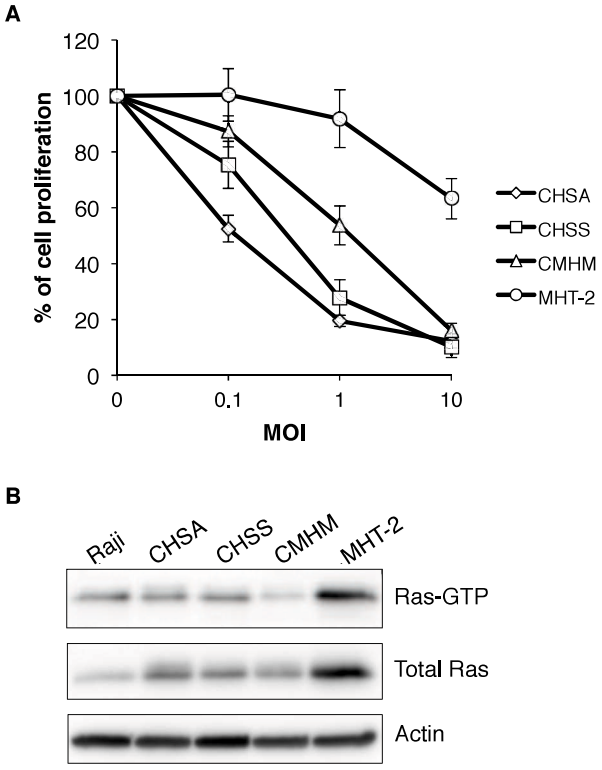

Fig. II-1. Canine histiocytic sarcoma cell lines are susceptible to reovirus, but not correlated to Ras status

(A) Four canine histiocytic sarcoma cell lines (CHSA, CHSS, CMHM, and MHT-2) in triplicates were mock or infected with reovirus at the indicated MOI. After 72 hours post-infection, cell proliferation was quantified by MTT assay. Data are expressed as the Mean ± SD from at least three independent experiments. (B) Ras-GTP from cell lysates of canine histiocytic sarcoma cell lines and Raji was affinity-precipitated with GST-RBD protein. The affinity-precipitated Ras-GTP was subjected to SDS-PAGE, followed by western blotting with anti-Ras antibody. Results shown are one representative result from two repeats.

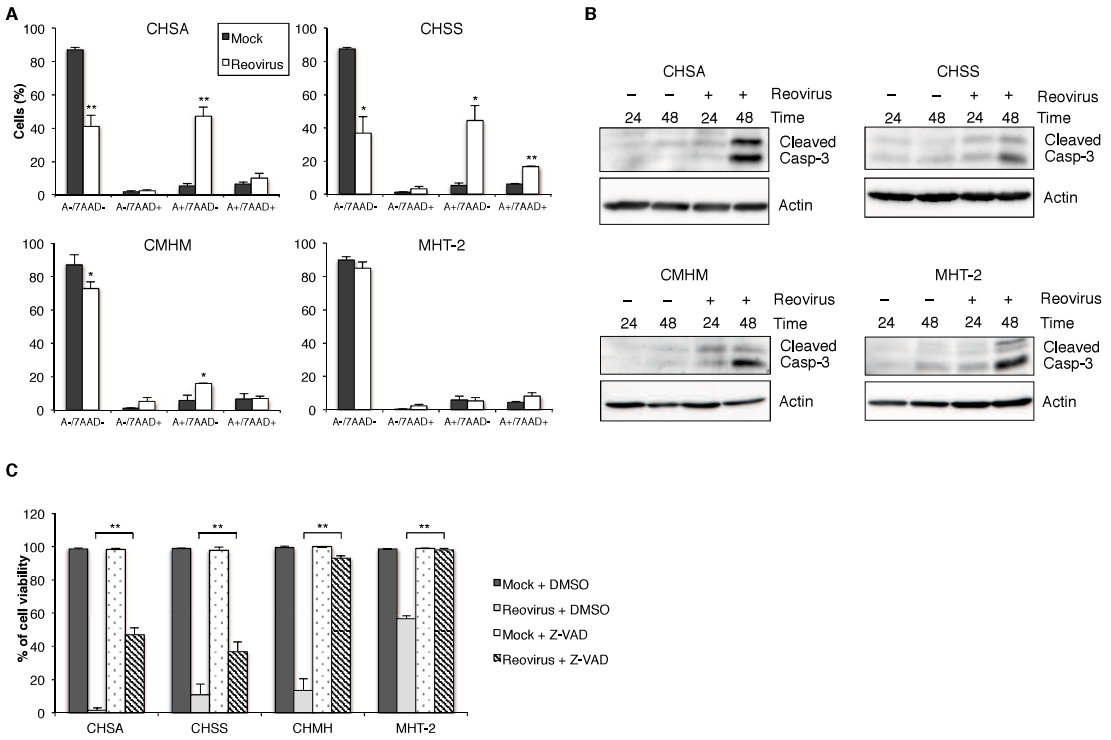

Fig. II-2. Reovirus induces caspase-dependent apoptotic cell death

(A) Reovirus-infected (MOI 10) cell lines were harvested at 48 hours post-infection and stained with PE-Annexin V/ 7-AAD assay before flow cytometry analysis. From the analyzed results, the cell population of apoptotic and necrotic cells was evaluated. Data are expressed as the Mean + SD from at least three independent experiments. Student's t test. *$p < 0.05$, ** $p < 0.01$. (B) Cleaved caspase-3 expression levels in each cell line treated with reovirus (MOI 10) for 24 or 48 hours are shown. Actin was used as a protein loading control. (C) Each cell line in triplicates was pre-incubated with DMSO or 50 ㎛ M of Z-VAD-FMK for 1 hour and followed by treating with reovirus at MOI of 10 for 72 hours. Cell viability was assessed by trypan blue exclusion test. Data are expressed as the Mean + SD from at least three independent experiments. Student's t test. *$p < 0.05$, ** $p < 0.01$.

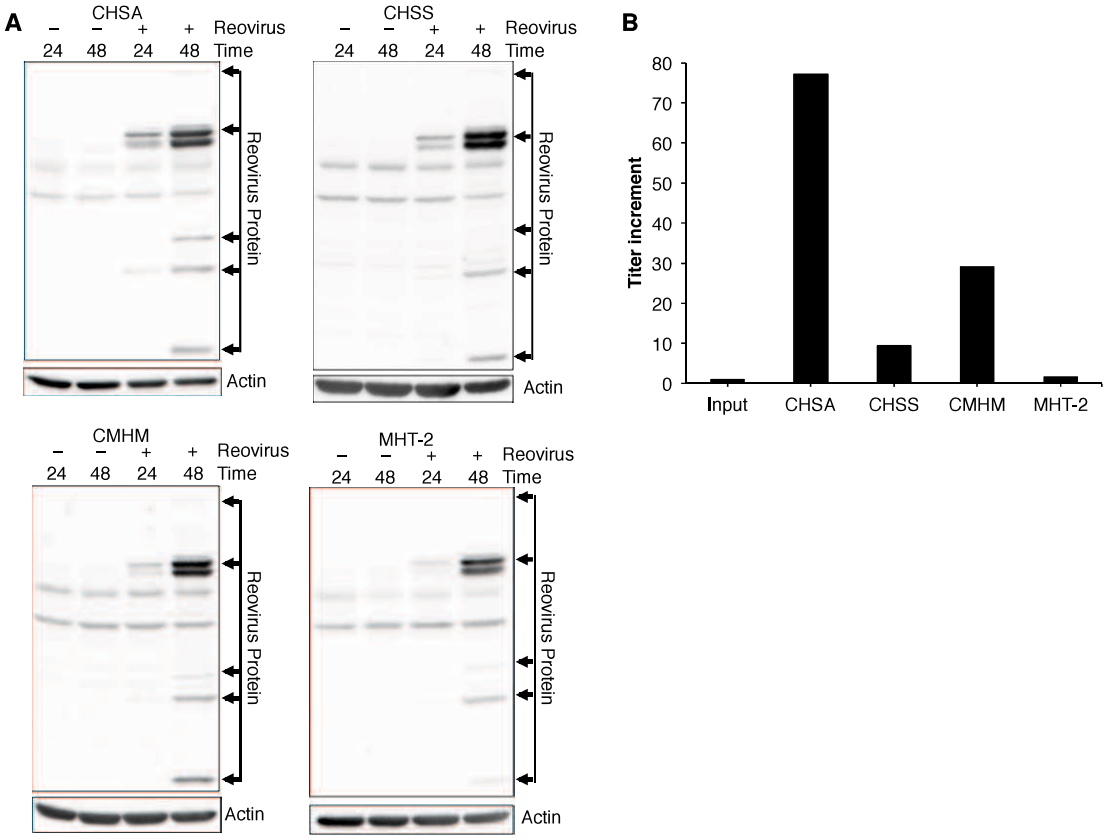

Fig. II-3. Reovirus replication and production of progeny virus in reovirus-infected cells (A) Reovirus structural proteins were detected using anti-reovirus polyclonal antibody. Cell lysates were collected from each cell line treated with reovirus (MOI 10) at indicated times. Actin was used as a protein loading control. (B) Supernatant of reovirus-infected each cell line was harvested at 72 hours post-infection, and virus titer were determined using $TCID_{50}$ assay. The fold increase of reovirus represents the mean values calculated from the titer of progeny virus divided by that of input virus form three independent expereiments.

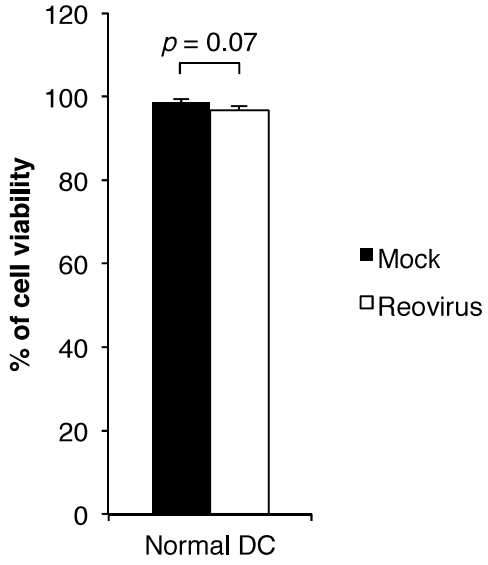

Fig. II-4. Canine immature dendritic cells are not susceptible to reovirus

Normal DCs differentiated from PBMCs of three healthy beagles in triplicates were treated with reovirus (MOI 10) for 72 hours. Cell viability was assessed by trypan blue exclusion test. Data are expressed as the Mean + SD from at least three independent experiments. Student's t test.

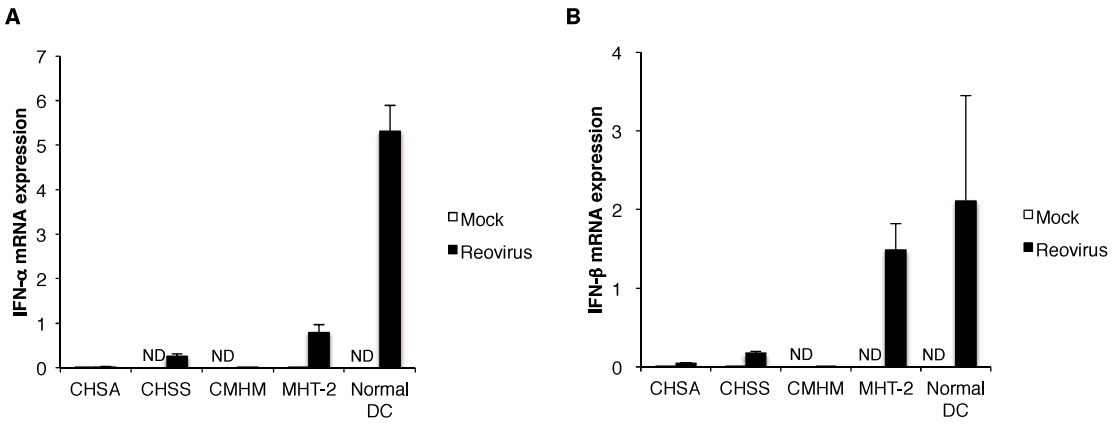

Fig. II-5. Reovirus infection triggers to express type I interferon genes

Histiocytic sarcoma cell lines and normal DCs were treated with reovirus (MOI 10) for 24 hours. The expression levels of *IFN-α* (A) and *IFN-β* (B) were determined by real-time PCR. The data were normalized to *RPL13A* gene. ND means that gene amplification cannot be detected by real-time PCR.

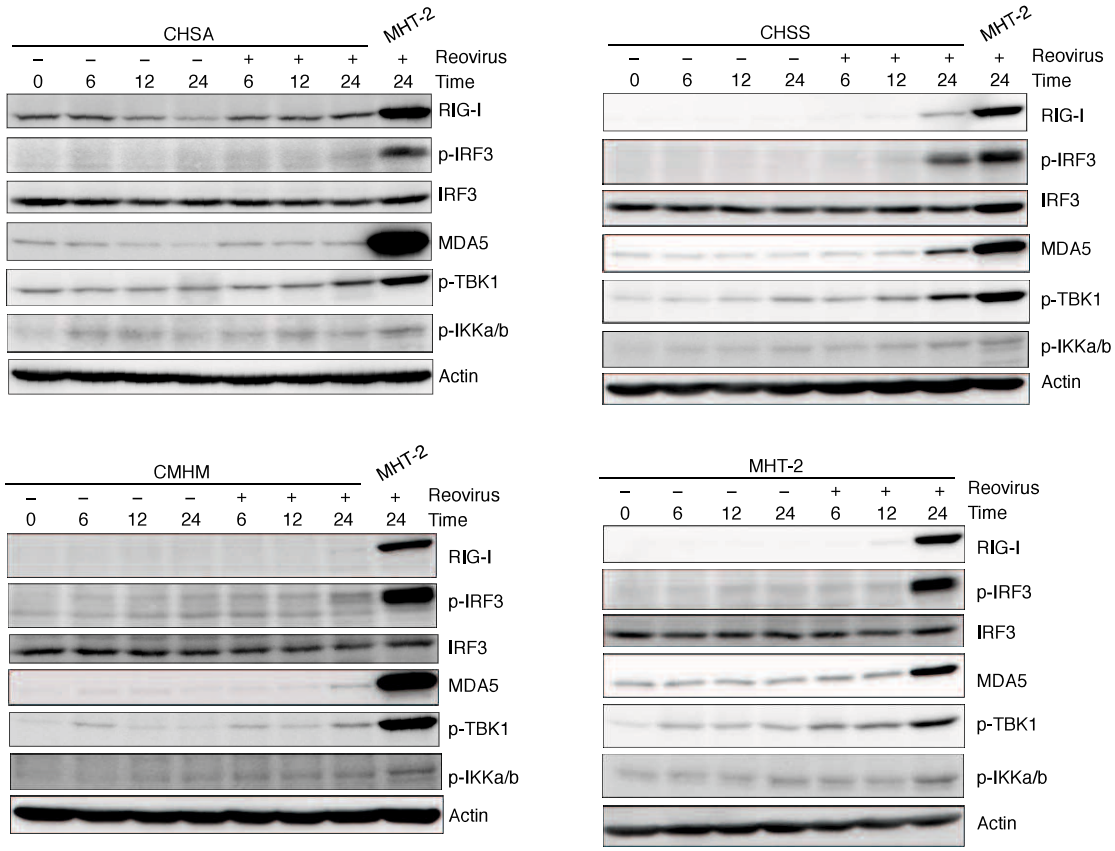

Fig. II-6. Expression of signaling proteins of innate immune responses in reovirus-infected canine histiocytic sarcoma cell lines

Cell lysates were collected from each cell line treated with reovirus (MOI 10) at indicated times. To monitor the activation of innate immune response, the expression of RIG-I, phospho-IRF3, IRF3, MDA5, phospho-TBK1, and phospho-IKKα/β was assessed by western blotting. Actin was used as a protein loading control.

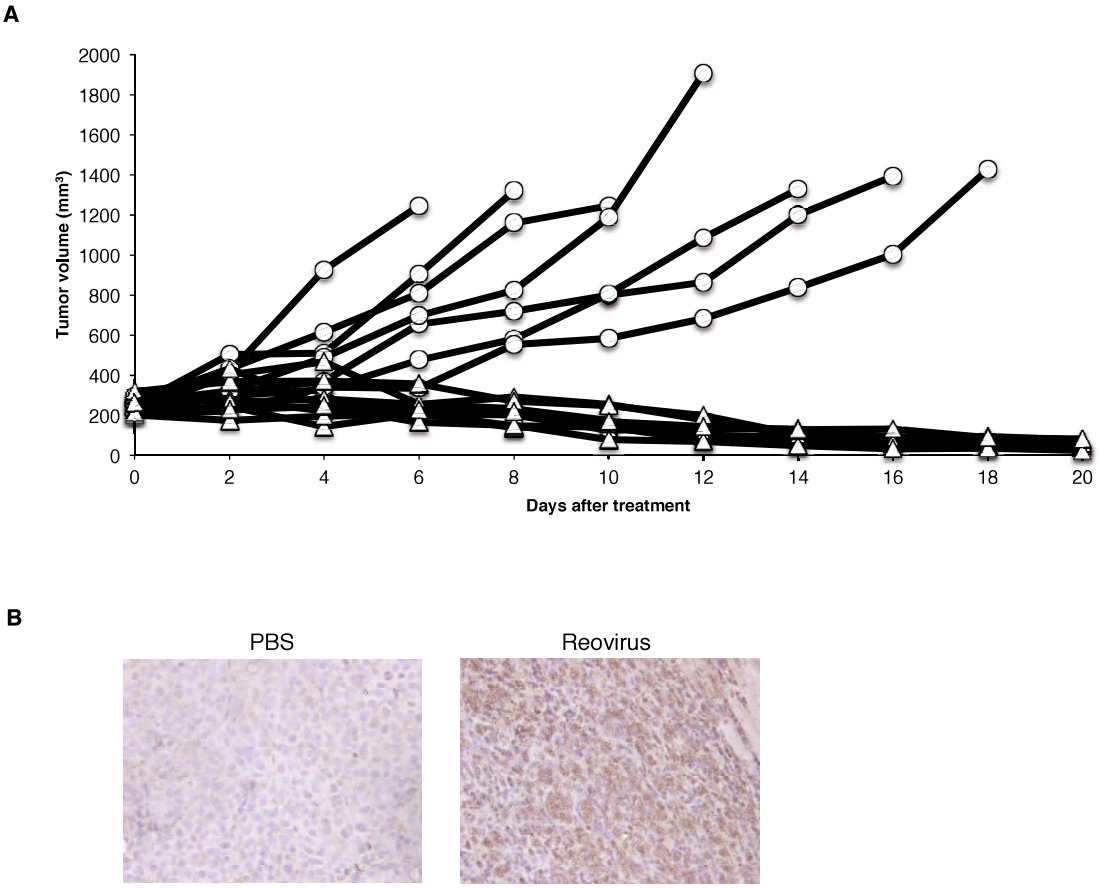

Fig. II-7. Reovirus suppresses the tumor growth in canine histiocytic sarcoma xenograft mouse model

CHSSv1 (4.0 x 10^6 cells) was implanted subcutaneously at the right flank of each mouse. When the tumor volume reached 200 mm^3, the mass was treated with a single intra-tumor injection of 1.0 x 10^8 PFUs of reovirus (open triangles) or PBS (open circles). (A) Tumor size was measured with a caliper. Data represents the tumor volume of each mouse. (B) IHC staining results using anti-reovirus antibody from the samples of representative mice in control and reovirus-treated group at the end point of this experiment are shown.

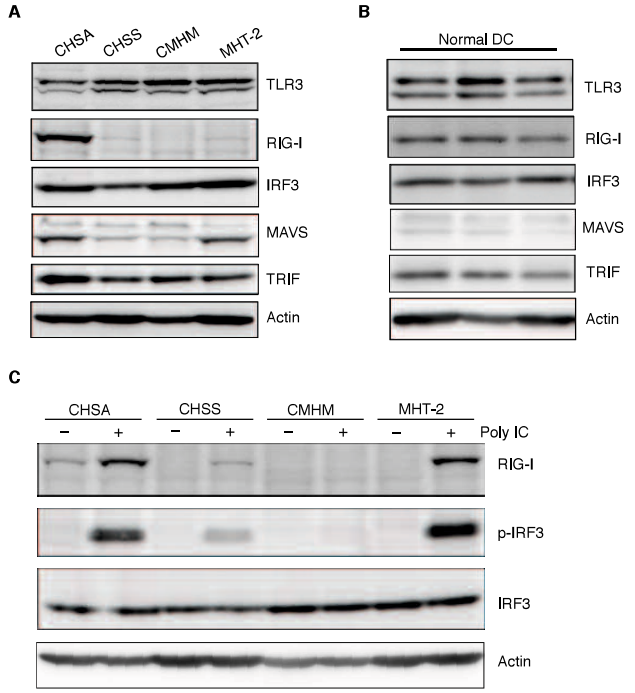

Fig. II-7. Expression of signaling proteins of innate immune responses in canine histiocytic sarcoma cell lines and immature dendritic cells

(A, B) Protein lysates in each sample were harvested at normal culture conditions. The expression of TLR3, RIG-I, MAVS, TRIF, and IRF3 was analyzed by western blotting. (C) Canine histiocytic sarcoma cell lines were treated with poly IC (10 μg/ml) for 2 hours. The expression of RIG-I, phospho-IRF3 and IRF3 was assessed by western blotting. Actin was used as a loading control.

Chapter 3

Oncolytic reovirus synergizes with chemotherapeutic agents to promote cell death in canine mammary gland tumor

SUMMARY

The oncolytic effects of reovirus in various cancers have been proven by the encouraging results of many clinical trials in human medicine. At the same time, oncolytic virotherapy using reovirus for canine cancers is being developed in our laboratory. The first part of this study demonstrated the efficacy of reovirus in canine mammary gland tumor (MGT) *in vitro* and *in vivo*. Reovirus alone exerted significant cell death via caspase-dependent apoptosis in canine MGT cell lines. Single injection of reovirus impeded canine MGT tumor growth in xenografted mice, but was insufficient to induce complete tumor regression. The second part of this study highlighted the anti-tumor effects of reovirus in combination with paclitaxel, carboplatin, gemcitabine or toceranib. Enhanced synergistic activity was observed in the MGT cell line treated concomitantly with reovirus and the chemotherapeutic agents, except toceranib. In addition, combination of reovirus with paclitaxel or gemcitabine at half dosage of IC50 enhanced cytotoxicity via caspase 3 activation. My data suggested that the combination of reovirus and low dose chemotherapeutic agents provides an attractive option in canine cancer therapy.

RESULTS

Reovirus is highly infective and induces cell-death in canine MGT cell lines

Chpater 1 in this thesis focused on various canine MGT cell lines as potential candidates for reovirus therapy. In this study, two canine MGT cell lines, CHMp-13a and CHMp-5b, were chosen due to the published biological behavior of these cell lines in xenotransplanted mice (Murai, K. et al., 2012). Firstly, examination of the susceptibility of the cell lines towards reovirus was carried out. CHMp-13a and CHMp-5b showed more than 50% of inhibition of cell proliferation by reovirus at MOI of 100 and inhibition was affected in a dose-dependent manner (Fig. III-1A). In addition to MTT assay, trypan blue exclusion test revealed that reovirus induced cell death in both of the cell lines (Fig. III-1B). Viral progeny was measured by $TCID_{50}$ assay to determine reovirus replication (Fig. III-1C). Both of the cell lines had increment of viral progeny titer, which was consistent with the detection of viral proteins using flow cytometric analysis (Fig. III-1D). These results indicated that CHMp-13a and CHMp-5b are highly susceptible to reovirus as observed in the parental CHMp cells (as shown in Chapter 1).

The baseline GTP-loading status of Ras was determined in both of the cell lines in order to investigate the involvement of Ras activation as the molecular determinant for reovirus susceptibility. Ras activity of the cell lines was higher than Raji (Fig. III-1E). Raji was used as a control because Raji is moderately susceptible towards reovirus-induced cell death and has a certain level of Ras activation as shown in previous study (Alain, T. *et al*., 2006).

Reovirus induces caspase-dependent apoptosis in canine MGT cell lines

Previous reports have indicated that caspase-dependent apoptosis is one of the mechanisms of reovirus-induced cell death in susceptible cell lines (Hwang, CC. *et al*., 2013, Hwang, CC. *et al*., 2016). Therefore, Annexin V/ PI assay was carried out to assess the amount of apoptotic cells in reovirus-infected culture. In both of the cell lines, the percentage of early apoptotic cells (A+/P-) increased over time after reovirus infection as compared to mock-infected cells (Fig. III-2A). At the same time, the percentage of necrotic cells (A-/P+) also increased in CHMp-13a after reovirus infection.

In order to prove that apoptosis of reovirus-infected cells occurred via caspase 3 activation, western blot analysis was performed using anti-caspase 3 and anti-PARP antibodies. As shown in Fig. III-2B and III-2C, cleavage of caspase 3 and PARP was shown in both of the cell lines at 48 hpi. Furthermore, both of the cell lines were pre-treated with Z-VAD-FMK before reovirus infection and cell viability was determined by trypan blue dye exclusion at 72 hpi. Cytotoxicity of reovirus infection was completely inhibited by Z-VAD-FMK in the cell lines (Fig. III-2D). In order to confirm that caspase 3 activation was inhibited by Z-VAD-FMK, the cleavage of caspase 3 was also examined via western blotting (Fig. III-2E). The level of cleaved caspase 3 decreased in the Z-VAD-FMK-treated CHMp-13a but an unexpected increment was observed in the Z-VAD-FMK-treated CHMp-5b. These results indicated that reovirus-induced cell death in CHMp-13a and CHMp-5b cell lines is predominantly via apoptosis related to a caspase inhibitor-sensitive pathway.

Reovirus inhibits growth of canine MGT engrafted in NOD/SCID mice

In order to assess the oncolytic potential of reovirus *in vivo*, subcutaneous

xenograft models were created using NOD/SCID mice. In a previously published study, tumour growth of CHMp-13a stopped a week after inoculation, indicating the difficulty of creating the subcutaneous CHMp-13a mouse models as compared to the subcutaneous CHMp-5b tumors that increased in size over time (Murai, K. *et al*., 2012). Therefore, the CHMp-5b subcutaneous xenograft models were chosen and treated with a single intratumoral injection of reovirus. All mice were treated with reovirus or UV-inactivated reovirus 14 days post-transplantation of CHMp-5b. Tumor growth was significantly limited by reovirus 21 days post-transplantation of CHMp-5b when compared to the UV-inactivated reovirus-treated group (Fig. III-3A). H&E-stained histopathological samples from the CHMp-5b xenograft models showed extensive necrotic lesions within the reovirus-treated tumors, in contrast to the untreated tumors and UV-inactivated reovirus-treated tumors (Fig. III-3B). Immunohistochemical staining using the anti-reovirus antibody demonstrated the presence of reovirus proteins in the reovirus-treated tumors (Fig. III-3B). These results confirmed that reovirus infected the tumor cells and suppressed the growth of tumors *in vivo*.

Reovirus cytotoxicity is enhanced in CHMp-5b with the combination of chemotherapeutic agents

Reovirus treatment regressed tumor growth in NOD/SCID mice engrafted with CHMp-5b cells, but the effects were weaker than expected. Therefore, I hypothesized that the synergistic effects of other anti-cancer agents can enhance the effects of reovirus therapy. This led me to examine the effects of reovirus in combination with chemotherapeutic agents, mainly paclitaxel, carboplatin, gemcitabine and toceranib, in CHMp-5b. Firstly, drug-induced cytotoxicity in CHMp-5b was assessed as a single agent, and the IC50 of each of the chemotherapeutic agents in CHMp-5b was determined (Table III-1). Similarly, the IC50 was determined for reovirus. In order to evaluate the synergistic effects of reovirus and the chemotherapeutic agents, CHMp-5b was treated with reovirus, chemotherapeutic agents or a combination of reovirus and the chemotherapeutic agents, at doses representing 4, 2, 1, 0.5 and 0.25 times of the calculated IC50 in a constant ratio, according to previously reported methods (Chou, TC., 2010, Chou, TC. and Talalay, P., 1984). The combination of reovirus and chemotherapeutic agents enhanced the tumour cell killing

effects, as compared to each of the agent alone, except toceranib (Fig. III-4). Based on this data, I analyzed the combination index (CI) using the isobologram analysis to determine whether the enhanced cell death was synergistic. CI provides a quantitative measurement of the degree of interaction between two or more cytotoxic agents. The combination of reovirus and paclitaxel, carboplatin or gemcitabine demonstrated synergistic cytotoxic effects against CHMp-5b at the indicated concentrations (Table III-1). In contrast, the combination with toceranib was shown to be less synergistic at those concentrations.

The combination of reovirus and chemotherapeutic agents activates the caspase-pathway

In order to assess the relationship between the synergistic cytotoxicity effects of reovirus-chemotherapeutic agents and the caspase pathway, the expression of cleaved caspase 3 was analyzed by western blotting. Similar to reovirus, paclitaxel and gemcitabine alone induced cleavage of caspase 3 in CHMp-5b while carboplatin did not. On the other hand, a combination of reovirus and paclitaxel or gemcitabine induced

significant levels of cleaved caspase 3 when compared to reovirus alone (Fig. III-5). The combination of reovirus and carboplatin showed a slight increment of cleaved caspase 3 but the combination was not statistically significant against reovirus alone. These data suggested that, depending on the type of chemotherapeutic agents, the synergistic effects seen in CHMp-5b with the combination of reovirus are mediated by apoptosis.

DISCUSSION

As CHMp-13a and CHMp-5b are clones derived from CHMp (Murai, K. *et al*., 2012), the susceptibility of these two cell lines towards reovirus was similar to their parental cell line (as shown in Chapter 1). Despite the common origin, CHMp-13a and CHMp-5b express different tumor-related proteins and exhibit distinctive cellular morphology and growth pattern. CHMp-5b expresses the mesenchymal genes, and is concomitantly more malignant and tumorigenic *in vitro* and *in vivo* than the epithelial CHMp-13a (Murai, K. *et al*., 2012). In my study, both cell lines showed reovirus susceptibility to a similar degree, where more than 40% of the cells were killed by reovirus infection (Fig. III-1B).

Annexin V/ PI staining and the cleavage of caspase 3 and PARP confirmed that reovirus-induced cytotoxicity was due to caspase-dependent apoptosis. Moreover, treatment with a pan-caspase inhibitor, Z-VAD-FMK, inhibited the reovirus-induced cytotoxicity (Fig. III-2D), which was also consistent with reports in canine mast cell tumors and lymphoma cell lines (Hwang, CC. *et al*., 2013, Hwang, CC. *et al*., 2016). As expected, caspase 3 activation induced by reovirus decreased in CHMp-13a treated with

Z-VAD-FMK (Fig. III-2E). However, contrasting result was obtained in CHMp-5b. Although I do not have any evidence-based explanation, I speculate that this phenomenon in CHMp-5b might involve other caspases. Since Z-VAD-FMK is a pan-caspase inhibitor, it can also inhibit other caspases besides caspase 3, such as caspase 8 and caspase 7. In CHMp-13a, reovirus-induced apoptosis is completely dependent on caspase 3, but reovirus-induced apoptosis in CHMp-5b might involve another caspase like caspase 7, which can compensate the loss of caspase 3 in certain cells.

Even though further studies are necessary to elucidate the complete mechanism of reovirus-induced cell death in CHMp-5b, I strongly believe that reovirus-induced cell death occurs via caspase-dependent pathways. Fig. III-2A showed that necrosis is also involved in reovirus-induced cell death in CHMp-13a. It remains unclear how necrosis contributes to this phenomenon. Besides apoptosis, reports of some human cancers have also shown that reovirus induces cell death through necrosis, necroptosis or autophagy (Ikeda, Y. *et al*., 2004, Berger, AK. *et al*., 2013, Thirukkumaran, CM. *et al*., 2013). It is a possibility that the mechanism of reovirus-induced cell death in CHMp-13a is partly associated with those pathways.

In addition to the *in vitro* study, I also confirmed the susceptibility of reovirus in subcutaneous xenograft mouse models using CHMp-5b (Fig. III-3A). Although tumor growth was impeded, complete tumor regression was not observed in mice treated with single injection of reovirus. In clinical cases, multiple injections of reovirus are warranted to exert prominent tumor lytic effects due to the additional antibody neutralizing effects as a result of treatment (Hirasawa, K. *et al*., 2003, Yang, WQ. *et al*., 2004). Data from this study suggests that reovirus as monotherapy for canine solid tumor has a limited efficacy, unlike the previous study in which single injection of reovirus completely regressed MCT in xenotransplanted mice (Hwang, CC. *et al*., 2013).

Recently, new approaches using a combination of reovirus and chemotherapeutic agents have been tested in various human cancer cell lines of different origins, and also in a number of clinical trials (Maitra, R. *et al*., 2014, Heinemann, L. *et al*., 2011, Galanis, E. *et al*., 2012, Comins, C. *et al*., 2010, Twigger, K. *et al*., 2008, Sei, S. *et al*., 2009). In order to assess the enhancement of reovirus-induced cytotoxicity in CHMp-5b, I chose chemotherapeutic agents such as paclitaxel,

carboplatin and gemcitabine, which are commonly used for tumor treatment, and toceranib, which is the first FDA-approved receptor tyrosine kinase inhibitor for the treatment of cancer in dogs (London, CA. *et al*., 2009). These agents exert cytotoxic effects through different mechanisms of action. Paclitaxel works as a taxane, carboplatin is a pseudo-alkylating agent, and gemcitabine is an anti-metabolite agent, while toceranib is a molecular-targeted drug inhibiting multiple tyrosine kinase. Combination analysis using the Chou-Talalay's method (Chou, TC., 2010) showed significant levels of synergistic effects between reovirus and the chemotherapeutic agents tested, except toceranib. These results indicate that paclitaxel, carboplatin, and gemcitabine are suitable candidates for combination therapy with reovirus in canine MGT (Table III-1). Even though the CI value of toceranib and reovirus was <1, it is the highest among the chemotherapeutic agents, indicating that toceranib showed the least synergistic effects with reovirus.

The canine Cmax levels of paclitaxel, carboplatin, gemcitabine and toceranib are 3.95 μg/ml (4.6 μM), 14.1 μg/ml (38 μM), 10.7 μg/ml (36 μM) and 109 ng/ml (0.27 μM), respectively. The IC50 of toceranib in the *in vitro* studies is higher than the canine

Cmax levels. When the canine Cmax levels are compared to the IC50, toceranib is the only agent in this study with IC50 that was higher than the canine Cmax level. Even though the relationship of IC50 and canine Cmax levels for paclitaxel, gemcitabine and carboplatin was not assessed in this study, the combination of reovirus and chemotherapeutic agents that demonstrated synergistic effects had IC50 that are either lower or equivalent to the Cmax levels. These results suggest that synergistic anti-tumor activities can also be achieved in tumor-bearing dogs when reovirus and the three chemotherapeutic agents are used in combination at the IC50 value.

Interestingly, the combination treatment of reovirus and paclitaxel or gemcitabine in CHMp-5b led to an increased activation of caspase 3 as compared to reovirus treatment alone (Fig. III-5). Some reports showed that the combination treatment of reovirus and chemotherapeutic agents (paclitaxel, gemcitabine and vinblastine) enhances cell death via the caspase pathway (Roulstone, V. *et al*., 2013, Sei, S. *et al*., 2009). On the other hand, the combination of reovirus and alkylating agent (cisplatin)-induced cell death is not caspase-dependent (Pandha, HS. *et al*., 2009, Sei, S. *et al*., 2009). Similarly, in this study, the combination of reovirus and carboplatin did

not induce any obvious enhancement of caspase activation even though CI for reovirus and carboplatin indicated a synergistic relationship. This suggests that the synergistic cell killing of reovirus and carboplatin might involve other mechanisms but concrete evidence is yet to be found.

In this study, I used immunocompromised mouse models engrafted with canine MGT cell line to examine the direct cytotoxic effect of reovirus to canine MGT. In order to apply these results as actual canine cancer treatment, I need to consider the involvement of host immune system and assess these effects in immunocompetent mouse models in future studies. Reovirus infection may be hindered by existing neutralizing antibody in immunocompetent hosts. However, this can be overcome as reovirus has an avoidance mechanism against those antibodies by hitchhiking into PBMCs and dendritic cells, as suggested by results from human clinical trials (Adair, RA. *et al*., 2012).

In addition to the synergistic effects shown in this study and previous studies (Qiao, J. *et al*., 2008, Roulstone, V. *et al*., 2015), simultaneous usage of chemotherapeutic agents with reovirus may induce immunosuppressive effects on the

host immune response, which can possibly limit the production of anti-reovirus neutralizing antibodies. Furthermore, reovirus stimulates both the innate and adaptive immunity as an indirect mean against the targeted tumor (Errington, F. *et al*., 2008, Errington, F. *et al*., 2008, Prestwich, RJ. *et al*., 2009). Even though I did not examine the efficacy of the combination of reovirus and chemotherapeutic agent *in vivo*, previous reports (Errington, F. *et al*., 2008, Errington, F. *et al*., 2008, Prestwich, RJ. *et al*., 2009) suggest that more profound effects can be expected from the combination therapy in immunocompetent models.

The process of optimizing the effectual dose of a chemotherapeutic agent can be exhausting for both veterinarians and pet owners. Moreover, this is often carried out while risking the quality of life of a beloved pet with the possibility of over-dosing. Based on the results of this study, the efficacy of reovirus as a monotherapy is limited in canine solid tumor. On the other hand, synergistic data obtained from this study showed that the combination of reovirus and a chemotherapeutic agent at a lower dosage enhanced the anti-tumor effects in canine MGT. This provides a particularly attractive alternative since the adverse events from chemotherapy can be reduced or even

completely eliminated. With continuous effort, this novel therapeutic approach for canine MGT is expected to be one of the forerunners of anti-cancer therapy in the veterinary field.

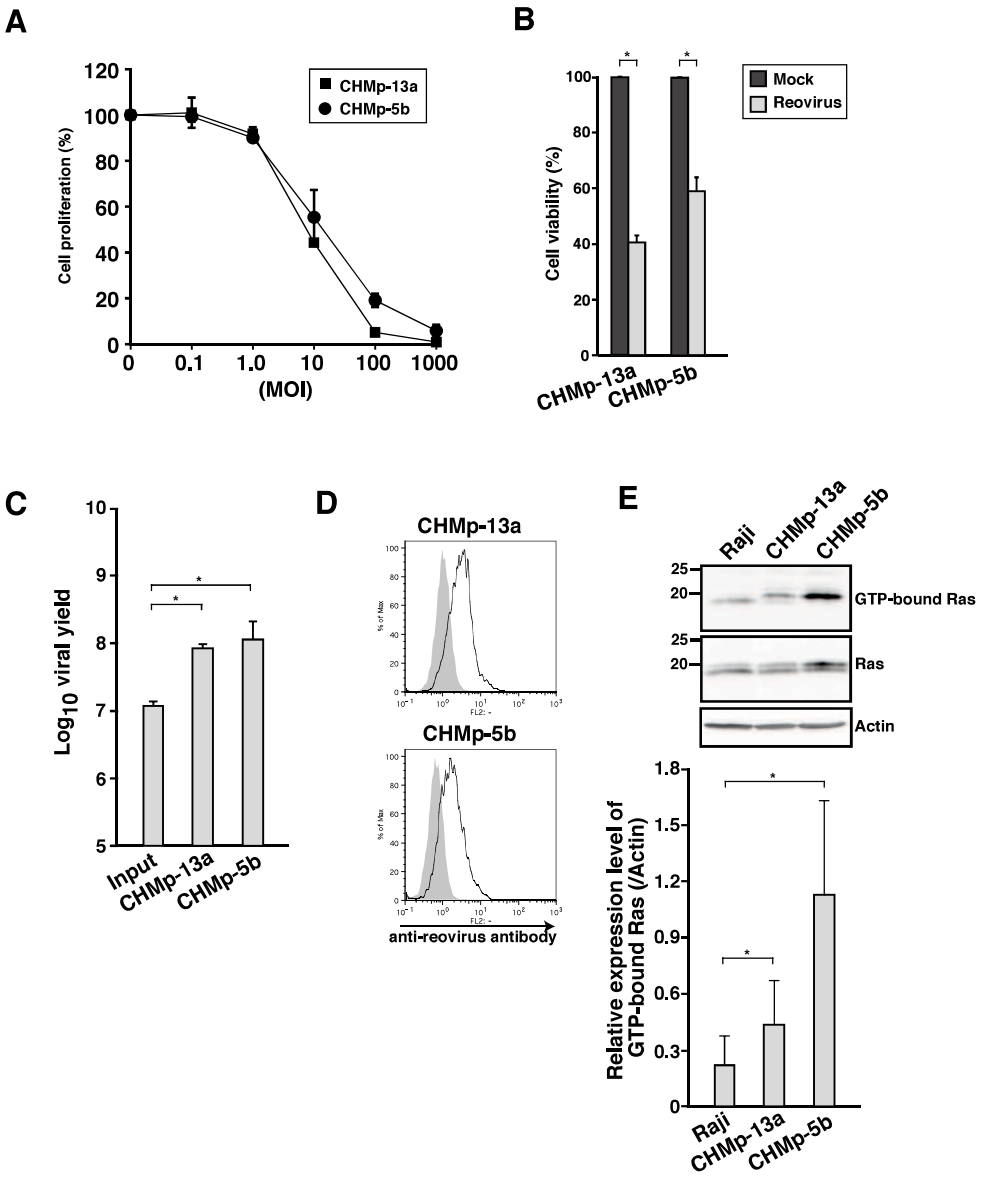

Fig. III-1. Evaluation of reovirus susceptibility in canine mammary gland tumor (MGT) cell lines.

(A) Two canine MGT cell lines in triplicate wells were mock-infected or infected with reovirus at the indicated MOI. After 72 hr post-infection (hpi), cell proliferation was quantified by MTT assay. Mean ± SD of three independent experiments is shown. (B)

Cell lines in triplicate wells were mock-infected or infected with reovirus at MOI 70. After 72 hpi, cell viability was quantified by trypan blue exclusion test. Mean ± SD of three independent experiments is shown. * indicates $p < 0.05$. (C) Supernatant of reovirus-infected (MOI 70) cell lines was harvested at 72 hpi, and virus titer were determined by $TCID_{50}$ assay. Input indicates the initial virus titer used in the infection of cells. Mean ± SD of three independent experiments is shown. * indicates $p < 0.05$. (D) Cell lines were infected with reovirus at MOI 70. Reovirus-infected cell lines were harvested at 48 hpi. Cells were permeabilized, followed by staining with rabbit anti-reovirus polyclonal antibody and analyzed by flow cytometry. The shaded regions and regions below the black line in the histograms indicate staining with isotype control and anti-reovirus antibody, respectively. Results shown are representatives of two repeats. (E) Ras-GTP from cell lysates of Raji and canine MGT cell lines was affinity-precipitated with GST-RBD protein. The affinity-precipitated Ras-GTP was subjected to SDS-PAGE, followed by western blotting with anti-Ras antibody. Actin was used as control for protein loading. Results shown are representatives of three repeats. Quantification of GTP-Ras by densitometry is shown below images. Mean ± SD of three independent experiments is shown. * indicates $p < 0.05$.

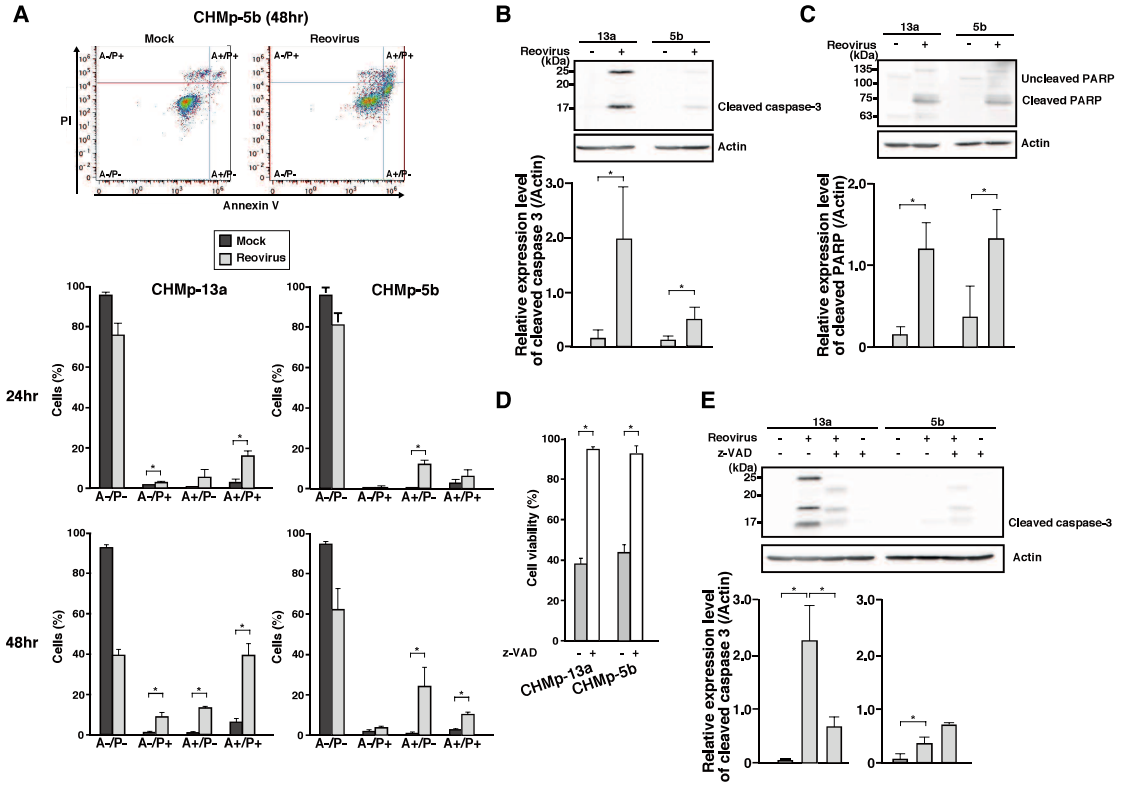

Fig. III-2. Reovirus induced cell death in canine MGT cell lines via the caspase-dependent apoptosis pathway.

(A) Reovirus-infected (MOI 70) cell lines were harvested at 24 or 48 hpi and stained with Annexin V/ PI assay before flow cytometric analysis. The population of living (A-/P-), necrotic (A-/P+), early apoptotic (A+/P-) and late apoptotic/ necrotic (A+/P+) cells was summarized. Dot plots shown are representatives for CHMp-5b at 48 hpi. Mean ± SD of three independent experiments is shown. * indicates $p < 0.05$. (B, C) Cell lysates of reovirus-infected (MOI 70) cell lines at 48 hpi were prepared before proteins were separated using SDS-PAGE. Caspase 3 activation (B) and Poly (ADP-ribose) polymerase (PARP) cleavage (C) were detected using anti-caspase 3 antibody and anti-

PARP antibody, respectively. Actin was used as protein loading control. Bar graphs shown are densitometric quantifications of the relative expression level of each protein relative to actin. Mean ± SD of three independent experiments is shown. * indicates $p < 0.05$. (D) Cell lines in triplicate wells were pre-treated with DMSO or 50 μM of Z-VAD-FMK (Z-VAD) for 1 hr at 37°C incubator before being infected with reovirus at MOI 70. Cell viability was quantified by trypan blue exclusion test at 72 hpi. Mean ± SD of three independent experiments is shown. * indicates $p < 0.05$. (E) Cell lines were pre-treated with DMSO or 50 μM of Z-VAD-FMK (Z-VAD) for 1hr at 37°C incubator before infection with reovirus at MOI 70. At 72 hpi, lysates of harvested cells were prepared before proteins were separated using SDS-PAGE. Caspase activation was detected using anti-caspase 3 antibody. Actin was used as protein loading control. Bar graphs shown are densitometric quantifications of the relative expression levels of cleaved caspase 3 relative to actin. Mean ± SD of three independent experiments is shown. * indicates $p < 0.05$.

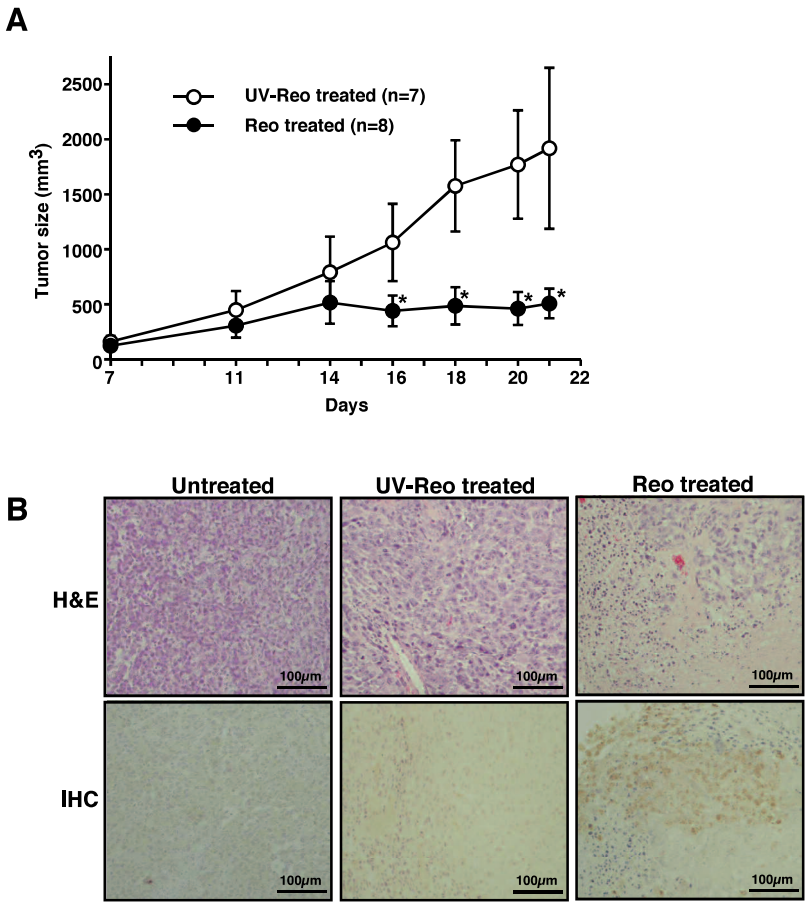

Fig. III-3. Reovirus suppressed tumor growth in canine MGT xenograft mouse models. CHMp-5b (1.0 x 10^7 cells) was implanted subcutaneously at the right flank of mice (Day 1). After 14 days, the tumors were treated with single intratumoral injection of 1.0 x 10^8 PFUs of reovirus or UV-inactivated reovirus (control). Tumor size was measured with a caliper (A). Data represents the mean ± SD of each treatment group.

* indicates $p < 0.05$. UV-inactivated reovirus did not show any infectivity to L929 cells. (B) H&E and immunohistochemical (IHC) results from representative mice with no treatment, UV-inactivated reovirus or reovirus 21 days post-transplantation are shown. Antibody used for IHC is targeted at the reoviral μ and σ proteins.

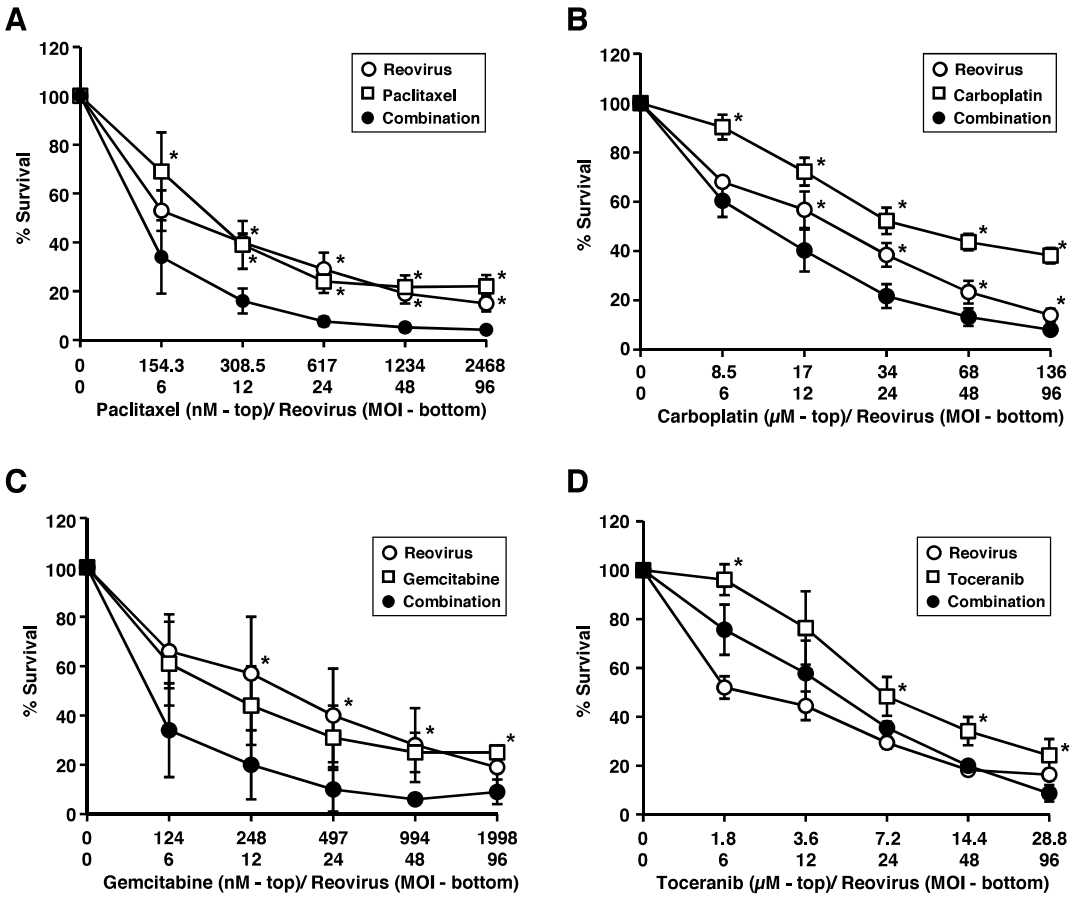

Fig. III-4. Evaluation of synergistic effects of reovirus and chemotherapeutic agents in CHMp-5b.

CHMp-5b cells were treated with reovirus alone (open circles), chemotherapeutic agent alone (open squares) or a combination of the two (closed circles) at the indicated concentrations for 72 hr. Cell proliferation was quantified by MTT assay. Mean ± SD of three independent experiments is shown. Statistical differences of % survival between single treatments (chemotherapeutic agent or reovirus) and combination treatment were evaluated using Dunnett's method. * indicates $p < 0.05$.

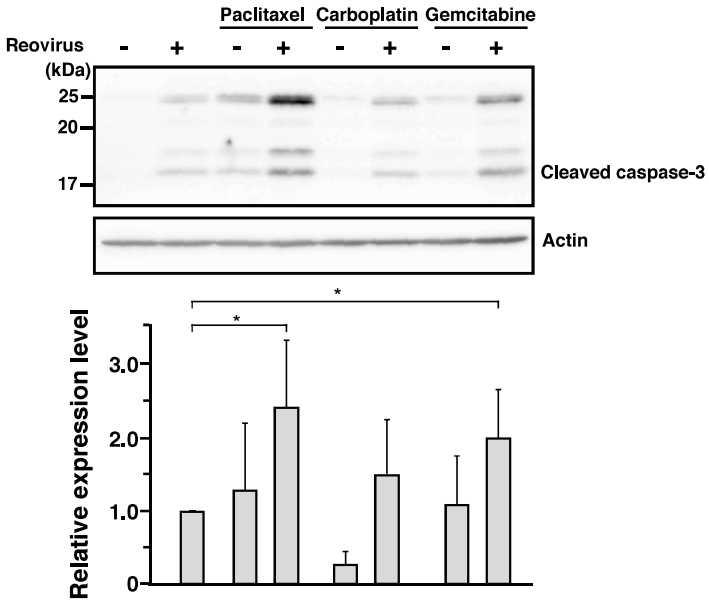

Fig. III-5. The combination of reovirus and chemotherapeutic agents enhanced cell death via caspase-dependent apoptosis.

Whole cell lysates were prepared from CHMp-5b treated with the chemotherapeutic agents at half of IC50 for 48 hr. Proteins were separated with SDS-PAGE before the cleavages of caspase 3 was assessed using Western blotting with anti-caspase 3 antibody. Actin was used as protein loading controls. Results shown are representatives of three repeats. Bar graphs shown are densitometric quantifications of the relative expression levels of cleaved caspase 3 of chemotherapeutic agents with or without reovirus relative to cleaved caspase 3 of reovirus alone. Mean ± SD of three independent experiments is shown. Statistical analysis was performed using t test between reovirus alone and chemotherapeutic agents with or without reovirus.

*indicates $p < 0.05$.

Table III-1.

Synergistic interaction of reovirus and chemotherapeutic agents on CHMp-5b

		mean of CI values ± SD*		
	IC50 ± SD	ED50	ED75	ED95
Reovirus	MOI 24 ± 5.7			
Paclitaxel	0.6 ± 0.04 (μM)	0.54 ± 0.04	0.58 ± 0.04	0.66 ± 0.03
Carboplatin	34 ± 7.9 (μM)	0.48 ± 0.04	0.52 ± 0.04	0.57 ± 0.03
Gemcitabine	0.39 ± 0.03 (μM)	0.51 ± 0.05	0.54 ± 0.05	0.60 ± 0.05
Toceranib	7.6 ± 1.9 (μM)	0.81 ± 0.06	0.83 ± 0.08	0.86 ± 0.10

* Data is calculated from 3 independent experiments at the ED (effective dose) indicated.

CI - combination index

Chapter 4

Combination Therapy with Reovirus and ATM inhibitor Enhances Cell Death and Virus Replication in Canine Melanoma and Human Cancer

SUMMARY

Oncolytic virotherapy using reovirus is a promising new anti-cancer treatment with potential for use in humans and dogs. Because reovirus monotherapy shows limited efficacy in human and canine cancer patients, the clinical development of a combination therapy is necessary. To identify candidate components of such a combination, I screened a 285-compound drug library for those that enhanced reovirus cytotoxicity in a canine melanoma cell line. Here, I show that exposure to an inhibitor of the ataxia telangiectasia mutated protein (ATM) enhances the oncolytic potential of reovirus in canine melanoma cell lines and in human cancer cell lines. Specifically, the ATM inhibitor potentiated reovirus replication in cancer cells by accelerating proteolysis of the reovirus particle coat via acidification of endosomes, resulting in an increased proportion of caspase-dependent apoptosis and cell cycle arrest at G2/M compared to those observed with reovirus alone. Therefore, my study suggests that the combination of reovirus and the ATM inhibitor may be an attractive option in cancer therapy.

RESULTS

The combination of an ATM inhibitor and reovirus enhances anti-tumor effects in cell lines

To identify drugs that enhance reovirus-induced anti-tumor effects, I screened a 285-compound signaling pathway inhibitor library for activity in the CMeC1 canine melanoma cell line (Fig. IV-S1). This screen revealed that the ATM inhibitor KU55933 showed no effect on cell proliferation by itself, but potentiated the cytotoxicity of reovirus when used in combination with reovirus. Moreover, the combination of KU55933 and reovirus yielded dose-dependent suppression of CMeC1 cell growth (Fig. IV-S2). For subsequent experiments, a higher specificity inhibitor of the ATM, KU60019 (Golding, SE. *et al*., 2009) was used in place of KU55933.

To confirm if KU60019 enhances reovirus-induced anti-tumor effects in other types of canine melanoma cell lines, I also examined *in vitro* cell survival using another 5 canine melanoma cell lines (Fig. IV-1). KU60019 combined with reovirus (multiplicity of infection (MOI) 100) significantly suppressed cell proliferation in CMeC1, KMeC, CMM12, LMeC, and CMM10 cell lines, as shown with KU55933.

These results indicated that the combination of KU60019 and reovirus yielded significant cell growth inhibition compared to compound or virus alone in 5 of 6 tested canine melanoma cell lines excepting CMGD2. In addition to cell proliferation, cell viability was examined in 4 of these cell lines (CMeC1, KMeC, LMeC, and CMGD2) by means of a trypan blue exclusion test (Fig. IV-2A). Compared to reovirus alone, the combination of KU60019 and reovirus strongly potentiated cell death in 3 of the 4 canine melanoma cell lines, excepting CMGD2. These results suggested that KU60019 has therapeutic potential for synergistic use in combination with reovirus for treatment of canine melanoma cells.

To translate these results from animals to humans, I evaluated the combination effects of KU60019 and reovirus in several human cancer cell lines (non-small-cell lung cancer A549, bladder cancer T-24, cutaneous melanomas A2058 and Colo679, and colorectal adenocarcinoma DLD-1). Consistent with the above results in canine melanoma cells, KU60019 enhanced reovirus-induced anti-tumor effects to greater in a dose-dependent manner in all of the tested human cancer cell lines excepting Colo679 (Fig. IV-S3). These data provided evidence that combination

treatment with reovirus and ATM inhibitor potentiated anti-tumor activity in human cancers as well as in canine melanomas.

To confirm the specificity of the ATM inhibitor, the ATM-encoding gene was knocked out in several canine melanoma cell lines (CMeC1, KMeC, CMM10, and CMM12) using a CRISPR/Cas9-based system (Fig. IV-S4A). At 48 hr after infection with reovirus, *ATM* knock-out cells showed greater inhibition of cell growth than did the respective ATM^{+} (wild type) cells (Fig. IV-S4B). These results confirmed that inhibition of ATM sensitizes canine melanoma cell lines to reovirus-induced cytotoxicity.

KU60019 enhances reovirus-induced apoptosis and cell cycle arrest

Next, I assessed the potential mechanism by which the combination of KU60019 and reovirus induces anti-tumor effects. As expected, the percentage of sub-G1 cells increased from 24 hr to 48 hr in CMeC1 cells subjected to the combination treatment compared to the percentage in cells treated with reovirus alone (Fig. IV-2B). At the earlier time point (24 hr), cleaved caspase-3 accumulated to higher levels in

CMeC1 cells subjected to the combination treatment than in the same cell line treated with reovirus alone (Fig. IV-2C). Notably, pre-treatment of CMeC1 and KMeC with 50 μM Z-VAD-FMK (carbobenzoxy-valyl-alanyl-aspartyl-[O-methyl]-fluoromethylketone, an irreversible caspase inhibitor), before exposure to the combination of reovirus and KU60019, resulted in the complete inhibition of reovirus-induced cell death, as assessed by the trypan blue exclusion test (Fig. IV-2D). However, in a cell proliferation assay, the combination treatment was not sufficient to completely abrogate cell growth in either of these cell lines (Fig. IV-2E). Therefore, I inferred that the combination of reovirus and KU60019 also affects cell cycle progression in canine melanoma cells.

Consistent with previous studies showing that reovirus infection results in cell cycle arrest at G2/ M in several cancer cell lines (Clarke, P. *et al*., 2005, Poggioli, GJ. *et al*., 2001, Maitra, R. *et al*., 2014, Twigger, K. *et al*., 2008, Sei, S. *et al*., 2009), I observed that treatment with reovirus alone induced cell cycle arrest at G2/M in CMeC1. Moreover, treatment of CMeC1 with the combination of KU60019 and reovirus resulted in strong cell cycle arrest at G2/ M and a reduction of the G1 interval (Fig. IV-3A). In a previous report, the viral nonstructural protein sigma 1s regulated the

activity of CDK1 (the G2/M cyclin-dependent kinase; cdc2), which was required for cell cycle arrest at G2/ M (Poggioli, GJ. *et al*., 2001). I sought to extend that analysis by using immunoblotting to test treated cells for their levels of CDK1 and p21 (the cyclin-dependent kinase inhibitor) (Fig. IV-3B). After 24 hr, cells treated with the combination of KU60019 and reovirus accumulated significantly lower levels of CDK1 than cells treated with either reagent alone. In contrast, the 24-hr levels of p21 did not differ significantly among cells treated with the combination or with KU60019 or reovirus alone. Together, these results indicated that the treatment of canine melanoma cells with the combination of KU60019 and reovirus induces both caspase-dependent apoptosis and cell cycle arrest at G2/M.

KU60019 increases reovirus replication and progeny virus number

Next, I assessed the correlation between reovirus replication and anti-tumor effect in canine melanoma cell lines. Western blotting detected reovirus proteins in reovirus-infected CMeC1 and KMeC cells, and further revealed that combination treatment (i.e., reovirus infection in the presence of KU60019) yielded increased levels

of these proteins at each time point (Fig. IV-4A). This analysis was extended by quantifying the progeny virus in the supernatant using the $TCID_{50}$ assay. In 3 of 4 tested canine melanoma cell lines (CMeC1, KMeC, and CMGD2, but not in LMeC), the combination treatment yielded apparent increases in the number of progeny viruses compared to treatment with reovirus alone (Fig. IV-4B). To prove that viral replication is involved in the cell death effect of the combination of reovirus and KU60019, I used western blotting to assess the accumulation of reovirus structural proteins and cleavage of caspase-3 in CMeC1 subjected to the combination treatment in the presence of ribavirin, an anti-viral reagent (Rankin, JT. *et al*., 1989). Notably, ribavirin treatment completely suppressed both reovirus replication and caspase-3 cleavage (Fig. IV-4C). Furthermore, to extend the observation above to human cancer cell lines, western blotting revealed that the reovirus structural proteins and cleaved caspase-3 accumulated to higher levels in T-24 cells subjected to the combination treatment than in those treated with either reagent alone (Fig. IV-S5A and IV-S5B).

The combination of KU60019 and reovirus enhances reovirus disassembly, but not

virus entry

To investigate the biological roles and functions of ATM in the reovirus replication cycle, each step of the replication cycle was analyzed during the treatment with reovirus and ATM inhibitor. The upregulation of JAM-A, the reovirus receptor, might be associated with sensitivity to virus-induced cell death (Stiff, A. *et al*., 2016, Kelly, KR. *et al*., 2015). Addressing the potential effect of the ATM inhibitor on expression of the reovirus receptor in canine cells was complicated by the lack of availability of an antibody with specificity for the canine-specific JAM-A protein. Instead, I employed another experimental approach (*See Methods*). As shown in Fig. IV-4D, pre-incubation of cells with KU60019 enhanced reovirus replication at 12 and 24 hr compared to cells exposed to reovirus alone. This result suggested that ATM inhibition had no effect on the expression of the virus receptor. Next, I sought to test whether the effect of ATM inhibition was mediated via the proteolytic step of reovirus replication. For this purpose, I examined the enhancement of viral replication using protease-stripped reovirus virions (infectious subviral particles, ISVPs), which are capable of infecting cells lacking virus receptors and cells that have lost their ability to

un-coat incoming virions (Alain, T. *et al*., 2006, Alain, T. *et al*., 2007, Marcato, P. *et al*., 2007). Subsequent western blotting (Fig. IV-4E) demonstrated that KU60019 showed no effect on reovirus replication after addition of ISVPs at early time points (at 6 hr and 12 hr), indicating that KU60019 influences an event before viral disassembly. However, at 24 hr, reovirus protein levels were elevated in CMeC1 cells treated with the combination of KU60019 and ISVPs; at 48 hr, the combination treatment yielded significant potentiation of cell growth inhibition compared to either component alone (Fig. IV-S6), in parallel to the results of Fig. IV-1. I infer that this delayed effect (at 24 hr and after) reflects the production of and infection by intact virus after one replication cycle (approximately 18 hr (Hiller, BE. *et al*., 2015)), given that the production of intact virus was potentiated by the combination treatment. These results suggested that the enhancement of reovirus replication in ATM inhibitor-treated cells represents an effect on some step in the interval from virus attachment to proteolysis.

Endosomal acidification and proteolytic activity by the combination of KU60019 and reovirus

Disassembly of the reovirus particle in the endosome is required for the replication cycle following internalization of the virus and depends on acidification of the endosome (Mainou, BA. and Dermody, TS., 2012, Sturzenbecker, LJ. *et al*., 1987). To analyze the effect of the ATM inhibitor on the pH of the endosome, we used LysoTracker-Red, a dye which exhibits increased fluorescence at the low pH typical of endosomes and lysosomes (Fig. IV-5A and IV-5B). Although the fluorescence intensity of LysoTracker-Red was not significantly altered compared to mock-treated cells following treatment with either reovirus or KU60019 alone, fluorescence was significantly increased with the combination treatment (Fig. IV-5B). Confocal microscopy confirmed this result, showing that the number of LysoTracker-positive dots was elevated in cells treated with combination of reovirus and KU60019 (Fig. IV-5B). These data suggested that the combination treatment potentiated the acidification of endosomes/lysosomes.

The endosomal acidification modulates the activity of some proteases such as cathepsins (Sturzenbecker, LJ. *et al*., 1987, Blum, JS. *et al*., 1991, Authier, F. *et al*., 1996). Therefore, we evaluated the cathepsin B activity in CMeC1 cells treated as in the

above experiments. Cells exposed to reovirus alone exhibited nominal decreases in cathepsin B activity, although the effect fell short of significance ($p = 0.06$ compared to mock-treated cells; Fig. IV-5C). However, combination treatment restored the level of cathepsin B activity to a value similar to that seen with mock treatment. These results implied that the effect of KU60019 treatment is mediated by enhanced proteolysis of the lysosomal-enclosed reovirus particle. Thus, I hypothesized that combination treatment potentiates reovirus replication by yielding decreased pH in endosomes and lysosomes, leading to increased cathepsin activation.

Reovirus infection induces the phosphorylation of ATM but not influences on V-ATPase complex

Infection by some viruses has been shown to induce phosphorylation of ATM, resulting in the induction of DNA damage (Passaro, C. *et al*., 2013, Sinclair, A. *et al*., 2006, Hau, PM. *et al*., 2015); however, the mechanism linking ATM activity to replication of mammalian reovirus remains unclear. At an early stage of infection (12 hr), reovirus induced phosphorylation of ATM in cell line CMeC1, but this modification

was abrogated by KU60019 (Fig. IV-6). A similar pattern was observed in A549 (Fig. IV-S7). Next, I examined whether reovirus induced DNA damage in cancer cells by determining the phosphorylation state of p53 and γH2A.X, proteins that are known to be regulated by ATM and are known to detect DNA damage (Kozlov, SV. *et al*., 2011). Notably, reovirus did not induce phosphorylation of these proteins (Fig. IV-S8, IV-S9A, and IV-S9B). This observation suggested that reovirus infection leads to increases in the phosphorylation of ATM in cancer cells without associated DNA damage, leading to the enhancement of reovirus replication.

Next, to reveal the mechanism of acidification of endosome, I conducted a co-immunoprecipitation assay of V-ATPase proton pump units. The V-ATPase, a biological rotary motor that mediates endosomal/lysosomal acidification, is a protein complex composed of two domains: a peripheral V1 domain, consisting of 8 subunits (A, B, C, D, E, F, G, and H); and a membrane-bound V0 domain, consisting of 5 subunits (a, b, c, d, and e)(Marshansky, V. *et al*., 2014). Assembly and/or disassembly of the V1 and V0 domains plays a crucial role in maintaining the vacuolar organelle's pH. A previous study showed that phosphorylated ATM interacts with the E-G

dimerization of the V-ATPase proton pump, leading in turn to an increase in the endosomal pH (Kang, HT. *et al*., 2017). In the present work, I was unable to detect interactions among V-ATPase subunits in A549/ATP6V1G1 treated with reovirus and KU60019 (Fig. IV-S10). However, this shortcoming may have reflected the low sensitivity of the co-immunoprecipitation assay. Further studies will be needed to elucidate the mechanism(s) linking reovirus-induced ATM phosphorylation and endosomal acidification.

DISCUSSION

In this study, I screened a drug library to identify new drugs that enhance reovirus cytotoxicity. As a result, I identified an ATM inhibitor. Previous reports demonstrated that many kinds of anti-cancer drugs have synergistic anti-tumor effects on cancer cells when combined with reovirus (Rajani, K. *et al.*, 2016, Sei, S. *et al*., 2009, Roulstone, V. *et al*., 2013, Heinemann, L. *et al*., 2011, Hamano, S. *et al*., 2014, Kelly, KR. *et al*., 2012). However, the present work represents the first report to my knowledge that an ATM inhibitor can be used as a combination drug with reovirus treatment. Based on my observations, the combinatorial effects of reovirus and the ATM inhibitor resulted in reovirus-related apoptosis and cell cycle arrest at G2/M in most canine melanoma cell lines as well as in human cancer cell lines, with the exception of CMGD2 (a canine melanoma line) and Colo679 (a human melanoma line). The specificity of the ATM inhibitor in our study was supported by a cell survival assay that treated *ATM* knock-out canine melanoma cell lines with reovirus. Although reovirus treatment yielded higher cytotoxicity when combined with KU60019 than with the *ATM* knock-out, all knock-out cell lines exhibited higher susceptibility to reovirus

compared to the isogenic wild-type (ATM^{+}) cell lines. I hypothesize that KU60019 inhibits not only ATM but also other kinases (members of the phosphatidylinositol 3-kinase (PI3K)-related kinase (PIKK) family)) (Golding, SE. *et al*., 2009), in a dose-dependent manner, leading to high-efficiency virus replication and cytotoxicity.

I further examined the effect of the combination treatment on the ATM phosphorylation that is associated with reovirus replication in cancer cells. These experiments were inspired by observations of the effects of human herpes simplex virus-1 (HSV-1), hepatitis C virus and human immunodeficiency virus-1 infection in other cell lines (Li, H. *et al*., 2008, Alekseev, O. *et al*., 2014, Machida, K. *et al*., 2006, Ryan, EL. *et al*., 2016). For those viruses, ATM activation supports viral replication, such that the inhibition of ATM negatively regulates replication. In contrast, it was unknown whether ATM activation is associated with mammalian reovirus replication. I am aware of only one relevant report, which demonstrated that two ATM-deficient cell lines (L3 lymphoblastoid cells and Granta mantle cell lymphoma cells) were more susceptible to reovirus than were other cell lines (Kim, M. *et al*., 2010). However, the relationship between reovirus replication, oncolysis, and ATM deficiency was not

proven in that study. In the present work, I identified a putative mechanism for the potentiation of reoviral replication by the inhibition of ATM. To confirm the biological roles and functions of ATM in the reovirus replication cycle, each step of the replication cycle was analyzed. I found that inhibition of ATM enhanced the endosomal proteolysis of the reovirus particle via endosomal acidification and re-activation of protease. Previous work has shown that endosomal acidification and protease activity are essential for reovirus replication (Alain, T. *et al*., 2007, Sturzenbecker, LJ. *et al*., 1987, Ebert, DH. *et al*., 2002). Therefore, upregulation of the proteolysis step was expected to enhance the efficiency of reovirus-mediated cell killing. However, in the present study, I was unable to demonstrate a mechanism whereby ATM inhibition leads to acidification of the endosome.

Compared to KU55933 (the library-identified compound), KU60019 has greater specificity and is considered a much improved ATM kinase inhibitor. However, neither KU55933 or KU60019 are suitable for *in vivo* studies, given the low aqueous solubility and low bioavailability of these compounds (Biddlestone-Thorpe, L. *et al*., 2013, Pike, KG. *et al*., 2018, Vecchio, D. *et al*., 2015). The ATM inhibitor AZD0156

was recently reported (Pike, KG. *et al*., 2018) and shown to exhibit superior pharmacokinetics with the potential for oral dosing; this compound is the subject of an ongoing phase I clinical trial being performed by AstraZeneca. I hope to evaluate the combination of reovirus and AZD0156 in xenograft mice harboring canine melanoma cell lines.

Taken together, my results suggested that the ATM inhibitor KU60019 enhances reovirus-induced anti-tumor effects in canine and human cancers. This synergy may provide a route to resolving the limited efficacy of reovirus treatment of cancers. Although the mechanism linking ATM activity and endosomal acidification remains unknown, I confirmed that treatment with the ATM inhibitor up-regulated viral proteolysis, resulting in increased viral replication. Given that the incidence of adverse events may be increased in combination treatment, *in vivo* experiments (e.g., mouse xenograft studies) will be needed to test this combination therapy. Nonetheless, these findings support further investigation of this combination therapy for the treatment of canine and human cancer patients.

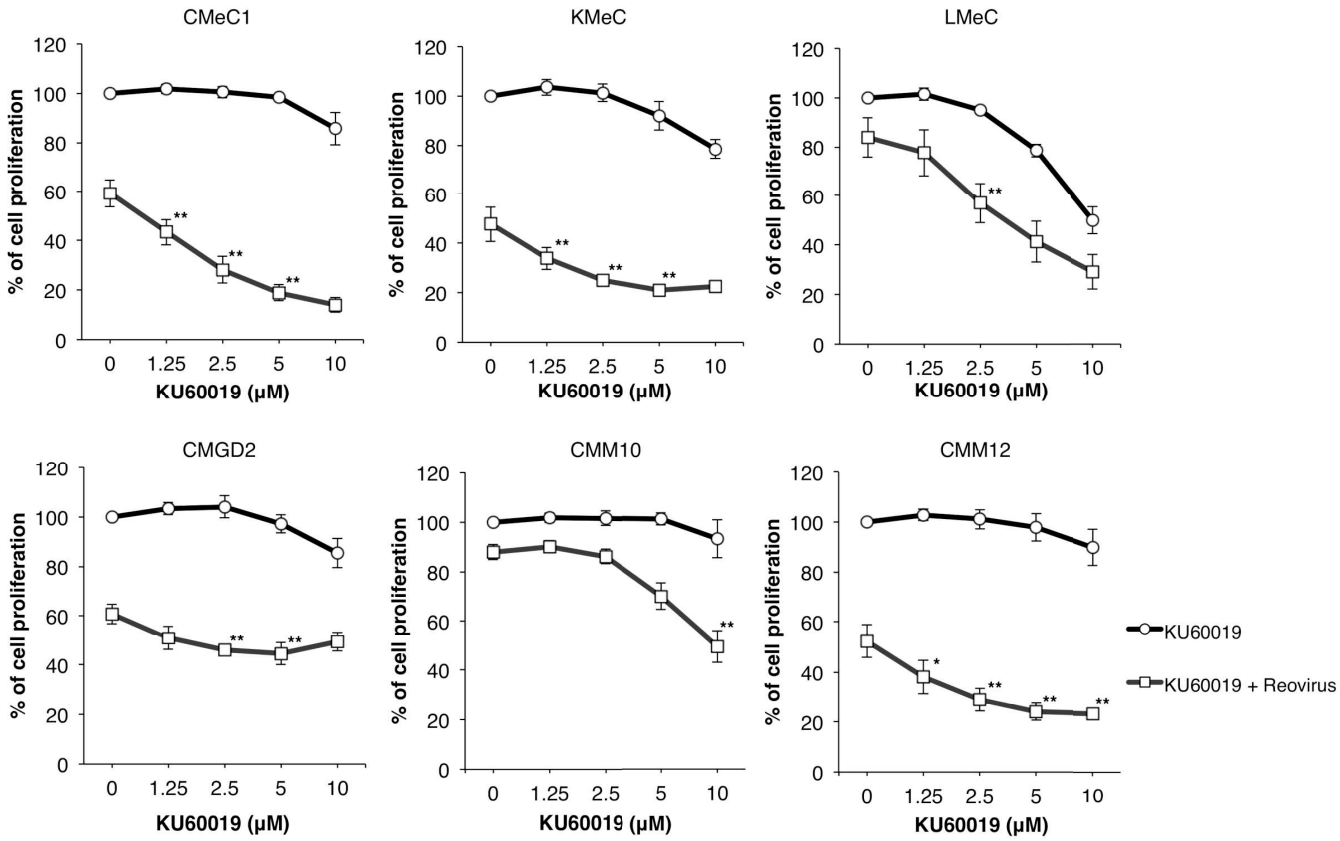

Fig. IV-1. ATM inhibitor KU60019 enhances reovirus-induced cell growth inhibition in canine melanoma cell lines

To evaluate cell proliferation, canine melanoma cell lines (CMeC1, KMeC, LMeC, CMM10, CMM12, and CMGD2) were treated with reovirus (MOI 100 for all cell lines except CMGD2 at MOI 10) and KU60019 (indicated concentration) for 48 hr before adding CCK-8 reagent. Data are expressed as the mean ± SD from at least three independent experiments. *p* values were calculated for the comparison between reovirus alone and reovirus combined with KU60019. To focus on the additional effects provided by KU60019, significance was tested only where no significant difference was

observed between mock control and KU60019 alone. Turkey-Kramer test, *$p < 0.05$, **$p < 0.01$.

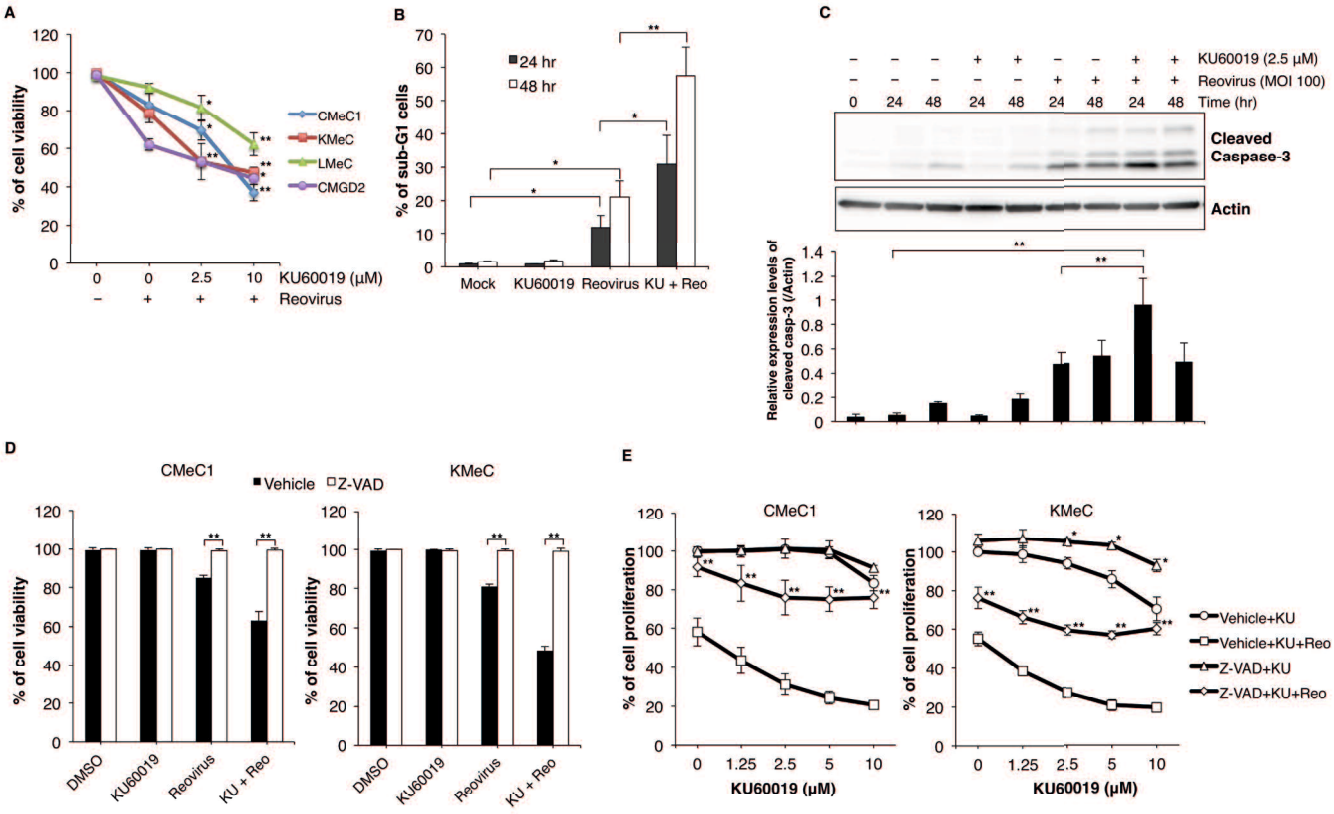

Fig. IV-2. The combination of KU60019 and reovirus induces apoptotic cell death

(A) CMeC1, KMeC, and LMeC were treated with reovirus (MOI 100) and KU60019 (2.5 and 10 μM), and CMGD2 was treated with reovirus (MOI 10) and KU60019 (2.5 and 10 μM). After a 48-hr incubation, cell viability was quantified by the trypan blue exclusion test. Data are expressed as the mean ± SD from at least three independent experiments. *p* values were calculated for the comparison to reovirus alone. Turkey-Kramer test, $*p < 0.05$, $**p < 0.01$. (B) The sub-G1 population was analyzed in CMeC1 treated with reovirus (MOI 100) and KU60019 (2.5 μM) for 24 and 48 hr. The cell numbers and stages were quantified using flow cytometry. Data are expressed as the mean + SD derived from three independent experiments. Student's t-test, $*p < 0.05$, $**p$

< 0.01. (C) Cleaved caspase-3 levels in CMeC1 treated with reovirus (MOI 100) and KU60019 (2.5 μM) for the indicated time are shown in the upper panel. The relative level of cleaved caspase-3 normalized to actin was quantified from three independent experiments. Data are expressed as the mean + SD. Turkey-Kramer test, *$p < 0.05$, **$p < 0.01$. (D, E) The effects of co-treatment for 48 hr with Z-VAD-FMK (50 μM) along with the combination of reovirus (MOI 100) and KU60019 (2.5 μM or indicated various concentrations) were quantified using the trypan blue exclusion test (D) or the CCK-8 cell viability assay (E). Data are expressed as the mean ± SD from at least three independent experiments. *p* values were calculated for the comparison to the vehicle sample. Student's t-test, *$p < 0.05$, **$p < 0.01$.

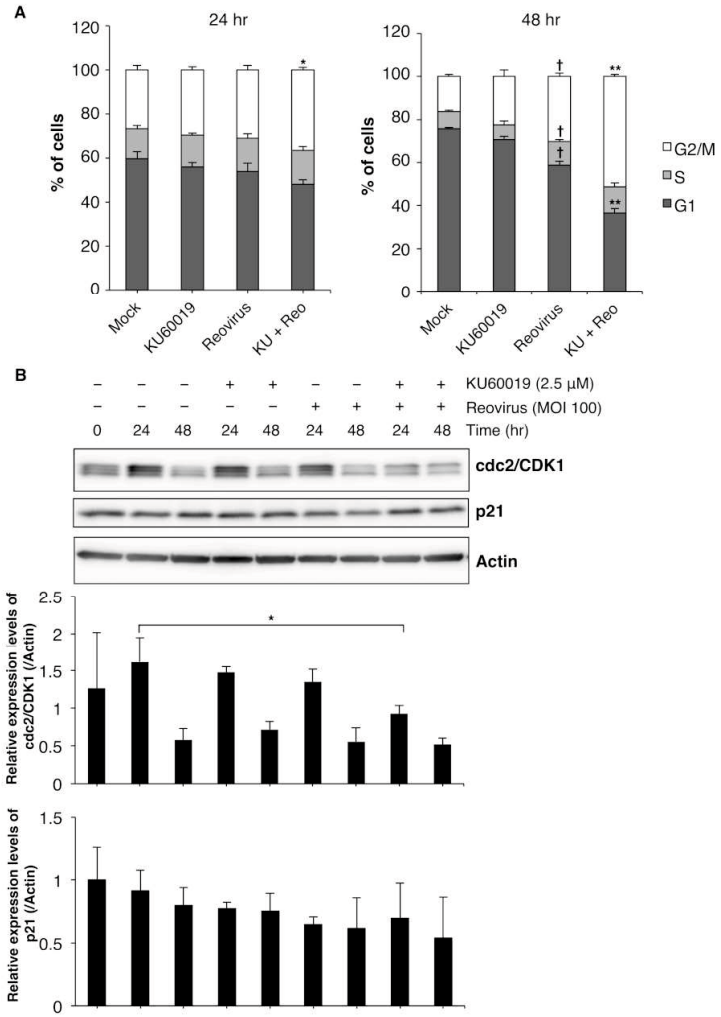

Fig. IV-3. The combination of KU60019 and reovirus induces cell cycle arrest at G2/M in canine melanoma cells

(A) CMeC1 was treated with reovirus (MOI 100) and KU60019 (2.5 μM). After a 48-hr incubation, the cell cycle of CMeC1 cells was assessed with propidium iodide (PI) staining. The mean + SD were derived from three independent experiments. *p* values were calculated for the comparison between "Reo" and "KU+Reo". Student's t-test, $*p < 0.05$, $**p < 0.01$. In addition, *p* values were calculated for the comparison between "Mock" and "Reo". Student's t-test, $^{\dagger}p < 0.01$. (B) cdc2 and p21 protein expression levels in CMeC1 treated as described in (A) are shown in the upper panel. The relative

level of each protein normalized to actin was quantified from three independent experiments. Mean + SD are shown. Turkey-Kramer test, *$p < 0.05$, **$p < 0.01$. The membrane in Fig. IV-2C was reprobed and used for this panel.

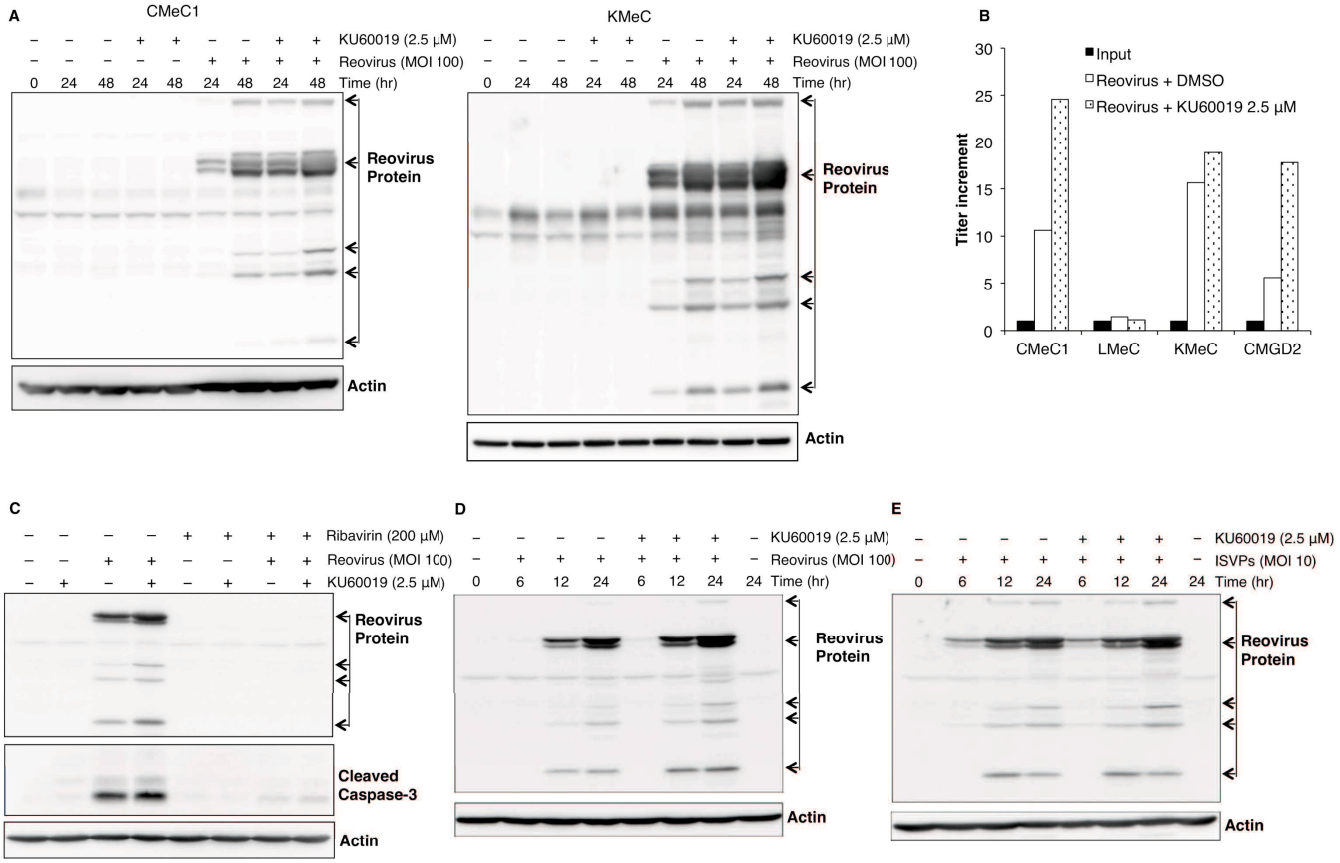

Fig. IV-4. Reovirus replication is enhanced by KU60019 treatment

(A) Reovirus structural proteins were detected using anti-reovirus polyclonal antibody. Cell lysates were collected from CMeC1 and KMeC cells treated as indicated. Actin was used as a protein loading control. (B) Supernatants of reovirus (MOI 100 for CMeC1, KMeC, and LMeC, or MOI 10 for CMGD2) -infected cell lines treated with KU60019 (2.5 μM) were harvested after a 48-hr incubation, and virus titers were determined by the $TCID_{50}$ assay. The fold increase of reovirus titer represents values calculated from the titer of progeny virus divided by the titer of input virus. (C) Effects of ribavirin (200 μM) in CMeC1 treated with combination of reovirus (MOI 100) and KU60019 (2.5 μM) for 24 hr were assessed by western blotting using anti-reovirus

antibody and anti-cleaved caspase-3 antibody. Actin was used as a protein loading control. (D, E) CMeC1 cells were treated with the combination of KU60019 (2.5 μM) and reovirus virions (MOI 100) or ISVPs (MOI 10), and reovirus structural proteins were detected by western blotting using anti-reovirus polyclonal antibody. Actin was used as a protein loading control.

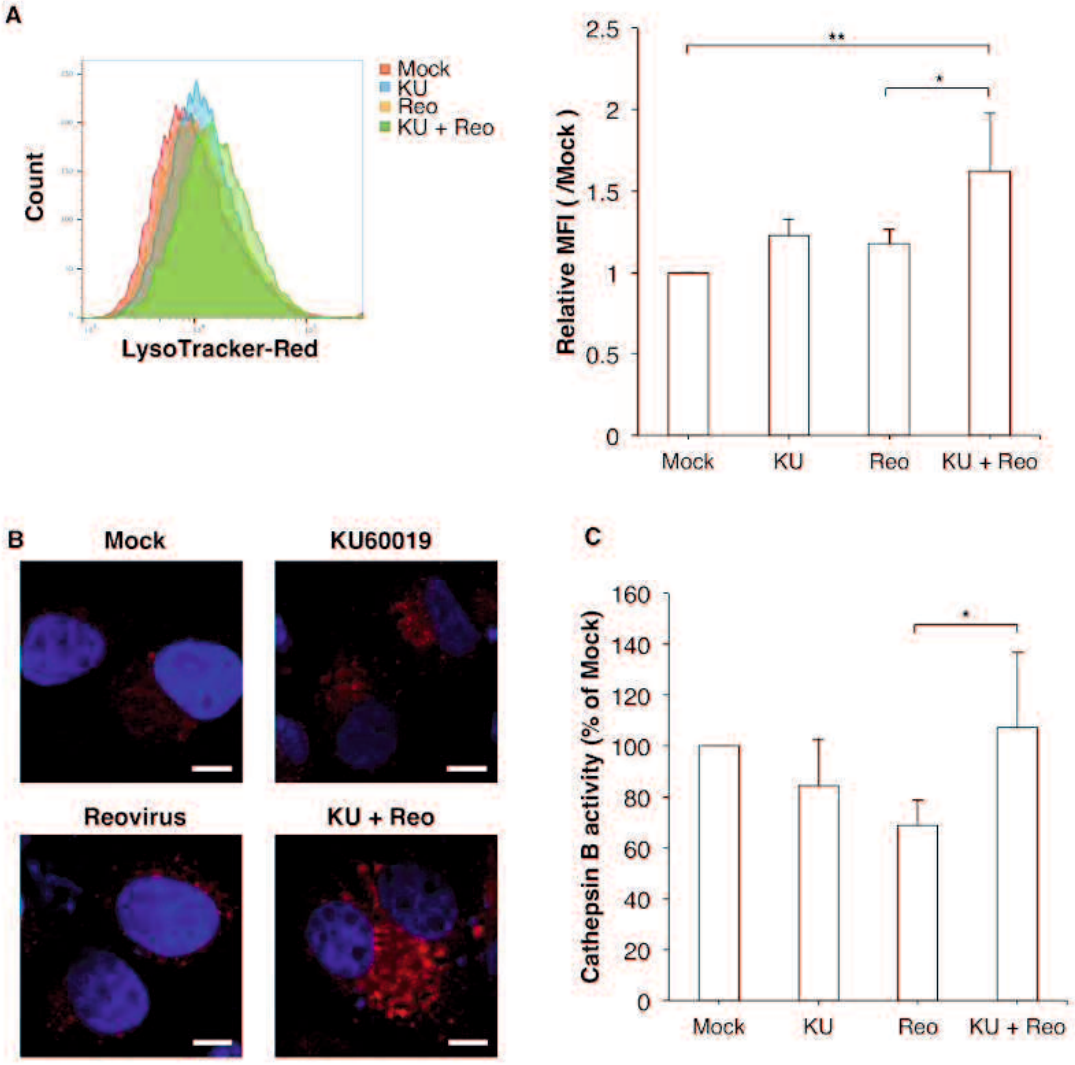

Fig. IV-5. The combination of reovirus and KU60019 promotes the proteolysis of reovirus via endosomal acidification and activation of cathepsin B

(A, B) The acidification of endosomes/lysosomes was determined by LysoTracker-Red staining. CMeC1 cells were treated with reovirus (MOI 100) and KU60019 (2.5 μM) for 24 hr before staining. (A) Histogram overlay of LysoTracker-Red staining of each

sample is shown for representative data from one of four independent experiments. Relative median fluorescence intensity (MFI) values relative to mock treatment are indicated. Mean + SD are shown from four independent experiments. Turkey-Kramer test, *$p < 0.05$, **$p < 0.01$. (B) Representative images of samples from each treatment groups are visualized using confocal microscopy at a 100x magnification. Nuclei were stained with DAPI. Scale bar: 10 μm. (C) The enzyme activity of cathepsin B in CMeC1 cells treated as described above was measured and normalized to the value obtained with mock treatment. Mean + SD are shown from five independent experiments. Turkey-Kramer test, *$p < 0.05$.

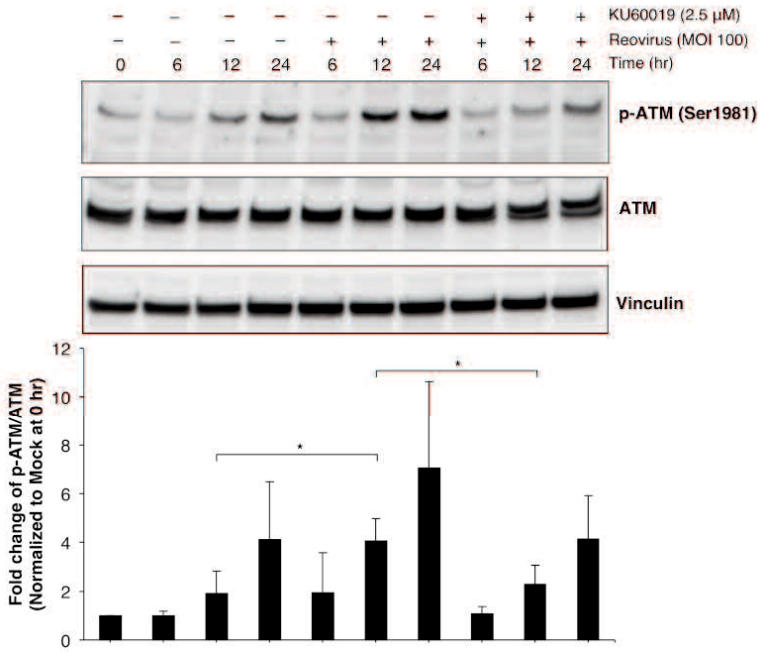

Fig. IV-6. Reovirus infection induces the phosphorylation of ATM in cancer cells

Phospho-ATM and total ATM expression levels were assessed by western blotting of lysates from CMeC1 cells treated with reovirus (MOI 100) and KU60019 (2.5 μM) for the indicated times. Vinculin was used as a protein loading control. The graph shows the relative level of each protein (normalized to vinculin) quantified from four independent experiments. The fold change of phospho-ATM divided by total ATM was normalized to the value of Mock at 0 hr. Mean + SD are shown. Turkey-Kramer test, $*p < 0.05$.

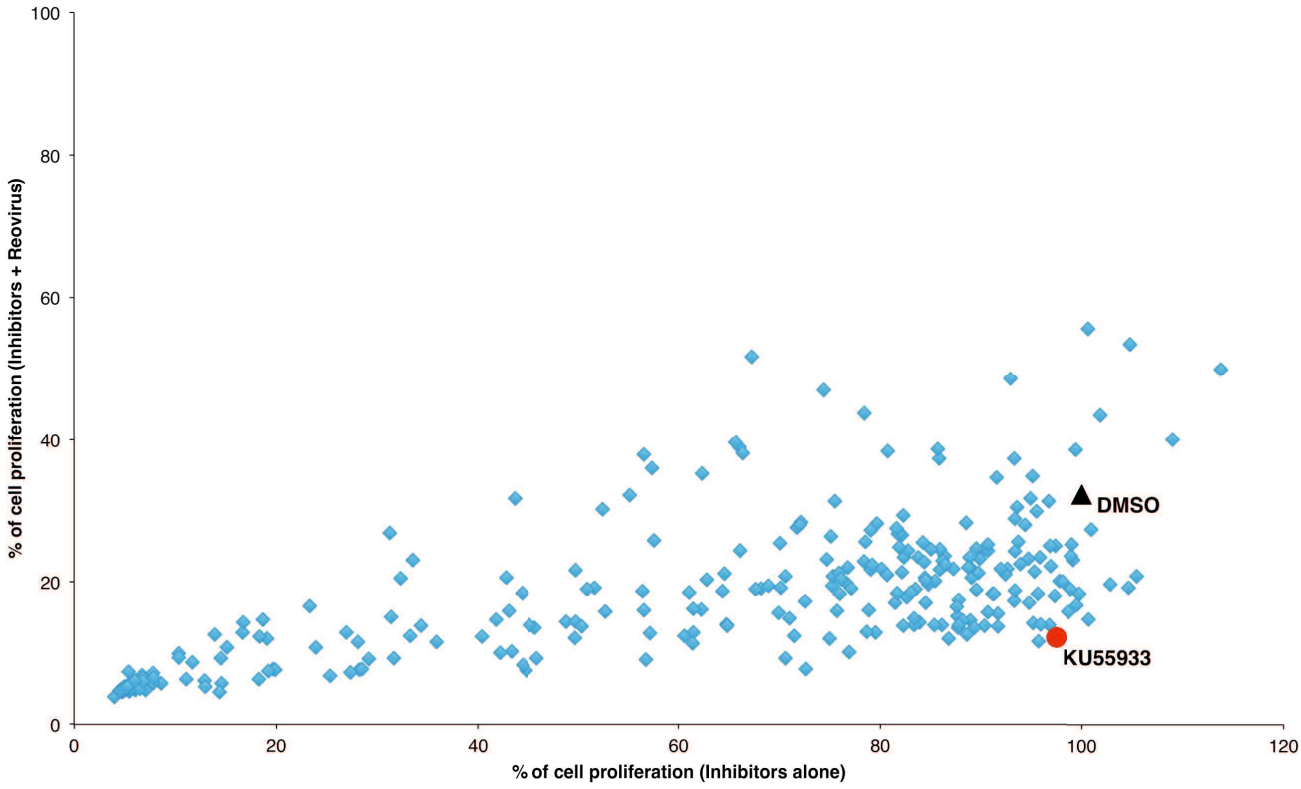

Fig. IV-S1. Drug screening in a reovirus-infected canine melanoma cell line

To identify drugs that potentiate reovirus cytotoxicity, we screened SCADS inhibitor kits (Kits 1, 2, and 3) comprising a total of 285 compounds. CMeC1 cells were treated with 10 μM of each inhibitor alone (x-axis), or each inhibitor and reovirus (MOI 100) (y-axis) for 48 hr, followed by the addition of the CCK-8 reagent. Both axes indicated the % of cell proliferation as compared with the untreated cells. The diamond-dots, the triangle, and the circle, represented each compound, DMSO, and KU55933-treated samples, respectively. KU55933 alone showed no effect on cell proliferation by itself (x-axis), but combination with reovirus yielded more cytotoxicity (y-axis).

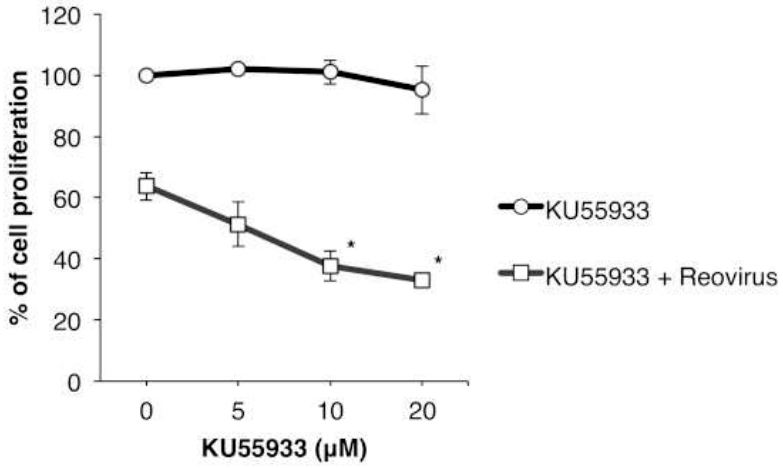

Fig. IV-S2. ATM inhibitor KU55933 enhances reovirus-induced cell growth inhibition in the CMeC1 canine melanoma cell line

To evaluate cell proliferation, a canine melanoma cell line (CMeC1) was treated with reovirus (MOI 100) and KU55933 (indicated concentration) for 48 hr before adding the CCK-8 reagent. Data are expressed as the mean ± SD of three independent experiments. *p* values were calculated for the comparison between reovirus alone and reovirus combined with KU55933. To focus on the additional effects provided by KU55933, significance was tested only where no significant difference was observed between mock control and KU55933 alone. Turkey-Kramer test, $*p < 0.05$.

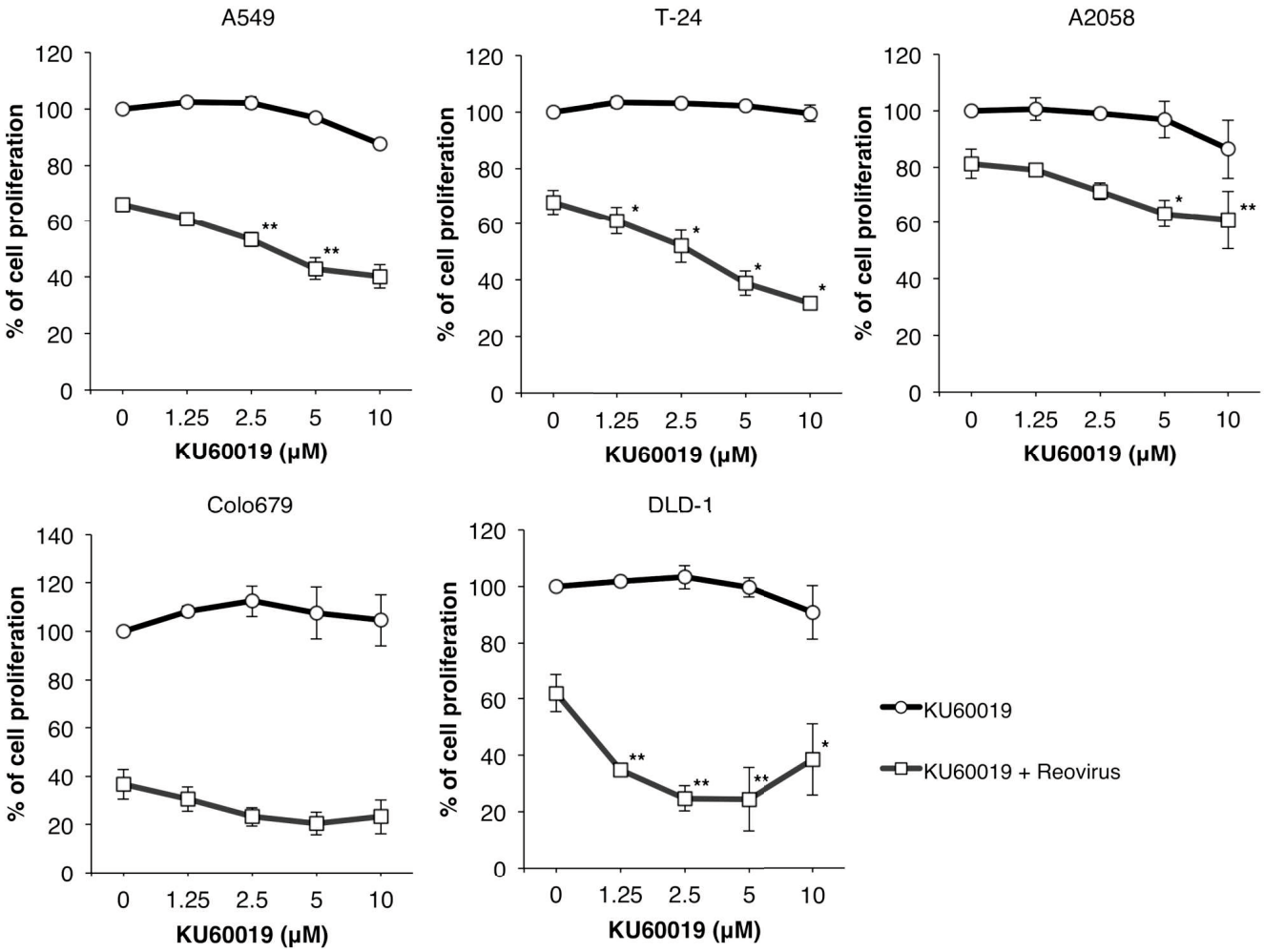

Fig. IV-S3. ATM inhibitor KU60019 enhances reovirus-induced cell growth inhibition in human cancer cell lines

To evaluate cell proliferation, five human cancer cell lines (A549, T-24, A2058, Colo679, and DLD-1) were treated with reovirus (MOI 10) and KU60019 (indicated concentration) for 48 hr before adding the CCK-8 reagent. Data are expressed as the mean ± SD from at least three independent experiments. *p* values were calculated for the comparison between reovirus alone and reovirus combined with KU60019. To focus on the additional effects provided by KU60019, significance was tested only where no

significant difference was observed between mock control and KU60019 alone. Turkey-Kramer test, *$p < 0.05$, **$p < 0.01$.

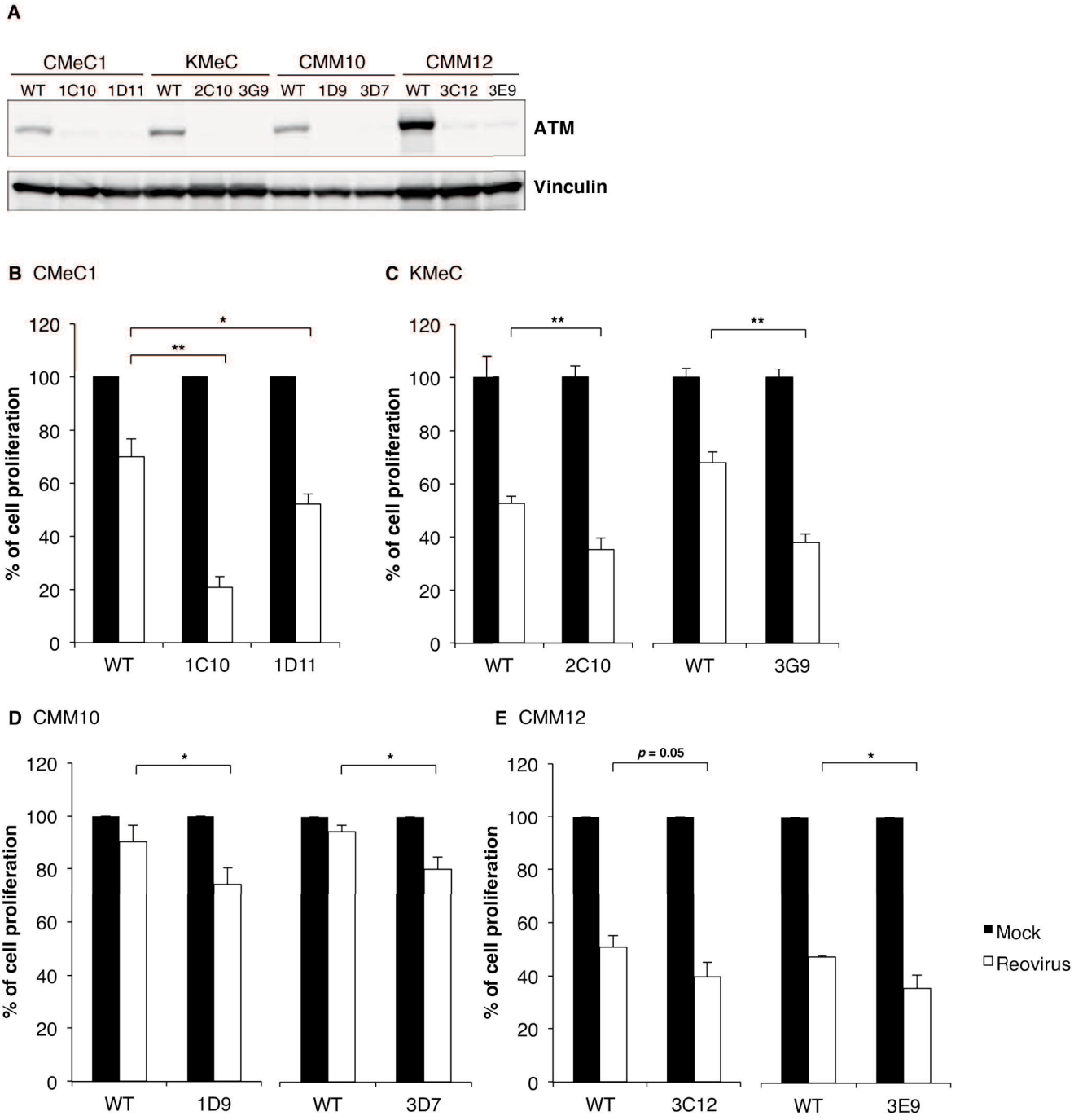

Fig. IV-S4. Reovirus susceptibility is enhanced by *ATM* knock-out

(A) The accumulation of ATM in the indicated melanoma cell lines was examined by western blotting. Vinculin was used as a protein loading control. (B) To evaluate cell

proliferation, *ATM* knock-out canine melanoma cell lines (CMeC1, KMeC, CMM10, and CMM12) were treated with reovirus (MOI 100) for 48 hr before adding the CCK-8 reagent to determine cell viability. Mean + SD are shown. Student's t-test, $*p < 0.05$, $**p < 0.01$.

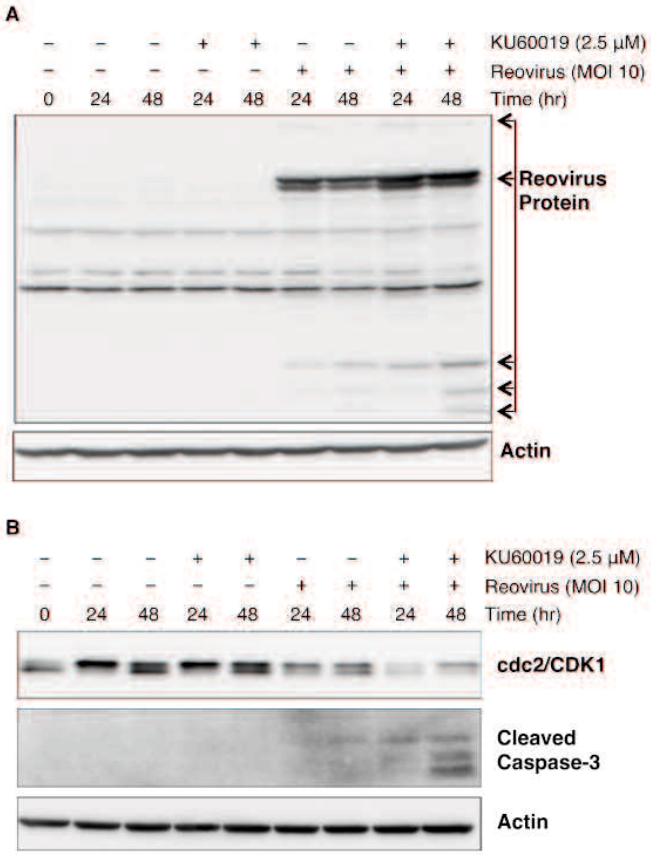

Fig. IV-S5. Protein expression in a human cancer cell line treated with the combination of KU60019 and reovirus

(A, B) The cell lysates were collected from T-24 cells treated with KU60019 (2.5 μM) and reovirus (MOI 10) for the indicated times. The levels of reovirus structural proteins, cdc2/CDK1, and cleaved caspase-3 were determined by western blotting. Actin was used as a protein loading control.

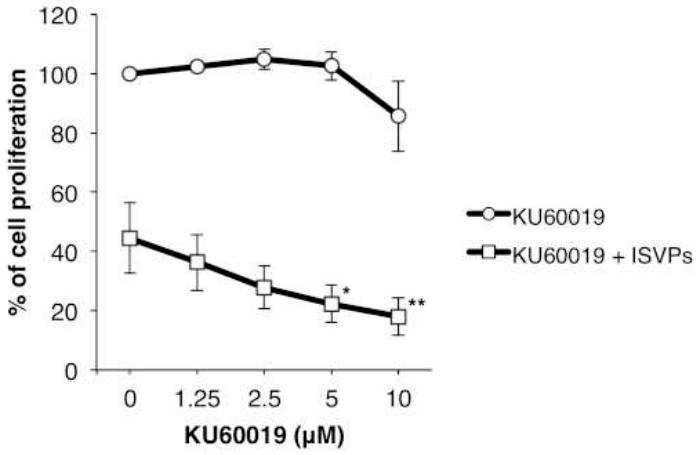

Fig. IV-S6. The combination of KU60019 and ISVPs enhances cell growth inhibition in a canine melanoma cell line

ISVPs were generated using chymotrypsin (see *Methods*). To evaluate cell proliferation, cells of the canine melanoma cell line CMeC1 were treated with ISVPs (MOI 10) and KU60019 (indicated concentration) for 48 hr before adding the CCK-8 reagent. Data are expressed as the mean ± SD from three independent experiments. *p* values were calculated for the comparison between ISVPs alone and ISVPs combined with KU60019. To focus on the additional effects provided by KU60019, significance was tested only where no significant difference was observed between mock control and KU60019 alone. Turkey-Kramer test, $*p < 0.05$, $**p < 0.01$.

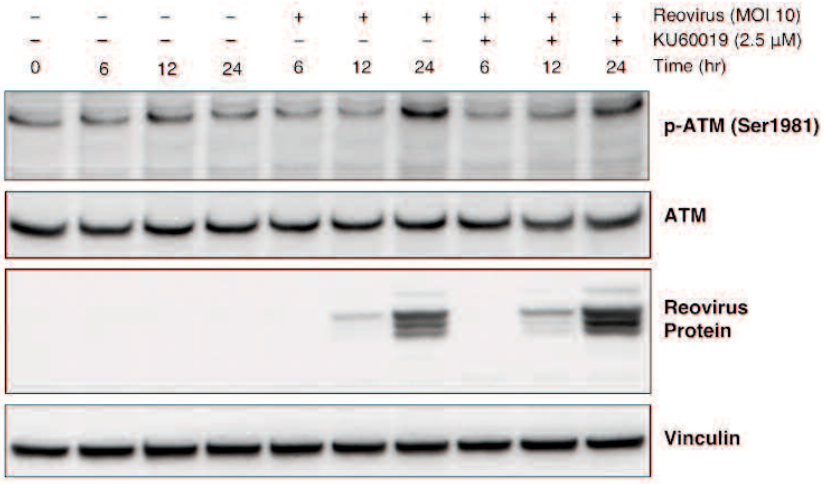

Fig. IV-S7. Reovirus infection induces phosphorylation of ATM in a human cancer cell line

The levels of phospho-ATM, total ATM, and reovirus structural proteins were determined by western blotting of lysates from A549 cells treated for the indicated times with reovirus (MOI 10) and KU60019 (2.5 μM). Vinculin was used as a protein loading control.

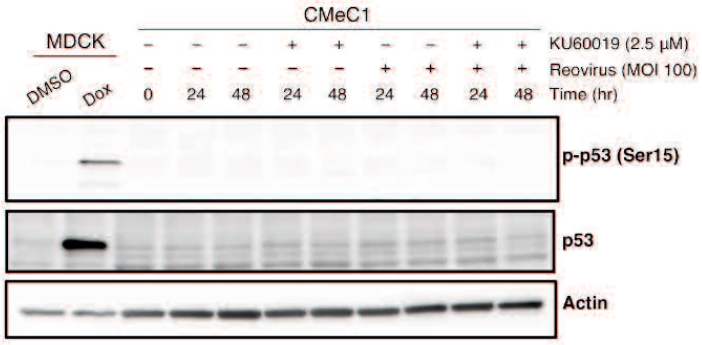

Fig. IV-S8. Reovirus does not induce the DNA damage response in a canine melanoma cell line

The levels of phopho-p53 and total p53 were determined by western blotting of lysates from CMeC1 cells treated for the indicated times with reovirus (MOI 100) and KU60019 (2.5 μM). MDCK (Madin-Darby canine kidney epithelial cells) treated with doxorubicin (Dox; MP BIOMEDICALS, LLC, Santa Ana, CA; 0.5 μM) for 12 hr was used as a positive control for DNA damage response. Actin was used as a protein loading control.

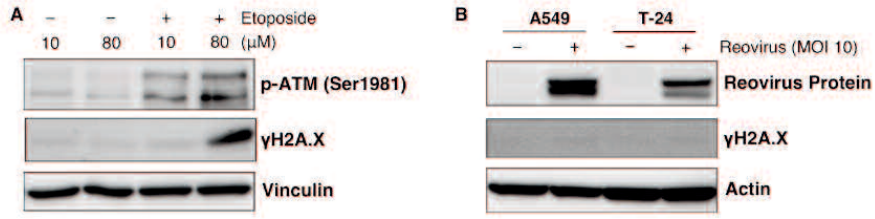

Fig. IV-S9. Reovirus does not induce the DNA damage response in human cancer cell lines

(A) As a positive control for γH2A.X accumulation, we used cell lysates from A549 cells treated with 10 or 80 μM etoposide (Wako, Tokyo, Japan) for 12 hr. The levels of γH2A.X and phospho-ATM were determined by western blotting. Vinculin was used as a protein loading control. (B) To evaluate the DNA damage response induced by reovirus, A549 and T-24 cells were treated with reovirus at MOI 10 for 24 hr. The levels of γH2A.X and reovirus structural proteins were determined by western blotting. Actin was used as a protein loading control.

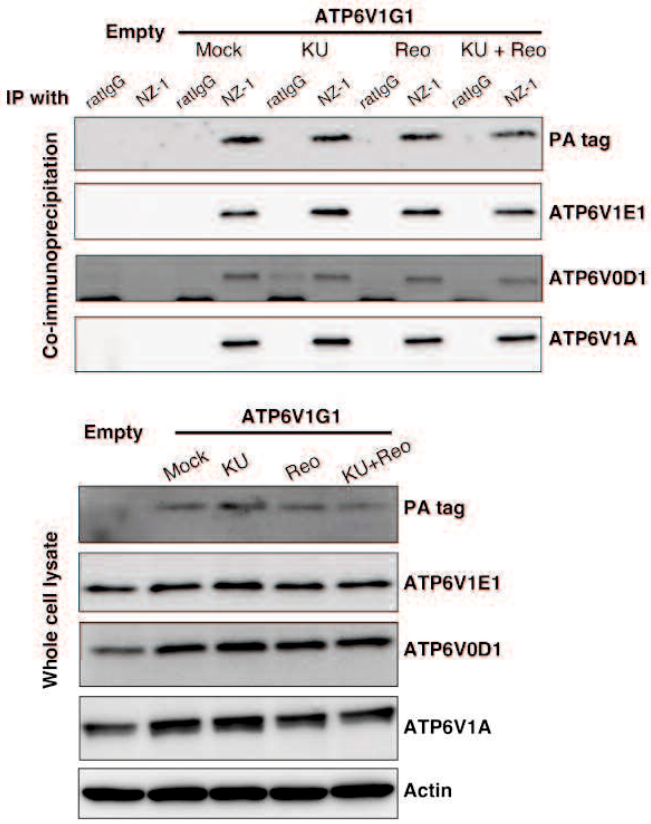

Fig. IV-S10. Co-immunoprecipitation assay with the PA-tagged protein in a human cancer cell line

The interactions of individual V-ATPase subunits were assessed by co-immunoprecipitation with the PA-tagged protein. Cell lysates were collected from A549/ATP6V1G1 treated with reovirus (MOI 10) and KU60019 (2.5 μM) for 24 hr. A549/Empty (empty vector) was used as a negative control for co-immunoprecipitation of PA-tagged protein. Actin was used as a protein loading control.

Table IV-1. Antibodies used for Western blotting

No	Antibody	Product no.	Source
1	Rabbit monoclonal anti-cleaved caspase-3(Asp175)	#9661	Cell Signaling Technology, Danvers, MA
2	Rabbit polyclonal anti-cdc2	#77055	Cell Signaling Technology
3	Rabbit polyclonal anti-p21	sc-397	Santa Cruz Biotechnology, Dallas, TX
4	Rabbit polyclonal anti-reovirus	-	Produced by our laboratory
5	Mouse monoclonal anti-ATM	sc-377293	Santa Cruz Biotechnology
6	Mouse monoclonal anti-phospho-ATM(Ser1981)	NB100-306	Novus Biologicals, Littleton, CO
7	Mouse monoclonal anti-p53	ADI-KAM-CC002	Enzo Life Science, Farmingdale, NY
8	Rabbit monoclonal anti-phospho-p53(Ser15)	#9284	Cell Signaling Technology
9	Mouse monoclonal anti-Vinculin	14-9777-80	eBioscience, San Diego, CA
10	Mouse monoclonal anti-V-ATPase D1	sc-393322	Santa Cruz Biotechnology
11	Mouse monoclonal anti-ATP6V1A	GTX633544	GeneTex, Irvine, CA
12	Rabbit polyclonal anti-ATP6E	GTX114056	GeneTex
13	Mouse monoclonal anti-beta-actin	A2228	Sigma-Aldrich, St. Louis, MO
14	Rabbit monoclonal anti-phospho-Histone H2AX(Ser139)	#9718	Cell Signaling Technology
15	Rat monoclonal anti-PA-tag (Biotin conjugated)	-	Dr. Yukinari Kato, Tohoku University, Sendai, Japan
16	Rat IgG2a isotype control	-	Dr. Yukinari Kato
17	Goat anti-mouse IgG-HRP	STAR117P	Bio-rad Laboratories, Hercules, CA
18	Donkey anti-rabbit IgG-HRP	711-035-152	Jackson ImmunoResearch Laboratories, West Grove, PA
19	Streptavidin-HRP	ab7403	Abcam, Cambridge, UK

Chapter 5

Oncolytic reovirus therapy: Pilot study in dogs with spontaneously occurring tumors

SUMMARY

Oncolytic virotherapy is a novel treatment involving replication-competent virus in the elimination of cancer. I have previously reported the oncolytic effects of reovirus in various canine cancer cell lines. This study aims to evaluate the safety profile of reovirus and determine a recommended dosing regimen in canine cancer. Nineteen dogs with various tumors, mostly of advanced stages, were treated with reovirus, ranging from 1.0×10^8 to 5.0×10^9 $TCID_{50}$ given as intratumor injection (IT) or intravenous infusion (IV) daily for up to five consecutive days in one or multiple treatment cycles. Adverse events (AEs) were graded according to the Veterinary Cooperative Oncology Group- Common Terminology Criteria for Adverse Events (VCOG-CTCAE) v1.1. Viral shedding, neutralizing anti-reovirus antibody (NARA) production and immunohistochemical (IHC) detection of reovirus protein in the tumors were also assessed. AE was not observed in most dogs and events were limited to Grade I or II fever, vomiting, diarrhea and inflammation of the injected tumor. No infectious virus was shed and all dogs had elevated NARA levels post-treatment. Although IHC results were only available in six dogs, four were detected positive for reovirus protein. In conclusion, reovirus is well-tolerated and can be given safely to tumor-bearing dogs according to the dosing regimen used in this study without significant concerns of viral

shedding. Reovirus is also potentially effective in various types of canine tumors.

RESULTS

Characteristics of study dogs

Information of the study dogs, including tumor grading, tumor staging and treatment history, is shown in Table V-2. A total of 19 dogs with a range of naturally occurring tumors were enrolled in this study. MCT, lymphoma, oral melanoma and soft tissue sarcoma represented the most common tumors in this study. Tumor metastasis was present in eight dogs and more than half of the dogs were in advanced tumor stages with associated systemic signs. All dogs, except Dogs 2, 4 and 11, had been previously treated with some form of cancer therapy prior to study enrollment.

Treatment course

The dosing regimen and route of administration are shown in Table V-2. Reovirus was given directly into the tumor in ten dogs while the other nine were given IV. Twelve dogs were given more than one cycle of reovirus, where up to 18 treatments were given in two dogs. The highest reovirus titer was 2.5×10^{10} $TCID_{50}$ per cycle, which comprised of five injections of 5.0×10^{9} $TCID_{50}$. The median number of cycles administered was two (range one to eight). No dose reduction due to AEs was implemented in this study.

Adverse events (AEs)

No AE of Grade 3 and above was observed in this study (Table V-3). The most common AEs were Grade 1 and 2 fever and diarrhea. Vomiting, bleeding and pain of the treated tumor were observed infrequently. These AEs were observed within a few days after administration of reovirus but resolved within a couple of days with supportive medical treatment. No hematological-based AE was seen.

Virology and virokinetics

Viral RNA fragments can be detected via RT-PCR in at least one of the samples, except for Dogs 4, 8, 16, 18 and 19 (Table V-4). Inactive virus fragments can be found most commonly in the serum, far exceeding virus fragments detected in the saliva, urine and feces. Only 2 serum samples (collected during Cycle 1, Day 3 and Day 5 from Dog 5) tested positive for live virus.

Detection of neutralizing anti-reovirus antibodies (NARA)

As compared to the other dogs, Dogs 9, 10 and 18 had high NARA titer pre-treatment. Despite that, all dogs experienced an increase of NARA titer during the study (Fig. V-1A). Dog 2 represents dogs with a low NARA titer fold increase at 1,024 (Fig.

V-1B), while NARA titer fold increase as high as 65,536 can be observed (Dog 5; Fig. V-1C).

Treatment response

Although response evaluation was not the primary objective of this study, I noted that five dogs had size reduction of the target lesion as the best outcome while six dogs experienced some notable form of alleviation of clinical symptoms related to the disease such as improved urination, reduced tumor pain, increased mobility or recovery of lost appetite. Tumor biopsies were also obtained from six dogs for immunohistochemical (IHC) staining and four samples were positively stained for reovirus.

Case examples are shown in Figures V-2 (MCT; Dog 2) and V-3 (oral melanoma; Dog 18). Both these cases were treated with IT administration of reovirus. In Figure V-2, a single injection of reovirus in Cycle 1 induced an inflammation that lasted for a few days. Treatment was repeated once a day for three consecutive days in Cycle 2, which did not induce an inflammatory response that was observed in Cycle 1. The course of treatment in a case with oral melanoma (Dog 18) is shown in Figure V-3A. The dog was given six cycles of reovirus once a day for three consecutive days in

each cycle. As the tumor was located at the caudal of the soft palate, measurement using a caliper was not possible. Nonetheless, photographic recordings were able to capture the anti-tumor effects (Fig. V-3B). The positive results of IHC staining provided further evidence that the tumor size reduction was due to reovirus replication (Fig. V-3C). With reovirus treatment, the dog became able to swallow its food again due to relief of the blockage in the oral cavity. Unfortunately, extensive tumor invasion into the nasal turbinate was discovered at Day 53 post-treatment (Fig. V-3D), suggesting that reovirus directly induced its effects only at the injection site but did not exert adequate anti-tumor effects at the inaccessible side of the tumor.

Based on these preliminary results, I came to a conclusion that reovirus has the potential to be effective as a treatment for many spontaneous tumors in dogs.

DISCUSSION

Oncolytic viruses, especially reovirus, have been receiving an increased interest in recent years due to their remarkable potential to treat various human cancers. Reovirus is ubiquitous in geographical distribution and has the capacity to infect nearly every known mammalian species, including humans and dogs (Rosen, L., 1962). Natural reovirus infection often goes unnoticed due to its asymptomatic nature (Fukumi, H. *et al*., 1969, Hwang, CC. *et al*., 2014). This unmodified virus works through three major mechanisms namely direct tumor lysis (Etoh, T. *et al*., 2003, Norman, KL. *et al*., 2002, Thirukkumaran, CM. *et al*., 2010), the innate immunity involving natural killer cells (Adair, RA. *et al*., 2012, Hall, K. *et al*., 2012, Zhao, X. *et al*., 2015), and the adaptive immunity via tumor-associated antigens (TAA) educated T cells (White, CL. *et al*., 2008, Gujar, SA. *et al*., 2010, Prestwich, RJ. *et al*., 2008). Based on this multimodal anti-tumor mode of action, I am confident of the potential of reovirus as a potent oncolytic virus in canine cancers. This study reports the results of a pilot study of reovirus given to canine patients with various tumors. Three major findings were confirmed in this study: reovirus is safe and well-tolerated, doses up to 5.0×10^9 $TCID_{50}$ can be given either IT or IV, and reovirus is potentially effective in various types of canine tumors.

Based on information derived from mouse models and humans (Gollamudi, R. *et al*., 2010), I postulated that the starting reovirus dose would be safe at 1.0 x 10^8 $TCID_{50}$. This dose was given as a single injection to the first two dogs, and since no serious AE was observed, the dose and dosing frequency were increased. The highest dose used in this study was 5.0 x 10^9 $TCID_{50}$, which was still notably lower than reovirus doses used in human. I did not pursue higher reovirus doses even though in human clinical trials, the maximum tolerated dose (MTD) has not been reached even at reovirus doses as high as 1.0 x 10^{10} $TCID_{50}$ was given IT (Forsyth, P. *et al*., 2008, Harrington, KJ. *et al*., 2010, Morris, DG. *et al*., 2013) and 3.0 x 10^{10} $TCID_{50}$ was given IV (Gollamudi, R. *et al*., 2010, Vidal, L. *et al*., 2008)

The IT and IV routes of administration each presents unique pros and cons in terms of ease of administration, virus dispersion and anti-tumor effects. IT allows immediate and direct exposure of the target tumor to a high dose of reovirus. By comparison, diluted reovirus given IV will be indirectly presented to the target tumor via cell carriage (Ilett, EJ. *et al*., 2011, Jennings, VA. *et al*., 2014). Nonetheless, reovirus given IT is limited to target tumors that are accessible and have a defined structure.

Almost half of the dogs (9 out of 19) did not show any AE, despite most of the dogs were considered to be in severe tumor stages. The observed AEs in dogs were

similar to those in humans, which were limited to low grade events resembling symptoms of a mild flu-like syndrome typical of a natural reovirus infection. Elevation of the NARA titer was observed in all dogs after reovirus treatment (Fig. V-1A) regardless of route of administration, which is consistent with the phenomenon observed in humans (Morris, DG. *et al*., 2013). The production of neutralizing antibodies and absence of significant AEs, even in dogs with severe disease, suggests that the antiviral defense mechanisms of the body are sufficiently protective against uncontrolled virus replication. The only concern is that neutralizing antibody might be the impeding factor for systemic delivery of reovirus (White, CL. *et al*., 2008), which should be further explored in studies using combination therapies such as gemcitabine (Lolkema, MP. *et al*., 2011), paclitaxel and carboplatin (Karapanagiotou, EM. *et al*., 2012) that have been reported to attenuate the NARA response and enhances clinical efficacy.

Besides taking into consideration AEs, viral shedding detection also plays an essential part in the risk analysis for this novel therapy. The first six dogs (Dogs 1, 2, 3, 4, 5 and 6) were hospitalized for a week after reovirus administration and bodily fluid samples were collected daily to monitor for viral shedding. Although inactive reovirus fragments can be detected in some of the saliva, feces and urine samples using RT-PCR,

the virus was not infectious. Therefore, decision was made to reduce the frequency of sample collection in subsequently enrolled dogs. Human studies detected a lower frequency of positive viral fragment detection in bodily fluids (Forsyth, P. *et al*., 2008, Morris, DG. *et al*., 2013) as compared to this study. The discrepancy might reflect a more extensive RT-PCR cycles (45 cycles) used in this study, leading to a higher sensitivity in viral fragment detection. Nonetheless, RT-PCR can only detect the presence of viral RNA fragments, which include non-infectious viral particles. The infectivity assay remains the only accurate method to assess the presence of live virus. In this study, none of the bodily fluids was tested positive for reovirus in the infectivity assay.

As this study was not designed to evaluate the anti-tumor activity of reovirus, dogs enrolled had heterogenous tumor types with variable tumor grading, and were not uniform in disease staging. Even so, size reduction of the target lesion were observed as the best outcome in some of the dogs after reovirus treatment, and owners were extremely satisfied with the minimal AEs and improvement of quality of life.

In conclusion, this study has provided evidence that reovirus serotype 3 Dearing (REOLYSIN®), up to a dose of 5.0×10^9 $TCID_{50}$ given by IT or IV, was safe and well-tolerated in tumor-bearing dogs. The recommended dose to be used in a

pivotal study will be between 1.0 x 10^9 $TCID_{50}$ and 5.0 x 10^9 $TCID_{50}$ daily for at least three consecutive days every two weeks. Treatment can be continued as long as it is tolerated and there is no evidence of disease progression. The best route of administration will depend on tumor type, location and extent of tumor metastasis. Reovirus treatment on an outpatient basis is considered suitable since there is no significant concern related to excretion of infectious virus. Evaluation of treatment response was highly suggestive that reovirus is effective in various canine tumor types. The results of this pilot study warrant further clinical trials to confirm these expectations in dogs.

A

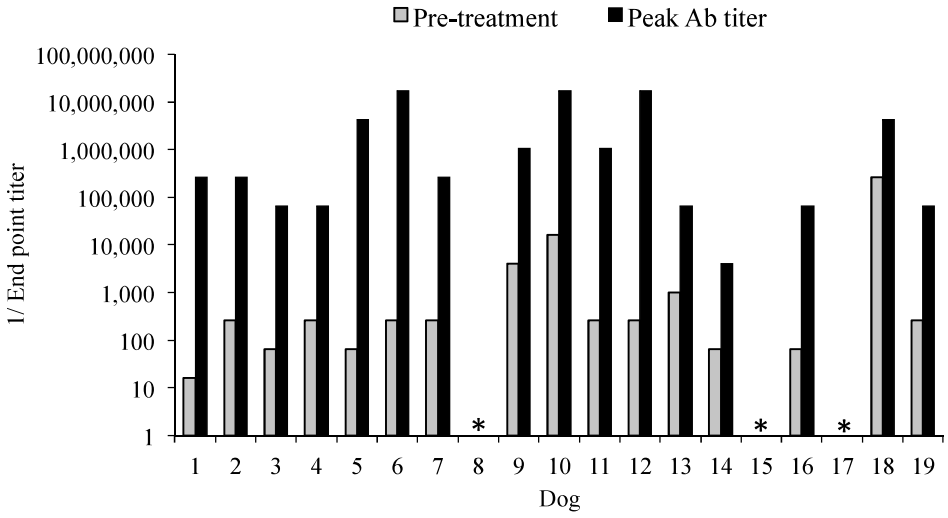
Pre-treatment
Peak Ab titer
1/ End point titer
100,000,000
10,000,000
1,000,000
100,000
10,000
1,000
100
10
1
*
1 2 3 4 5 6 7 8 9 10 11 12 13 14 15 16 17 18 19
Dog

B

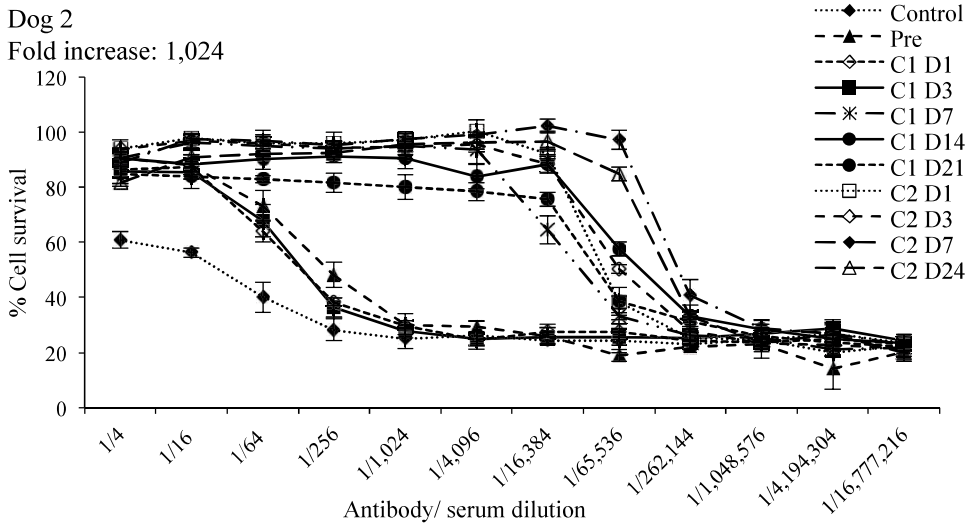
Dog 2
Fold increase: 1,024
Control
Pre
C1 D1
C1 D3
C1 D7
C1 D14
C1 D21
C2 D1
C2 D3
C2 D7
C2 D24
% Cell survival
120
100
80
60
40
20
0
1/4
1/16
1/64
1/256
1/1,024
1/4,096
1/16,384
1/65,536
1/262,144
1/1,048,576
1/4,194,304
1/16,777,216
Antibody/ serum dilution

C

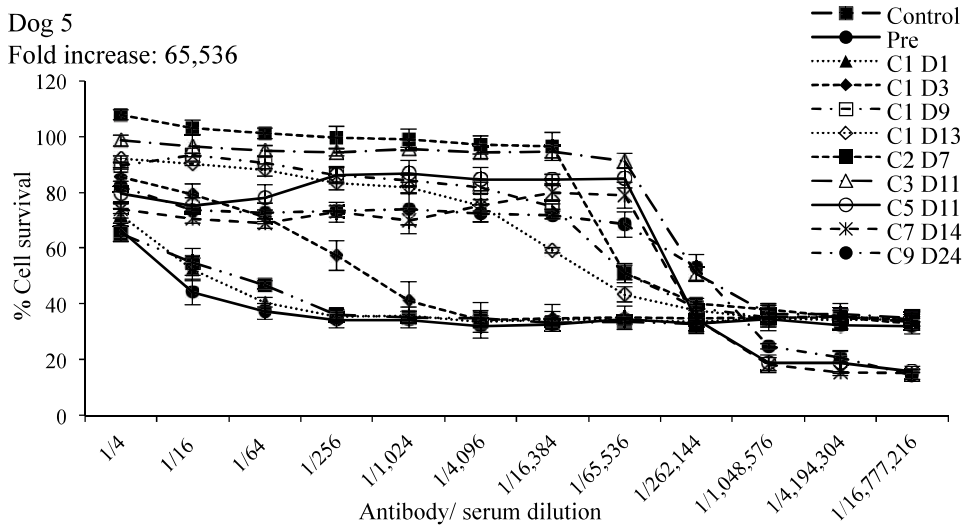
Dog 5
Fold increase: 65,536
Control
Pre
C1 D1
C1 D3
C1 D9
C1 D13
C2 D7
C3 D11
C5 D11
C7 D14
C9 D24
% Cell survival
120
100
80
60
40
20
0
1/4
1/16
1/64
1/256
1/1,024
1/4,096
1/16,384
1/65,536
1/262,144
1/1,048,576
1/4,194,304
1/16,777,216
Antibody/ serum dilution

Fig. V-1. Detection of neutralizing anti-reovirus antibodies (NARA).

(A) Pre-treatment (grey bars) and peak post-treatment (dark bars) NARA titer. Adequate serum samples were not collected from Dogs 8, 15 and 17 for analysis (*). (B) Dogs 2 and (C) Dog 5 are representatives of NARA profiles with low and high fold increase, respectively. MTT assay was performed with absorbance read at 550 nm and cell survival expressed as a percentage of a control population of untreated L929 cells. The control curve represents data using canine polyclonal antibody from naïve dog. The value of $n = 3$ replicates and error bars represent the standard deviation.

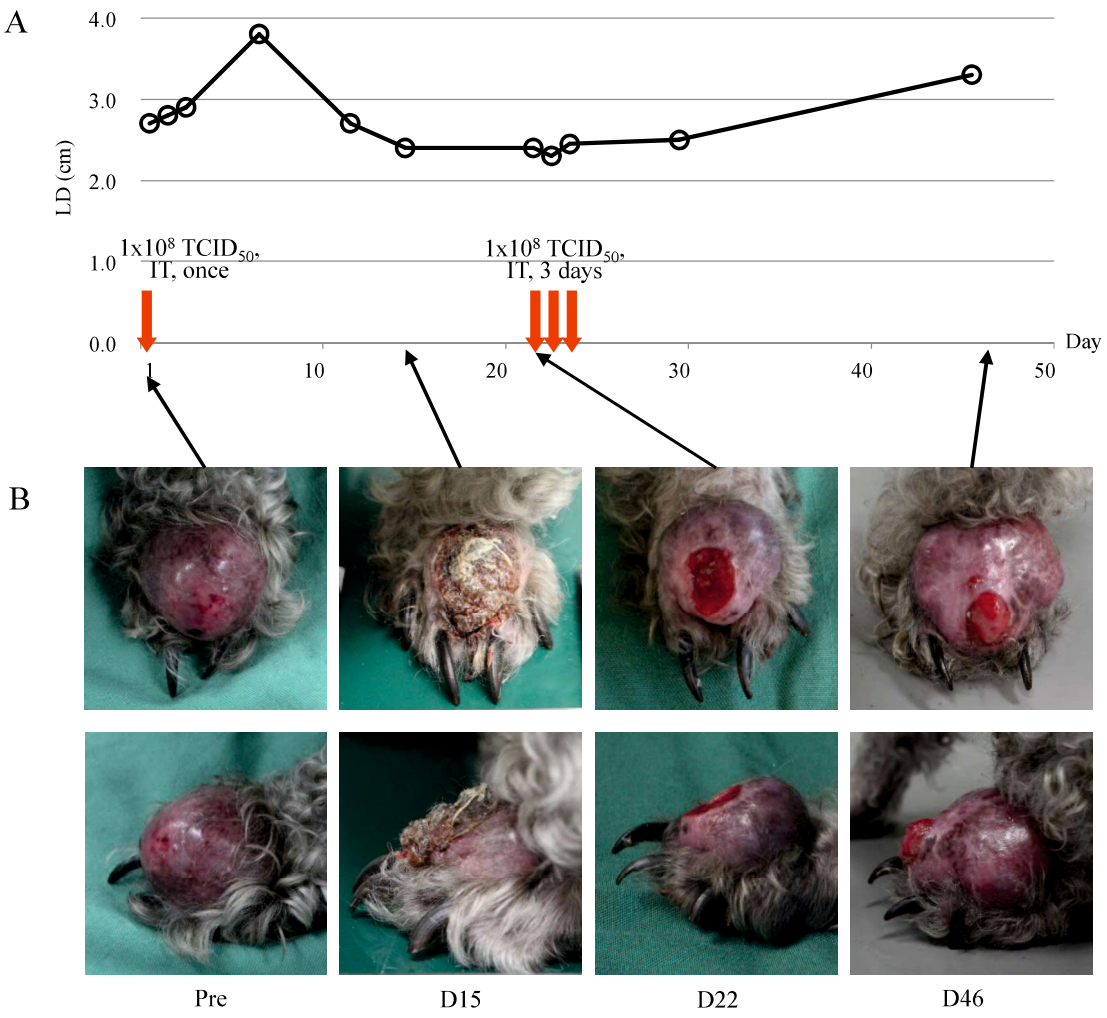

Fig. V-2. Anti-tumor response in a dog with canine mast cell tumor.

(A) Measurement of the longest diameter (LD) of the mast cell tumor (MCT) treated with intratumor injection (IT) of 1 x 10^8 $TCID_{50}$ reovirus in Dog 2. Red arrows indicate days of reovirus administration. (B) Pictures of the target tumor pre-treatment, Day 15, Day 22 and Day 46 post-treatment.

A

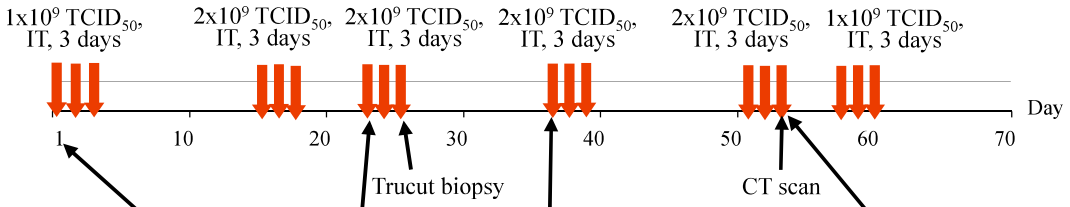

B

Pre

D37

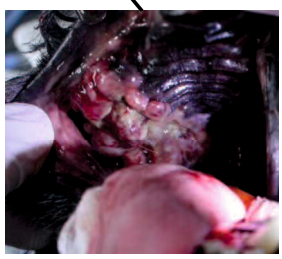

D23

D53

C

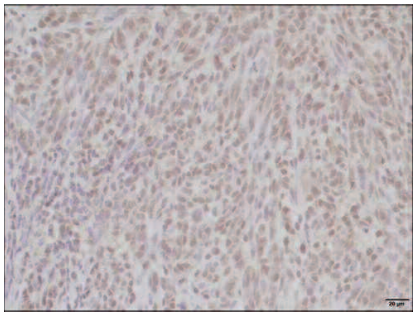

D

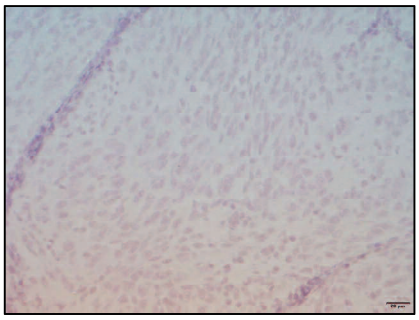

E

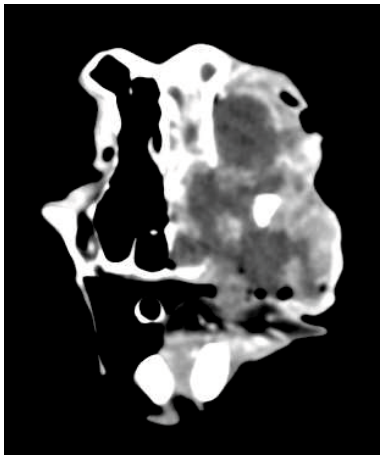

Fig. V-3. Anti-tumor response in a dog with canine oral melanoma.

(A) Dosing regimen of Dog 18 with oral melanoma treated with intratumor injection (IT) of 1 x 10^9 and 2 x 10^9 $TCID_{50}$ reovirus. Red arrows indicate days of reovirus administration. (B) Pictures of the target tumor pre-treatment, Day 23, Day 37 and Day 53 post-treatment. Immunohistochemical (IHC) staining of tumor biopsy taken at Day 25 post-treatment using (C) rabbit anti-reovirus antibody or (D) serum from non-immunized rabbit (isotype control). (E) CT scan performed at Day 53 indicating extensive tumor invasion into the nasal turbinate.

Table V-1. Study events

Event	Before enrollment	Treatment cycle*		Final visit**
		First injection	Subsequent injection(s)	
Demographics, medical history	✓			
Physical examination	✓	✓	✓	✓
CBC/ serum biochemistry	✓	✓		✓
Urinalysis	✓	✓		✓
Confirmatory diagnosis, including grading and staging	✓			
Measurement of target/ non-target lesion(s)	✓	✓	✓	✓
Photographic recording of target/ non-target lesion(s)	✓	✓	✓	✓
Inclusion/ exclusion	✓			
Owner consent	✓			
Reovirus administration		✓	✓	
Adverse event reporting		✓	✓	✓
Serum, saliva, feces and urine sample collection***		✓	✓	✓

* Treatment cycle consisted of a single injection, once a day injection for 3 or 5 consecutive days. For treatment cycle that consisted only of a single injection, events under first injection were performed. For treatment cycle that consisted of once a day injection for 3 or 5 consecutive days, events under first and subsequent injection(s) were performed. Treatment cycles were carried out continuously until refusal by owner or deterioration of the dog's condition.
** Events under final visit were carried out if the dog's condition allowed.
*** Serum, saliva, feces and urine samples were collected daily for the first week after reovirus administration in Dogs 1, 2, 3, 4, 5 and 6 as they were hospitalized for a week post-treatment.

Table V-2. Characteristics of study dogs and treatment course

Dog	Breed (Age)	Diagnosis, Tumor Grading (Metastatic Site)	Tumor Staging	Prev. Rx	Dose/ Tumor ($TCID_{50}$), No. of injection/ cycle, Route
1	Maltese (5Y8M)	Cutaneous MCT, Grade II [a] (submandibular LN)	T2N1M0 (Stage IIa)	Targeted therapy	1 x 10^8, 1x, IT
2	Toy poodle (15Y)	Cutaneous MCT [b]	T1N0M0 (Stage Ia)	-	Cycle 1: 1 x 10^8, 1x, IT; Cycle 2 (3 weeks apart): 1 x 10^8, 3x, IT
3	Dalmatian (12Y9M)	Inflammatory mammary CA, Grade III [c] (abdominal LN)	T3N0M0 (Stage IIIb)	Surgery, radiation therapy	Cycle 1: 1 x 10^9, 3x, IV; Cycle 2 (3 weeks apart): 5 x 10^9, 5x, IV
4	Shih tzu (11Y1M)	Esophageal cancer [d]	T2N0M0 (syst. signs present)	-	1 x 10^9, 5x, IV
5	Toy poodle (10Y2M)	TCC [d] (lung, Iliac LN)	T2N1M0 (syst. signs present)	Surgery, chemotherapy	Cycle 1: 1 x 10^9, 5x, IV; Cycle 2, 3, 4, 5, 6, 7 and 8 (1 to 2 week apart): 5 x 10^9, 1x, IV
6	FC retriever (12Y5M)	OSA [d] (lung)	T2N0M1 (syst. signs present)	Radiation therapy, chemotherapy	Cycle 1, 2 and 3 (2 weeks apart): 5 x 10^9, 5x, IV
7	M dachshund (14Y)	Extraskeletal OSA [d] (lung)	T2N1M1 (no syst. sign)	Surgery	1 x 10^9, 3x, IT
8	Papillon (11Y1M)	Multicentric and splenic LSA, high-grade [e] B cell	Stage Vb	Chemotherapy	Cycle 1: 1 x 10^9, 3x, IT (1 target tumor); Cycle 2 (5 days apart): 1 x 10^9, 3x, IT (2 target tumors)
9	Mix breed (12Y)	Cutaneous MCT [b]	T3N0M0 (Stage IIIa)	Surgery, medical	1 x 10^9, 3x, IT (3 target tumors)
10	M dachshund (10Y9M)	Oral melanoma [d] (lung)	T0N0M1 (Stage IVb)	Surgery	Cycle 1, 2, 3, 4, 5 and 6 (2 weeks apart): 1 x 10^9, 3x, IV
11	Beagle (Age Unk.)	Liposarcoma [b,f]	T2bN0M0 (Stage IIIa)	-	1 x 10^9, 3x, IT
12	AC spaniel (10Y2M)	Mammary CA, Grade II [c] (lung)	T0N1M1 (Stage Va)	Surgery	Cycle 1 and 2 (2 weeks apart): 1 x 10^9, 3x, IV
13	Beagle (9Y3M)	Hemangiopericytoma, Grade II [f]	T2aN0M0 (Stage IIb)	Radiation therapy	Cycle 1, 2 and 3 (2 weeks apart): 1 x 10^9, 3x, IT
14	M dachshund (8Y)	Hodgkin's lymphoma, Low grade [e]	Stage IVb	Chemotherapy	1 x 10^9, 3x, IV
15	Welsh corgi (10Y5M)	TCC [d] (inguinal LN)	T3N2M0 (syst. signs present)	Surgery	2.5 x 10^9, 5x, IV
16	Beagle (13Y10M)	Hemangiopericytoma, Grade I [f]	T1aN0M0 (Stage Ib)	Surgery, radiation therapy	Cycle 1: 1 x 10^9, 3x, IT; Cycle 2 and 3 (2 weeks apart): 5 x

Dog	Breed (Age)	Diagnosis, Tumor Grading (Metastatic Site)	Tumor Staging	Prev. Rx	Dose/ Tumor ($TCID_{50}$), No. of injection/ cycle, Route
					10^9, 3x, IT
17	M dachshund (12Y3M)	LSA, low/ int.-grade [e] B cell	Stage IVb	Chemotherapy	Cycle 1 and 2 (1 week apart): 1 x 10^9, 3x, IV
18	Toy poodle (11Y4M)	Oral melanoma [d]	T3N0M0 (Stage IIIb)	Surgery, radiation therapy, laser vaporization	Cycle 1: 1 x 10^9, 3x, IT; Cycle 2, 3, 4, 5 and 6 (1 to 2 weeks apart): 2 x 10^9, 3x, IT
19	M dachshund (13Y)	Oral melanoma [d]	T1N1M0 (Stage IIIa)	Radiation therapy, chemotherapy	Cycle 1: 1 x 10^9, 3x, IT; Cycle 2 and 3 (2 and 4 weeks apart): 1 x 10^9, 3x, IT (2 target tumors)

[a] Patnaik system for grading of canine mast cell tumor (London, CA. and Thamm, DH., 2013)

[b] Grading not determined

[c] Tumor grade based on histologic score in canine mammary neoplasms (Sorenmo, KU. et al., 2013)

[d] Grading not available

[e] Lymphoma histopathological grade

[f] Soft Tissue Sarcomas Grading System (Liptak, JM. and Forrest, LJ., 2013)

Abbreviations: AC spaniel American cocker spaniel CA Carcinoma, FC retriever Flat-coated retriever, LN Lymph Node, LSA Lymphosarcoma, M dachshund Miniature dachshund, M month, MCT Mast Cell Tumor, NA Not Available, ND Not Determined, OSA Osteosarcoma, Prev. Rx Previous Treatment, Syst. Systematic, TCC Transitional Cell Carcinoma, Unk. Unknown, Y year.

Table V-3. Adverse events (AEs)

Event	**Grade 1**	**Grade 2**	**Grade 3/ 4/ 5**	**Total, *n* = 19 (%)**
Fever	5	2	0	7 (36.8)
Diarrhea	3	3	0	6 (31.6)
Vomiting	1	1	0	2 (10.5)
Bleeding of injected tumor	2	2	0	4 (21.1)
Pain of injected tumor	1	1	0	2 (10.5)

Table V-4. Viral dissemination

Dog	RT-PCR serum	RT-PCR saliva	RT-PCR urine	RT-PCR feces
1	Pos D1	Pos D1, D3, D7, D9, D11 [a]	Neg	Pos D9, D13, D14 [a]
2	Pos C2D4	Pos C1D4, C1D5, C1D6 [a]	Pos C1D5, C1D7	Pos C1D6, C1D7 [a]
3	Pos C1D2, C1D3, C1D4	Neg	Pos C1D2	Neg
4	Neg	Neg	Neg	Neg
5	Pos C1D2, C1D3 [b], C1D4, C1D5 [b], C1D6, C3D7, C9D18, C9D21	Neg	Pos C1D1, C1D2, C1D3, C1D5, C4D10, C8D15, C9D18	Neg
6	Pos C1D1, C1D2, C1D3, C1D4, C1D5, C2D1, C2D2, C2D3, C2D4, C2D27	Pos C1D16, C2D4	Neg	Neg
7	Pos D4	Neg	-	Neg
8	Neg	Neg	Neg	Neg
9	Pos D3, D5	Pos D7	Neg	Neg
10	Pos C1D7	Neg	Neg	Neg
11	Pos D3, D5, D7	Neg	-	Neg
12	Pos C1D7, C2D9	-	-	-
13	Pos D7	-	-	-
14	Pos D3, D5	-	-	-
15	Pos D2	-	-	-
16	Neg	-	-	-
17	Pos D2, D7	-	-	-
18	Neg	-	-	-
19	Neg	-	-	-

Infectivity test was performed for samples that are positive in RT-PCR. All infectivity test results were negative unless stated otherwise.
[a] Infectivity test not done
[b] Positive for infectivity test
Abbreviations: Pos Positive, Neg Negative, - Not Available.

CONCLUSION

Recently, oncolytic viruses are gaining ground as a novel approach for cancer treatment in dogs (Sanchez, D. *et al*., 2018). Researchers have reported *in vitro* and *in vivo* studies using oncolytic viruses, which leads to growing interests in performing clinical trials. Our laboratory published the first report that reovirus can be an effective therapy in canine cancers. Of that, previous Ph. D. student, Dr. Hwang Chung Chew, investigated the anti-tumor effects of reovirus in canine mast cell tumor and lymphoma. Therefore, I focused on canine solid tumor such as melanoma, mammary gland tumor, osteosarcoma, and histiocytic sarcoma.

In Chapters 1 and 2, reovirus was shown to exhibit superior oncolytic activities in melanoma, mammary gland tumor and histiocytic sarcoma cell lines. We also found *in vitro* assay that reovirus induced cell death through caspase-3-dependent apoptosis and production of progeny viruses in susceptible cell lines. Among them, histiocytic sarcoma xenografted mice were treated with reovirus and showed complete suppression of tumor growth as compared to PBS-treated xenografted mice. These results suggest that a wide range of canine cancers is a potential candidate for oncolytic virotherapy using reovirus.

In human clinical trials, reovirus is usually used in combination therapy with chemotherapeutic drugs (Clements, D. *et al*., 2014). Chapter 3 shows that combination with reovirus and paclitaxel, gemcitabine, or carboplatin demonstrated synergistic anti-tumor effects against a canine mammary gland tumor cell line. Interestingly, we found that the combination treatments led to an increased activation of caspase-3 compared to reovirus alone. In addition, by screening many small molecule inhibitors in combination with reovirus, I identified the new role of ATM inhibitor KU60019 in Chapter 4. KU60019 enhanced the oncolytic potentials of reovirus in canine melanoma and human

cancer cell lines. I also elucidated this mechanism, and showed that ATM inhibition increased the virus replication through the upregulation of the endosomal proteolysis steps. To our best knowledge, this is a first report of combination treatment with reovirus and ATM inhibitor in human and canine cancer. Unfortunately, I could not carry out *in vivo* experiments in both Chapters. Even though further studies will be needed, these synergic effects may provide a route to resolve the limited efficacy of sole reovirus treatment against cancers.

The final chapter, Chapter 5 is the most important chapter in my PhD thesis and our laboratory works. Chapter 1 to 4 elucidated the oncolytic activity of reovirus at the bench. However, the most important question was whether this new therapy was safe and effective in clinical cancer patients. Therefore, I conducted the first reovirus clinical study in 19 dogs with various spontaneously occurring tumors, aligned with the progress of human clinical trials. The primary objectives of this chapter were to establish the safety profile of reovirus in treated dogs and to determine the recommended dosing regimen. As a result, adverse events were not observed in most of dogs and events were limited to Grade I and II. I showed that the recommended dose to be used in a next clinical study will be between 1.0×10^9 $TCID_{50}$ and 5.0×10^9 $TCID_{50}$ daily for at least three consecutive days every two weeks. Although response evaluation is not the primary objective of this study, I noted that five dogs had the size reduction of the target lesions as the best outcome while six dogs experienced some notable form of alleviation of clinical symptoms related to the disease such as improved urination, reduced tumor pain, increased mobility or recovery of anorexia. This final chapter warranted further large clinical trials to approve for clinical usage in canine cancers.

In my studies, I only focused on the direct cytotoxicity of reovirus against

cancer cells. However, reovirus also has the anti-tumor activity via innate and adaptive immune responses and renders it an attractive component of immunotherapy (Gong, J. *et al*., 2016). Pre-clinical and clinical data showed that injection of oncolytic viruses can inducd the infiltration of effector T cells, which is indicated that oncolytic virotherapy has a potential of changing the local tumor microenvironment from an immunologically cold to a hot tumor (LaRocca, CJ. and Warner SG, 2018). Therefore, as a next step, further investigation of immune profile in reovirus therapy will be required to reveal the robust mechanism of reovirus indirect cytotoxicity. I hope that oncolytic reovirus as a standard cancer therapy in dogs will be established near future.

ACKNOWLEDGMENTS

I would like to express my sincere gratitude and appreciation to *Prof. Takuya Mizuno* for being a truly ideal supervisor and for kindly guiding me all steps of the way. I am highly indebted to him for his stimulating suggestions and encouragement that helped me in all the time of research and writing of this thesis.

I would like to appreciate to *Assis. Prof. Yuki Nemoto* for assisting me with my experiments and English presentations. Her meticulous comments were an enormous help to me.

I am grateful to *Assoc. Prof. Shunsuke Noguchi* (*Laboratory of Veterinary Radiology, Graduate School of Life and Environmental Sciences, Osaka Prefecture University*), *Prof. Masaru Okuda* (*Laboratory of Veterinary Internal Medicine, Joint Faculty of Veterinary Medicine, Yamaguchi University*), *Prof. Yasuyuki Endo* (*Laboratory of Veterinary Internal Medicine, Joint Faculty of Veterinary Medicine, Kagoshima University*), *Assoc. Prof. Kenji Baba* (*Laboratory of Veterinary Internal Medicine, Joint Faculty of Veterinary Medicine, Yamaguchi University*), *Assoc. Prof. Takashi Ohama* (*Laboratory of Veterinary Pharmacology, Joint Faculty of Veterinary Medicine, Yamaguchi University*), *Assis. Prof. Satoshi Kambayashi* (*Laboratory of Veterinary Internal Medicine, Joint Faculty of Veterinary Medicine, Yamaguchi University*), and *Dr. Hwang Chung Chew* (*AstraZeneca Japan*) for all their help and kindness.

I wish to thank *Saori Umeki*, *Takuma Yanase*, *Kazuha Shousu*, *Kenta Fukushima*, *Noriyuki Fujiki*, *Yosuke Kurogouchi*, *Yuki Morinaga*, and all the lab. members for supporting me with my doctorial life.

Finally, I would like to give my thanks to my family and friends for the supports in everything I do.

REFERENCES

Adair RA, Roulstone V, Scott KJ, Morgan R, Nuovo GJ, Fuller M, Beirne D, West EJ, Jennings VA, Rose A, Kyula J, Fraser S, Dave R, Anthoney DA, Merrick A, Prestwich R, Aldouri A, Donnelly O, Pandha H, Coffey M, Selby P, Vile R, Toogood G, Harrington K, Melcher AA. Cell carriage, delivery, and selective replication of an oncolytic virus in tumor in patients. Sci Transl Med. 2012 Jun 13;4(138):138ra77.

Akira S, Uematsu S, Takeuchi O. Pathogen recognition and innate immunity. Cell. 2006 Feb 24;124(4):783-801.

Alain T, Kim M, Johnston RN, Urbanski S, Kossakowska AE, Forsyth PA, Lee PW. The oncolytic effect in vivo of reovirus on tumour cells that have survived reovirus cell killing in vitro. Br J Cancer. 2006 Oct 23;95(8):1020-7.

Alain T, Kim TS, Lun X, Liacini A, Schiff LA, Senger DL, Forsyth PA. Proteolytic disassembly is a critical determinant for reovirus oncolysis. Mol Ther. 2007 Aug;15(8):1512-21.

Alberts P, Olmane E, Brokāne L, Krastiņa Z, Romanovska M, Kupčs K, Isajevs S, Proboka G, Erdmanis R, Nazarovs J, Venskus D. Long-term treatment with the oncolytic ECHO-7 virus Rigvir of a melanoma stage IV M1c patient, a small cell lung cancer stage IIIA patient, and a histiocytic sarcoma stage IV patient-three case reports. APMIS. 2016 Oct;124(10):896-904.

Alekseev O, Donovan K, Azizkhan-Clifford J. Inhibition of ataxia telangiectasia mutated (ATM) kinase suppresses herpes simplex virus type 1 (HSV-1) keratitis. Invest Ophthalmol Vis Sci. 2014 Feb 3;55(2):706-15.

Alloussi SH, Alkassar M, Urbschat S, Graf N, Gärtner B. All reovirus subtypes show oncolytic potential in primary cells of human high-grade glioma. Oncol Rep. 2011 Sep;26(3):645-9.

Authier F, Posner BI, Bergeron JJ. Endosomal proteolysis of internalized proteins. FEBS Lett. 1996 Jun 24;389(1):55-60.

Azakami D, Bonkobara M, Washizu T, Iida A, Kondo M, Kato R, Niikura Y, Iwaki S, Tamahara S, Matsuki N, Ono K. Establishment and biological characterization of canine histiocytic sarcoma cell lines. J Vet Med Sci. 2006 Dec;68(12):1343-6.

Berger AK, Danthi P. Reovirus activates a caspase-independent cell death pathway. MBio. 2013 May 14;4(3):e00178-13.

Bianco SR, Sun J, Fosmire SP, Hance K, Padilla ML, Ritt MG, Getzy DM, Duke RC, Withrow SJ, Lana S, Matthiesen DT, Dow SW, Bellgrau D, Cutter GR, Helfand SC, Modiano JF. Enhancing antimelanoma immune responses through apoptosis. Cancer Gene Ther. 2003 Sep;10(9):726-36.

Biddlestone-Thorpe L, Sajjad M, Rosenberg E, Beckta JM, Valerie NC, Tokarz M, Adams BR, Wagner AF, Khalil A, Gilfor D, Golding SE, Deb S, Temesi DG, Lau A, O'Connor MJ, Choe KS, Parada LF, Lim SK, Mukhopadhyay ND, Valerie K. ATM kinase inhibition preferentially sensitizes p53-mutant glioma to ionizing radiation. Clin Cancer Res. 2013 Jun 15;19(12):3189-200.

Blum JS, Fiani ML, Stahl PD. Proteolytic cleavage of ricin A chain in endosomal vesicles. Evidence for the action of endosomal proteases at both neutral and acidic pH. J Biol Chem. 1991 Nov 25;266(33):22091-5.

Boerkamp KM, van Steenbeek FG, Penning LC, Groot Koerkamp MJ, van Leenen D, Vos-Loohuis M, Grinwis GC, Rutteman GR. The two main forms of histiocytic sarcoma in the predisposed Flatcoated retriever dog display variation in gene expression. PLoS One. 2014 Jun 2;9(6):e98258.

Chou TC, Talalay P. Quantitative analysis of dose-effect relationships: the combined effects of multiple drugs or enzyme inhibitors. Adv Enzyme Regul. 1984;22:27-55.

Chou TC. Drug combination studies and their synergy quantification using the Chou-Talalay method. Cancer Res. 2010 Jan 15;70(2):440-6.

Clarke P, Meintzer SM, Wang Y, Moffitt LA, Richardson-Burns SM, Johnson GL, Tyler KL. JNK regulates the release of proapoptotic mitochondrial factors in reovirus-infected cells. J Virol. 2004 Dec;78(23):13132-8.

Clarke P, Richardson-Burns SM, DeBiasi RL, Tyler KL. Mechanisms of apoptosis during reovirus infection. Curr Top Microbiol Immunol. 2005;289:1-24.

Clements D, Helson E, Gujar SA, Lee PW. Reovirus in cancer therapy: an evidence-based review. Oncolytic Virother. 2014 Jul 9;3:69-82.

Clifford CA, Skorupski KA, Moore PF. Histiocytic disorders. In: Small Animal Clinical Oncology. 5th edn. Withrow SJ, Vail DM, Page RL Eds., St. Louis, Saunders Elsevier, 2013: 710-713.

Coffey MC, Strong JE, Forsyth PA, Lee PW. Reovirus therapy of tumors with activated Ras pathway. Science. 1998 Nov 13;282(5392):1332-4.

Comins C, Spicer J, Protheroe A, Roulstone V, Twigger K, White CM, Vile R, Melcher A, Coffey MC, Mettinger KL, Nuovo G, Cohn DE, Phelps M, Harrington KJ, Pandha HS. REO-10: a phase I study of intravenous reovirus and docetaxel in patients with advanced cancer. Clin Cancer Res. 2010 Nov 15;16(22):5564-72.

Connolly JL, Rodgers SE, Clarke P, Ballard DW, Kerr LD, Tyler KL, Dermody TS. Reovirus-induced apoptosis requires activation of transcription factor NF-kappaB. J Virol. 2000 Apr;74(7):2981-9.

Dalia S, Shao H, Sagatys E, Cualing H, Sokol L. Dendritic cell and histiocytic neoplasms: biology, diagnosis, and treatment. Cancer Control. 2014 Oct;21(4):290-300.

Decaro N, Campolo M, Desario C, Ricci D, Camero M, Lorusso E, Elia G, Lavazza A, Martella V, Buonavoglia C. Virological and molecular characterization of a mammalian orthoreovirus type 3 strain isolated from a dog in Italy. Vet Microbiol. 2005 Aug 10;109(1-2):19-27.

Dernell WS, Ehrhart NP, Straw RC, Vail DM. Tumors of the Skeletal System. In: Small Animal Clinical Oncology. 4th edn. Withrow SJ, Vail DM Eds., St. Louis, Saunders Elsevier, 2007: 540-582.

Duncan MR, Stanish SM, Cox DC. Differential sensitivity of normal and transformed human cells to reovirus infection. J Virol. 1978 Nov;28(2):444-9.

Ebert DH, Deussing J, Peters C, Dermody TS. Cathepsin L and cathepsin B mediate reovirus disassembly in murine fibroblast cells. J Biol Chem. 2002 Jul 5;277(27):24609-17.

Emile JF, Abla O, Fraitag S, Horne A, Haroche J, Donadieu J, Requena-Caballero L, Jordan MB, Abdel-Wahab O, Allen CE, Charlotte F, Diamond EL, Egeler RM, Fischer A, Herrera JG, Henter JI, Janku F, Merad M, Picarsic J, Rodriguez-Galindo C, Rollins BJ, Tazi A, Vassallo R, Weiss LM; Histiocyte Society. Revised classification of histiocytoses and neoplasms of the macrophage-dendritic cell lineages. Blood. 2016 Jun 2;127(22):2672-81.

Errington F, Steele L, Prestwich R, Harrington KJ, Pandha HS, Vidal L, de Bono J, Selby P, Coffey M, Vile R, Melcher A. Reovirus activates human dendritic cells to promote innate antitumor immunity. J Immunol. 2008 May 1;180(9):6018-26.

Errington F, White CL, Twigger KR, Rose A, Scott K, Steele L, Ilett LJ, Prestwich R, Pandha HS, Coffey M, Selby P, Vile R, Harrington KJ, Melcher AA. Inflammatory tumour cell killing by oncolytic reovirus for the treatment of melanoma. Gene Ther. 2008 Sep;15(18):1257-70.

Etoh T, Himeno Y, Matsumoto T, Aramaki M, Kawano K, Nishizono A, Kitano S. Oncolytic viral therapy for human pancreatic cancer cells by reovirus. Clin Cancer Res. 2003 Mar;9(3):1218-23.

Farkona S, Diamandis EP, Blasutig IM. Cancer immunotherapy: the beginning of the end of cancer? BMC Med. 2016 May 5;14:73.

Filley AC, Dey M. Immune System, Friend or Foe of Oncolytic Virotherapy? Front Oncol. 2017 May 23;7:106.

Forsyth P, Roldán G, George D, Wallace C, Palmer CA, Morris D, Cairncross G, Matthews MV, Markert J, Gillespie Y, Coffey M, Thompson B, Hamilton M. A phase I trial of intratumoral administration of reovirus in patients with histologically confirmed recurrent malignant gliomas. Mol Ther. 2008 Mar;16(3):627-32.

Fujii Y, Kaneko M, Neyazaki M, Nogi T, Kato Y, Takagi J. PA tag: a versatile protein tagging system using a super high affinity antibody against a dodecapeptide derived from human podoplanin. Protein Expr Purif. 2014 Mar;95:240-7.

Fujii Y, Matsunaga Y, Arimori T, Kitago Y, Ogasawara S, Kaneko MK, Kato Y, Takagi J. Tailored placement of a turn-forming PA tag into the structured domain of a protein to probe its conformational state. J Cell Sci. 2016 Apr 1;129(7):1512-22.

Fukuhara H, Ino Y, Todo T. Oncolytic virus therapy: A new era of cancer treatment at dawn. Cancer Sci. 2016 Oct;107(10):1373-1379.

Fukumi H, Takeuchi Y, Ishida M, Saito H. Serological epidemiology of reovirus infection. 1. Jpn J Med Sci Biol. 1969 Feb;22(1):13-21.

Fulmer AK, Mauldin GE. Canine histiocytic neoplasia: an overview. Can Vet J. 2007 Oct;48(10):1041-3, 1046-50.

Galanis E, Markovic SN, Suman VJ, Nuovo GJ, Vile RG, Kottke TJ, Nevala WK, Thompson MA, Lewis JE, Rumilla KM, Roulstone V, Harrington K, Linette GP, Maples WJ, Coffey M, Zwiebel J, Kendra K. Phase II trial of intravenous administration of Reolysin(®) (Reovirus Serotype-3-dearing Strain) in patients with metastatic melanoma. Mol Ther. 2012 Oct;20(10):1998-2003.

Gillard M, Cadieu E, De Brito C, Abadie J, Vergier B, Devauchelle P, Degorce F, Dréano S, Primot A, Dorso L, Lagadic M, Galibert F, Hédan B, Galibert MD, André C. Naturally occurring melanomas in dogs as models for non-UV pathways of human melanomas. Pigment Cell Melanoma Res. 2014 Jan;27(1):90-102.

Golding SE, Rosenberg E, Valerie N, Hussaini I, Frigerio M, Cockcroft XF, Chong WY, Hummersone M, Rigoreau L, Menear KA, O'Connor MJ, Povirk LF, van Meter T, Valerie K. Improved ATM kinase inhibitor KU-60019 radiosensitizes glioma cells, compromises insulin, AKT and ERK prosurvival signaling, and inhibits migration and invasion. Mol Cancer Ther. 2009 Oct;8(10):2894-902.

Gollamudi R, Ghalib MH, Desai KK, Chaudhary I, Wong B, Einstein M, Coffey M, Gill GM, Mettinger K, Mariadason JM, Mani S, Goel S. Intravenous administration of Reolysin, a live replication competent RNA virus is safe in patients with advanced solid tumors. Invest New Drugs. 2010 Oct;28(5):641-9.

Gong J, Sachdev E, Mita AC, Mita MM. Clinical development of reovirus for cancer therapy: An oncolytic virus with immune-mediated antitumor activity. World J Methodol. 2016 Mar 26;6(1):25-42.

Gujar SA, Marcato P, Pan D, Lee PW. Reovirus virotherapy overrides tumor antigen presentation evasion and promotes protective antitumor immunity. Mol Cancer Ther. 2010 Nov;9(11):2924-33.

Hall K, Scott KJ, Rose A, Desborough M, Harrington K, Pandha H, Parrish C, Vile R, Coffey M, Bowen D, Errington-Mais F, Melcher AA. Reovirus-mediated cytotoxicity and enhancement of innate immune responses against acute myeloid leukemia. Biores Open Access. 2012 Jan;1(1):3-15.

Hamano S, Mori Y, Aoyama M, Kataoka H, Tanaka M, Ebi M, Kubota E, Mizoshita T, Tanida S, Johnston RN, Asai K, Joh T. Oncolytic reovirus combined with trastuzumab enhances antitumor efficacy through TRAIL signaling in human HER2-positive gastric cancer cells. Cancer Lett. 2015 Jan 28;356(2 Pt B):846-54.

Harrington KJ, Karapanagiotou EM, Roulstone V, Twigger KR, White CL, Vidal L, Beirne D, Prestwich R, Newbold K, Ahmed M, Thway K, Nutting CM, Coffey M, Harris D, Vile RG, Pandha HS, Debono JS, Melcher AA. Two-stage phase I dose-escalation study of intratumoral reovirus type 3 dearing and palliative radiotherapy in patients with advanced cancers. Clin Cancer Res. 2010 Jun 1;16(11):3067-77.

Hashiro G, Loh PC, Yau JT. The preferential cytotoxicity of reovirus for certain transformed cell lines. Arch Virol. 1977;54(4):307-15.

Hau PM, Deng W, Jia L, Yang J, Tsurumi T, Chiang AK, Huen MS, Tsao SW. Role of ATM in the formation of the replication compartment during lytic replication of Epstein-Barr virus in nasopharyngeal epithelial cells. J Virol. 2015 Jan;89(1):652-68.

Hedan B, Thomas R, Motsinger-Reif A, Abadie J, Andre C, Cullen J, Breen M. Molecular cytogenetic characterization of canine histiocytic sarcoma: A spontaneous model for human histiocytic cancer identifies deletion of tumor suppressor genes and highlights influence of genetic background on tumor behavior. BMC Cancer. 2011 May 26;11:201.

Heinemann L, Simpson GR, Boxall A, Kottke T, Relph KL, Vile R, Melcher A, Prestwich R, Harrington KJ, Morgan R, Pandha HS. Synergistic effects of oncolytic reovirus and docetaxel chemotherapy in prostate cancer. BMC Cancer. 2011 Jun 6;11:221. doi: 10.1186/1471-2407-11-221.

Hernandez B, Adissu HA, Wei BR, Michael HT, Merlino G, Simpson RM. Naturally Occurring Canine Melanoma as a Predictive Comparative Oncology Model for Human Mucosal and Other Triple Wild-Type Melanomas. Int J Mol Sci. 2018 Jan 30;19(2). pii: E394.

Hiller BE, Berger AK, Danthi P. Viral gene expression potentiates reovirus-induced necrosis. Virology. 2015 Oct;484:386-94.

Hirasawa K, Nishikawa SG, Norman KL, Coffey MC, Thompson BG, Yoon CS, Waisman DM, Lee PW. Systemic reovirus therapy of metastatic cancer in immune-competent mice. Cancer Res. 2003 Jan 15;63(2):348-53.

Holm GH, Zurney J, Tumilasci V, Leveille S, Danthi P, Hiscott J, Sherry B, Dermody TS. Retinoic acid-inducible gene-I and interferon-beta promoter stimulator-1 augment proapoptotic responses following mammalian reovirus infection via interferon regulatory factor-3. J Biol Chem. 2007 Jul 27;282(30):21953-61.

Hwang CC, Umeki S, Kubo M, Hayashi T, Shimoda H, Mochizuki M, Maeda K, Baba K, Hiraoka H, Coffey M, Okuda M, Mizuno T. Oncolytic reovirus in canine mast cell tumor. PLoS One. 2013 Sep 20;8(9):e73555.

Hwang CC, Mochizuki M, Maeda K, Okuda M, Mizuno T. Seroepidemiology of reovirus in healthy dogs in six prefectures in Japan. J Vet Med Sci. 2014 Mar;76(3):471-5.

Hwang CC, Umeki S, Igase M, Coffey M, Noguchi S, Okuda M, Mizuno T. The effects of oncolytic reovirus in canine lymphoma cell lines. Vet Comp Oncol. 2016 Aug;14 Suppl 1:61-73.

Hwang CC, Igase M, Sakurai M, Haraguchi T, Tani K, Itamoto K, Shimokawa T, Nakaichi M, Nemoto Y, Noguchi S, Coffey M, Okuda M, Mizuno T. Oncolytic reovirus therapy: Pilot study in dogs with spontaneously occurring tumours. Vet Comp Oncol. 2018 Jun;16(2):229-238.

Igase M, Hwang CC, Coffey M, Okuda M, Noguchi S, Mizuno T. The oncolytic effects of reovirus in canine solid tumor cell lines. J Vet Med Sci. 2015 May;77(5):541-8.

Igase M, Hwang CC, Kambayashi S, Kubo M, Coffey M, Miyama TS, Baba K, Okuda M, Noguchi S, Mizuno T. Oncolytic reovirus synergizes with chemotherapeutic agents to promote cell death in canine mammary gland tumor. Can J Vet Res. 2016 Jan;80(1):21-31.

Ikeda Y, Nishimura G, Yanoma S, Kubota A, Furukawa M, Tsukuda M. Reovirus oncolysis in human head and neck squamous carcinoma cells. Auris Nasus Larynx. 2004 Dec;31(4):407-12.

Ilett EJ, Bárcena M, Errington-Mais F, Griffin S, Harrington KJ, Pandha HS, Coffey M, Selby PJ, Limpens RW, Mommaas M, Hoeben RC, Vile RG, Melcher AA. Internalization of oncolytic reovirus by human dendritic cell carriers protects the virus from neutralization. Clin Cancer Res. 2011 May 1;17(9):2767-76.

Inoue K, Ohashi E, Kadosawa T, Hong SH, Matsunaga S, Mochizuki M, Nishimura R, Sasaki N. Establishment and characterization of four canine melanoma cell lines. J Vet Med Sci. 2004 Nov;66(11):1437-40.

Ito K, Kuroki S, Kobayashi M, Ono K, Washizu T, Bonkobara M. Identification of dasatinib as an in vitro potent growth inhibitor of canine histiocytic sarcoma cells. Vet J. 2013 Jun;196(3):536-40.

Jassies-van der Lee A, Rutten V, Spiering R, van Kooten P, Willemse T, Broere F. The immunostimulatory effect of CpG oligodeoxynucleotides on peripheral blood mononuclear cells of healthy dogs and dogs with atopic dermatitis. Vet J. 2014 Apr;200(1):103-8.

Jennings VA, Ilett EJ, Scott KJ, West EJ, Vile R, Pandha H, Harrington K, Young A, Hall GD, Coffey M, Selby P, Errington-Mais F, Melcher AA. Lymphokine-activated killer and dendritic cell carriage enhances oncolytic reovirus therapy for ovarian cancer by overcoming antibody neutralization in ascites. Int J Cancer. 2014 Mar 1;134(5):1091-101.

Kambayashi S, Igase M, Kobayashi K, Kimura A, Shimokawa Miyama T, Baba K, Noguchi S, Mizuno T, Okuda M. Hypoxia inducible factor 1 α expression and effects of its inhibitors in canine lymphoma. J Vet Med Sci. 2015 Nov;77(11):1405-12.

Kang DC, Gopalkrishnan RV, Wu Q, Jankowsky E, Pyle AM, Fisher PB. mda-5: An interferon-inducible putative RNA helicase with double-stranded RNA-dependent ATPase activity and melanoma growth-suppressive properties. Proc Natl Acad Sci U S A. 2002 Jan 22;99(2):637-42.

Kang HT, Park JT, Choi K, Kim Y, Choi HJC, Jung CW, Lee YS, Park SC. Chemical screening identifies ATM as a target for alleviating senescence. Nat Chem Biol. 2017 Jun;13(6):616-623.

Karapanagiotou EM, Roulstone V, Twigger K, Ball M, Tanay M, Nutting C, Newbold K, Gore ME, Larkin J, Syrigos KN, Coffey M, Thompson B, Mettinger K, Vile RG, Pandha HS, Hall GD, Melcher AA, Chester J, Harrington KJ. Phase I/II trial of carboplatin and paclitaxel chemotherapy in combination with intravenous oncolytic reovirus in patients with advanced malignancies. Clin Cancer Res. 2012 Apr 1;18(7):2080-9.

Kelly KR, Espitia CM, Mahalingam D, Oyajobi BO, Coffey M, Giles FJ, Carew JS, Nawrocki ST. Reovirus therapy stimulates endoplasmic reticular stress, NOXA induction, and augments bortezomib-mediated apoptosis in multiple myeloma. Oncogene. 2012 Jun 21;31(25):3023-38.

Kelly KR, Espitia CM, Zhao W, Wendlandt E, Tricot G, Zhan F, Carew JS, Nawrocki ST. Junctional adhesion molecule-A is overexpressed in advanced multiple myeloma and determines response to oncolytic reovirus. Oncotarget. 2015 Dec 1;6(38):41275-89.

Kim M, Williamson CT, Prudhomme J, Bebb DG, Riabowol K, Lee PW, Lees-Miller SP, Mori Y, Rahman MM, McFadden G, Johnston RN. The viral tropism of two distinct oncolytic viruses, reovirus and myxoma virus, is modulated by cellular tumor

suppressor gene status. Oncogene. 2010 Jul 8;29(27):3990-6.

Kim M. Naturally occurring reoviruses for human cancer therapy. BMB Rep. 2015 Aug;48(8):454-60.

Kozlov SV, Graham ME, Jakob B, Tobias F, Kijas AW, Tanuji M, Chen P, Robinson PJ, Taucher-Scholz G, Suzuki K, So S, Chen D, Lavin MF. Autophosphorylation and ATM activation: additional sites add to the complexity. J Biol Chem. 2011 Mar 18;286(11):9107-19.

LaRocca CJ, Warner SG. Oncolytic viruses and checkpoint inhibitors: combination therapy in clinical trials. Clin Transl Med. 2018 Nov 14;7(1):35.

Li H, Baskaran R, Krisky DM, Bein K, Grandi P, Cohen JB, Glorioso JC. Chk2 is required for HSV-1 ICP0-mediated G2/M arrest and enhancement of virus growth. Virology. 2008 May 25;375(1):13-23.

Linge C, Gewert D, Rossmann C, Bishop JA, Crowe JS. Interferon system defects in human malignant melanoma. Cancer Res. 1995 Sep 15;55(18):4099-104.

Liptak JM, Forrest LJ. Soft tissue sarcoma. In: Small Animal Clinical Oncology. 5th edn. Withrow SJ, Vail DM, Page RL Eds., St. Louis, Saunders Elsevier, 2013: 356-380.

Liu S, Cai X, Wu J, Cong Q, Chen X, Li T, Du F, Ren J, Wu YT, Grishin NV, Chen ZJ. Phosphorylation of innate immune adaptor proteins MAVS, STING, and TRIF induces IRF3 activation. Science. 2015 Mar 13;347(6227):aaa2630.

Loken SD, Norman K, Hirasawa K, Nodwell M, Lester WM, Demetrick DJ. Morbidity in immunosuppressed (SCID/NOD) mice treated with reovirus (dearing 3) as an anti-cancer biotherapeutic. Cancer Biol Ther. 2004 Aug;3(8):734-8.

Lolkema MP, Arkenau HT, Harrington K, Roxburgh P, Morrison R, Roulstone V, Twigger K, Coffey M, Mettinger K, Gill G, Evans TR, de Bono JS. A phase I study of the combination of intravenous reovirus type 3 Dearing and gemcitabine in patients with advanced cancer. Clin Cancer Res. 2011 Feb 1;17(3):581-8.

London CA, Malpas PB, Wood-Follis SL, Boucher JF, Rusk AW, Rosenberg MP, Henry CJ, Mitchener KL, Klein MK, Hintermeister JG, Bergman PJ, Couto GC, Mauldin GN, Michels GM. Multi-center, placebo-controlled, double-blind, randomized study of oral toceranib phosphate (SU11654), a receptor tyrosine kinase inhibitor, for the treatment of dogs with recurrent (either local or distant) mast cell tumor following surgical excision. Clin Cancer Res. 2009 Jun 1;15(11):3856-65.

London CA, Thamm DH. Mast cell tumors. In: Small Animal Clinical Oncology. 5th edn. Withrow SJ, Vail DM, Page RL Eds., St. Louis, Saunders Elsevier, 2013: 335-355.

Machida K, Cheng KT, Lai CK, Jeng KS, Sung VM, Lai MM. Hepatitis C virus triggers

mitochondrial permeability transition with production of reactive oxygen species, leading to DNA damage and STAT3 activation. J Virol. 2006 Jul;80(14):7199-207.

Maeda J, Yurkon CR, Fujisawa H, Kaneko M, Genet SC, Roybal EJ, Rota GW, Saffer ER, Rose BJ, Hanneman WH, Thamm DH, Kato TA. Genomic instability and telomere fusion of canine osteosarcoma cells. PLoS One. 2012;7(8):e43355.

Mainou BA, Dermody TS. Transport to late endosomes is required for efficient reovirus infection. J Virol. 2012 Aug;86(16):8346-58.

Maitra R, Seetharam R, Tesfa L, Augustine TA, Klampfer L, Coffey MC, Mariadason JM, Goel S. Oncolytic reovirus preferentially induces apoptosis in KRAS mutant colorectal cancer cells, and synergizes with irinotecan. Oncotarget. 2014 May 15;5(9):2807-19.

Marcato P, Shmulevitz M, Pan D, Stoltz D, Lee PW. Ras transformation mediates reovirus oncolysis by enhancing virus uncoating, particle infectivity, and apoptosis-dependent release. Mol Ther. 2007 Aug;15(8):1522-30.

Marelli G, Howells A, Lemoine NR, Wang Y. Oncolytic Viral Therapy and the Immune System: A Double-Edged Sword Against Cancer. Front Immunol. 2018 Apr 26;9:866.

Marshansky V, Rubinstein JL, Grüber G. Eukaryotic V-ATPase: novel structural findings and functional insights. Biochim Biophys Acta. 2014 Jun;1837(6):857-79.

Matin SF, Rackley RR, Sadhukhan PC, Kim MS, Novick AC, Bandyopadhyay SK. Impaired alpha-interferon signaling in transitional cell carcinoma: lack of p48 expression in 5637 cells. Cancer Res. 2001 Mar 1;61(5):2261-6.

Mito K, Sugiura K, Ueda K, Hori T, Akazawa T, Yamate J, Nakagawa H, Hatoya S, Inaba M, Inoue N, Ikehara S, Inaba T. IFN{gamma} markedly cooperates with intratumoral dendritic cell vaccine in dog tumor models. Cancer Res. 2010 Sep 15;70(18):7093-101.

Moore PF. A review of histiocytic diseases of dogs and cats. Vet Pathol. 2014 Jan;51(1):167-84.

Morris DG, Feng X, DiFrancesco LM, Fonseca K, Forsyth PA, Paterson AH, Coffey MC, Thompson B. REO-001: A phase I trial of percutaneous intralesional administration of reovirus type 3 dearing (Reolysin®) in patients with advanced solid tumors. Invest New Drugs. 2013 Jun;31(3):696-706.

Mostafa AA, Meyers DE, Thirukkumaran CM, Liu PJ, Gratton K, Spurrell J, Shi Q, Thakur S, Morris DG. Oncolytic Reovirus and Immune Checkpoint Inhibition as a Novel Immunotherapeutic Strategy for Breast Cancer. Cancers (Basel). 2018 Jun 15;10(6). pii: E205.

Murai K, Nakagawa T, Endo Y, Kamida A, Yoshida K, Mochizuki M, Nishimura R, Sasaki N. Establishment of a pair of novel cloned tumour cell lines with or without metastatic potential from canine mammary adenocarcinoma. Res Vet Sci. 2012 Aug;93(1):468-72.

Nakagawa T, Watanabe M, Ohashi E, Uyama R, Takauji S, Mochizuki M, Nishimura R, Ogawa H, Sugano S, Sasaki N. Cyclopedic protein expression analysis of cultured canine mammary gland adenocarcinoma cells from six tumours. Res Vet Sci. 2006 Jun;80(3):317-23.

Narváez CF, Angel J, Franco MA. Interaction of rotavirus with human myeloid dendritic cells. J Virol. 2005 Dec;79(23):14526-35.

Norman KL, Coffey MC, Hirasawa K, Demetrick DJ, Nishikawa SG, DiFrancesco LM, Strong JE, Lee PW. Reovirus oncolysis of human breast cancer. Hum Gene Ther. 2002 Mar 20;13(5):641-52.

Oncolytics Biotech Inc. News releases.
http://www.oncolyticsbiotech.com/news/oncolytics-biotech-inc-announces-positive-top-line-data-from-reo-018-randomized-study-of-reolysin-in-head-and-neck-cancers/
Accessed April 28, 2017.

Oncolytics Biotech Inc. News releases.
http://www.oncolyticsbiotech.com/news/oncolytics-biotech-inc-announces-fda-fast-track-designation-for-reolysin-in-metastatic-breast-cancer/ Accessed April 28, 2017.

Pandha HS, Heinemann L, Simpson GR, Melcher A, Prestwich R, Errington F, Coffey M, Harrington KJ, Morgan R. Synergistic effects of oncolytic reovirus and cisplatin chemotherapy in murine malignant melanoma. Clin Cancer Res. 2009 Oct 1;15(19):6158-66.

Passaro C, Abagnale A, Libertini S, Volpe M, Botta G, Cella L, Pacelli R, Halldèn G, Gillespie D, Portella G. Ionizing radiation enhances dl922-947-mediated cell death of anaplastic thyroid carcinoma cells. Endocr Relat Cancer. 2013 Aug 19;20(5):633-47.

Pike KG, Barlaam B, Cadogan E, Campbell A, Chen Y, Colclough N, Davies NL, de-Almeida C, Degorce SL, Didelot M, Dishington A, Ducray R, Durant ST, Hassall LA, Holmes J, Hughes GD, MacFaul PA, Mulholland KR, McGuire TM, Ouvry G, Pass M, Robb G, Stratton N, Wang Z, Wilson J, Zhai B, Zhao K, Al-Huniti N. The Identification of Potent, Selective, and Orally Available Inhibitors of Ataxia Telangiectasia Mutated (ATM) Kinase: The Discovery of AZD0156 (8-{6-[3-(Dimethylamino)propoxy]pyridin-3-yl}-3-methyl-1-(tetrahydro-2 H-pyran-4-yl)-1,3-dihydro-2 H-imidazo[4,5- c]quinolin-2-one). J Med Chem. 2018 May 10;61(9):3823-3841.

Pileri SA, Grogan TM, Harris NL, Banks P, Campo E, Chan JK, Favera RD, Delsol G, De Wolf-Peeters C, Falini B, Gascoyne RD, Gaulard P, Gatter KC, Isaacson PG, Jaffe

ES, Kluin P, Knowles DM, Mason DY, Mori S, Müller-Hermelink HK, Piris MA, Ralfkiaer E, Stein H, Su IJ, Warnke RA, Weiss LM. Tumours of histiocytes and accessory dendritic cells: an immunohistochemical approach to classification from the International Lymphoma Study Group based on 61 cases. Histopathology. 2002 Jul;41(1):1-29.

Pfankuche VM, Sayed-Ahmed M, Contioso VB, Spitzbarth I, Rohn K, Ulrich R, Deschl U, Kalkuhl A, Baumgärtner W, Puff C. Persistent Morbillivirus Infection Leads to Altered Cortactin Distribution in Histiocytic Sarcoma Cells with Decreased Cellular Migration Capacity. PLoS One. 2016 Dec 2;11(12):e0167517.

Pfankuche VM, Spitzbarth I, Lapp S, Ulrich R, Deschl U, Kalkuhl A, Baumgärtner W, Puff C. Reduced angiogenic gene expression in morbillivirus-triggered oncolysis in a translational model for histiocytic sarcoma. J Cell Mol Med. 2017 Apr;21(4):816-830.

Poggioli GJ, Dermody TS, Tyler KL. Reovirus-induced sigma1s-dependent G(2)/M phase cell cycle arrest is associated with inhibition of p34(cdc2). J Virol. 2001 Aug;75(16):7429-34.

Pol J, Bloy N, Obrist F, Eggermont A, Galon J, Cremer I, Erbs P, Limacher JM, Preville X, Zitvogel L, Kroemer G, Galluzzi L. Trial Watch:: Oncolytic viruses for cancer therapy. Oncoimmunology. 2014 Jun 1;3:e28694.

Pol J, Buqué A, Aranda F, Bloy N, Cremer I, Eggermont A, Erbs P, Fucikova J, Galon J, Limacher JM, Preville X, Sautès-Fridman C, Spisek R, Zitvogel L, Kroemer G, Galluzzi L. Trial Watch-Oncolytic viruses and cancer therapy. Oncoimmunology. 2015 Dec 8;5(2):e1117740.

Prestwich RJ, Errington F, Ilett EJ, Morgan RS, Scott KJ, Kottke T, Thompson J, Morrison EE, Harrington KJ, Pandha HS, Selby PJ, Vile RG, Melcher AA. Tumor infection by oncolytic reovirus primes adaptive antitumor immunity. Clin Cancer Res. 2008 Nov 15;14(22):7358-66.

Prestwich RJ, Errington F, Diaz RM, Pandha HS, Harrington KJ, Melcher AA, Vile RG. The case of oncolytic viruses versus the immune system: waiting on the judgment of Solomon. Hum Gene Ther. 2009 Oct;20(10):1119-32.

Qiao J, Wang H, Kottke T, White C, Twigger K, Diaz RM, Thompson J, Selby P, de Bono J, Melcher A, Pandha H, Coffey M, Vile R, Harrington K. Cyclophosphamide facilitates antitumor efficacy against subcutaneous tumors following intravenous delivery of reovirus. Clin Cancer Res. 2008 Jan 1;14(1):259-69.

Rajani K, Parrish C, Kottke T, Thompson J, Zaidi S, Ilett L, Shim KG, Diaz RM, Pandha H, Harrington K, Coffey M, Melcher A, Vile R. Combination Therapy With Reovirus and Anti-PD-1 Blockade Controls Tumor Growth Through Innate and Adaptive Immune Responses. Mol Ther. 2016 Feb;24(1):166-74.

Rankin JT Jr, Eppes SB, Antczak JB, Joklik WK. Studies on the mechanism of the antiviral activity of ribavirin against reovirus. Virology. 1989 Jan;168(1):147-58.

Rassnick KM, Moore AS, Russell DS, Northrup NC, Kristal O, Bailey DB, Flory AB, Kiselow MA, Intile JL. Phase II, open-label trial of single-agent CCNU in dogs with previously untreated histiocytic sarcoma. J Vet Intern Med. 2010 Nov-Dec;24(6):1528-31.

Reed LJ, Muench H. A simple method of estimating fifty per cent endpoints. Am. J. Epidemiol. 1938 May;27(3):493-497.

Rosen L. Reoviruses in animals other than man. Ann N Y Acad Sci. 1962 Nov;101(2):461-5.

Rosen L, Evans HE, Spickard A. Reovirus infections in human volunteers. Am J Hyg. 1963 Jan;77:29-37.

Roulstone V, Twigger K, Zaidi S, Pencavel T, Kyula JN, White C, McLaughlin M, Seth R, Karapanagiotou EM, Mansfield D, Coffey M, Nuovo G, Vile RG, Pandha HS, Melcher AA, Harrington KJ. Synergistic cytotoxicity of oncolytic reovirus in combination with cisplatin-paclitaxel doublet chemotherapy. Gene Ther. 2013 May;20(5):521-8.

Roulstone V, Khan K, Pandha HS, Rudman S, Coffey M, Gill GM, Melcher AA, Vile R, Harrington KJ, de Bono J, Spicer J. Phase I trial of cyclophosphamide as an immune modulator for optimizing oncolytic reovirus delivery to solid tumors. Clin Cancer Res. 2015 Mar 15;21(6):1305-12.

Ryan EL, Hollingworth R, Grand RJ. Activation of the DNA Damage Response by RNA Viruses. Biomolecules. 2016 Jan 6;6(1):2.

Sánchez D, Cesarman-Maus G, Amador-Molina A, Lizano M. Oncolytic Viruses for Canine Cancer Treatment. Cancers (Basel). 2018 Oct 27;10(11). pii: E404.

Sanjana NE, Shalem O, Zhang F. Improved vectors and genome-wide libraries for CRISPR screening. Nat Methods. 2014 Aug;11(8):783-784.

Sei S, Mussio JK, Yang QE, Nagashima K, Parchment RE, Coffey MC, Shoemaker RH, Tomaszewski JE. Synergistic antitumor activity of oncolytic reovirus and chemotherapeutic agents in non-small cell lung cancer cells. Mol Cancer. 2009 Jul 14;8:47.

Shmulevitz M, Marcato P, Lee PW. Unshackling the links between reovirus oncolysis, Ras signaling, translational control and cancer. Oncogene. 2005 Nov 21;24(52):7720-8.

Shmulevitz M, Pan LZ, Garant K, Pan D, Lee PW. Oncogenic Ras promotes reovirus spread by suppressing IFN-beta production through negative regulation of RIG-I signaling. Cancer Res. 2010 Jun 15;70(12):4912-21.

Shoji M, Arakaki Y, Esumi T, Kohnomi S, Yamamoto C, Suzuki Y, Takahashi E, Konishi S, Kido H, Kuzuhara T. Bakuchiol Is a Phenolic Isoprenoid with Novel Enantiomer-selective Anti-influenza A Virus Activity Involving Nrf2 Activation. J Biol Chem. 2015 Nov 13;290(46):28001-17.

Sinclair A, Yarranton S, Schelcher C. DNA-damage response pathways triggered by viral replication. Expert Rev Mol Med. 2006 Mar 3;8(5):1-11.

Skorupski KA, Clifford CA, Paoloni MC, Lara-Garcia A, Barber L, Kent MS, LeBlanc AK, Sabhlok A, Mauldin EA, Shofer FS, Couto CG, Sørenmo KU. CCNU for the treatment of dogs with histiocytic sarcoma. J Vet Intern Med. 2007 Jan-Feb;21(1):121-6.

Sorenmo KU, Worley DR, Goldschmidt MH. Tumors of the mammary gland. In: Small Animal Clinical Oncology. 5th edn. Withrow SJ, Vail DM, Page RL Eds., St. Louis, Saunders Elsevier, 2013: 538-556.

Sun WH, Pabon C, Alsayed Y, Huang PP, Jandeska S, Uddin S, Platanias LC, Rosen ST. Interferon-alpha resistance in a cutaneous T-cell lymphoma cell line is associated with lack of STAT1 expression. Blood. 1998 Jan 15;91(2):570-6.

Stanifer ML, Rippert A, Kazakov A, Willemsen J, Bucher D, Bender S, Bartenschlager R, Binder M, Boulant S. Reovirus intermediate subviral particles constitute a strategy to infect intestinal epithelial cells by exploiting TGF-β dependent pro-survival signaling. Cell Microbiol. 2016 Dec;18(12):1831-1845.

Stiff A, Caserta E, Sborov DW, Nuovo GJ, Mo X, Schlotter SY, Canella A, Smith E, Badway J, Old M, Jaime-Ramirez AC, Yan P, Benson DM, Byrd JC, Baiocchi R, Kaur B, Hofmeister CC, Pichiorri F. Histone Deacetylase Inhibitors Enhance the Therapeutic Potential of Reovirus in Multiple Myeloma. Mol Cancer Ther. 2016 May;15(5):830-41.

Sturzenbecker LJ, Nibert M, Furlong D, Fields BN. Intracellular digestion of reovirus particles requires a low pH and is an essential step in the viral infectious cycle. J Virol. 1987 Aug;61(8):2351-61.

Strong JE, Coffey MC, Tang D, Sabinin P, Lee PW. The molecular basis of viral oncolysis: usurpation of the Ras signaling pathway by reovirus. EMBO J. 1998 Jun 15;17(12):3351-62.

Thirukkumaran CM, Luider JM, Stewart DA, Cheng T, Lupichuk SM, Nodwell MJ, Russell JA, Auer IA, Morris DG. Reovirus oncolysis as a novel purging strategy for autologous stem cell transplantation. Blood. 2003 Jul 1;102(1):377-87.

Thirukkumaran CM, Nodwell MJ, Hirasawa K, Shi ZQ, Diaz R, Luider J, Johnston RN, Forsyth PA, Magliocco AM, Lee P, Nishikawa S, Donnelly B, Coffey M, Trpkov K, Fonseca K, Spurrell J, Morris DG. Oncolytic viral therapy for prostate cancer: efficacy

of reovirus as a biological therapeutic. Cancer Res. 2010 Mar 15;70(6):2435-44.

Thirukkumaran CM, Shi ZQ, Luider J, Kopciuk K, Gao H, Bahlis N, Neri P, Pho M, Stewart D, Mansoor A, Morris DG. Reovirus modulates autophagy during oncolysis of multiple myeloma. Autophagy. 2013 Mar;9(3):413-4.

Twigger K, Vidal L, White CL, De Bono JS, Bhide S, Coffey M, Thompson B, Vile RG, Heinemann L, Pandha HS, Errington F, Melcher AA, Harrington KJ. Enhanced in vitro and in vivo cytotoxicity of combined reovirus and radiotherapy. Clin Cancer Res. 2008 Feb 1;14(3):912-23.

Twigger K, Roulstone V, Kyula J, Karapanagiotou EM, Syrigos KN, Morgan R, White C, Bhide S, Nuovo G, Coffey M, Thompson B, Jebar A, Errington F, Melcher AA, Vile RG, Pandha HS, Harrington KJ. Reovirus exerts potent oncolytic effects in head and neck cancer cell lines that are independent of signalling in the EGFR pathway. BMC Cancer. 2012 Aug 24;12:368.

Vacchelli E, Eggermont A, Sautès-Fridman C, Galon J, Zitvogel L, Kroemer G, Galluzzi L. Trial watch: Oncolytic viruses for cancer therapy. Oncoimmunology. 2013 Jun 1;2(6):e24612.

van Houdt WJ, Smakman N, van den Wollenberg DJ, Emmink BL, Veenendaal LM, van Diest PJ, Hoeben RC, Borel Rinkes IH, Kranenburg O. Transient infection of freshly isolated human colorectal tumor cells by reovirus T3D intermediate subviral particles. Cancer Gene Ther. 2008 May;15(5):284-92.

van Meerloo J, Kaspers GJ, Cloos J. Cell sensitivity assays: the MTT assay. Methods Mol Biol. 2011;731:237-45.

Vecchio D, Daga A, Carra E, Marubbi D, Raso A, Mascelli S, Nozza P, Garrè ML, Pitto F, Ravetti JL, Vagge S, Corvò R, Profumo A, Baio G, Marcello D, Frosina G. Pharmacokinetics, pharmacodynamics and efficacy on pediatric tumors of the glioma radiosensitizer KU60019. Int J Cancer. 2015 Mar 15;136(6):1445-57.

Veterinary cooperative oncology group - common terminology criteria for adverse events (VCOG-CTCAE) following chemotherapy or biological antineoplastic therapy in dogs and cats v1.1. Vet Comp Oncol. 2016 Dec;14(4):417-446.

Vidal L, Pandha HS, Yap TA, White CL, Twigger K, Vile RG, Melcher A, Coffey M, Harrington KJ, DeBono JS. A phase I study of intravenous oncolytic reovirus type 3 Dearing in patients with advanced cancer. Clin Cancer Res. 2008 Nov 1;14(21):7127-37.

White CL, Twigger KR, Vidal L, De Bono JS, Coffey M, Heinemann L, Morgan R, Merrick A, Errington F, Vile RG, Melcher AA, Pandha HS, Harrington KJ. Characterization of the adaptive and innate immune response to intravenous oncolytic reovirus (Dearing type 3) during a phase I clinical trial. Gene Ther. 2008

Jun;15(12):911-20.

Yang WQ, Senger D, Muzik H, Shi ZQ, Johnson D, Brasher PM, Rewcastle NB, Hamilton M, Rutka J, Wolff J, Wetmore C, Curran T, Lee PW, Forsyth PA. Reovirus prolongs survival and reduces the frequency of spinal and leptomeningeal metastases from medulloblastoma. Cancer Res. 2003 Jun 15;63(12):3162-72.

Yang WQ, Lun X, Palmer CA, Wilcox ME, Muzik H, Shi ZQ, Dyck R, Coffey M, Thompson B, Hamilton M, Nishikawa SG, Brasher PM, Fonseca K, George D, Rewcastle NB, Johnston RN, Stewart D, Lee PW, Senger DL, Forsyth PA. Efficacy and safety evaluation of human reovirus type 3 in immunocompetent animals: racine and nonhuman primates. Clin Cancer Res. 2004 Dec 15;10(24):8561-76.

Yoshitake R, Saeki K, Watanabe M, Nakaoka N, Ong SM, Hanafusa M, Choisunirachon N, Fujita N, Nishimura R, Nakagawa T. Molecular investigation of the direct anti-tumour effects of nonsteroidal anti-inflammatory drugs in a panel of canine cancer cell lines. Vet J. 2017 Mar;221:38-47.

Zhao X, Rajasekaran N, Chester C, Yonezawa A, Dutt S, Coffey M, Kohrt HE. Reovirus activated NK cells show enhanced cetuximab mediated antibody-dependent cellular cytotoxicity against colorectal cancer cells. J Immunother Cancer. 2015 Nov;3(S2):340.